Novel functions of schizophrenia-related dysbindin-1 in the subventricular zone

A thesis submitted to the Department of Physiology, Anatomy and Genetics,

in partial fulfilment of the requirements for the degree of

Doctor of Philosophy

by

Abeer Al-Shammari

St Anne's College, University of Oxford, United Kingdom

Michaelmas Term, 2016

For my parents and siblings

Abstract

Abeer Al-Shammari. Novel functions of schizophrenia-related dysbindin-1 in the subventricular zone. St Anne's College. Submitted in partial fulfilment for the degree of Doctor of Philosophy. Michaelmas term, 2016.

Schizophrenia is a neurodevelopmental disorder that has widely been associated with environmental and genetic risk factors. However, direct functional interactions between the two risk factors remain unclear. Therefore, I sought to address how the schizophrenia-related dysbindin-1 may functionally mediate polyI:C-induced inflammation and the importance of this interaction on neurodevelopment in the subventricular zone (SVZ). I focused on the SVZ niche since it lies at the interface between systemic inflammation and neurogenic homeostasis. The interacting effects of dysbindin-1 and polyI:C on microglia, cytokine secretion and leukocyte permeability into the SVZ were also characterized.

Multiple systemic polyI:C injections during early postnatal development in dysbindin-1 mutant (Sandy, Sdy) mice resulted in reduced adult SVZ proliferation and reduced neuroblast populations in the rostral migratory stream (RMS). This was also correlated with reduced prepulse inhibition, decreased locomotor activity, object recognition deficit as well as long-term reduction in body weights in adulthood. Postnatal SVZ proliferation was also reduced in Sdy mice given postnatal polyI:C indicating a neurodevelopmental origin of these abnormalities in adulthood. In contrast to these results, adult SVZ proliferation as well as proliferation and neuroblast populations in the RMS were unaffected in transgenic mice overexpressing neuregulin-1 type I ($NRG1^{typeI\text{-}tg}$) and Snap25 mutant ($SNAP25^{+/-}$) mice that were not immune challenged.

I analyzed the expression of toll-like receptor 3 (Tlr3), RelA and Sp1 which are important in the innate immune response and cell proliferation in order to determine how dysbindin-1 and polyI:C mediate their expression. PolyI:C administration to WT SVZ *in vivo* and *in vitro* induced the expression of its receptor Tlr3 and the downstream transcription factors RelA and Sp1 indicating a normal inflammatory response. Unexpectedly, *in vitro* and *in vivo* polyI:C administration also increased dysbindin-1 expression in WT SVZ, suggesting an inflammatory role for dysbindin-1. This was confirmed in Sdy mice that showed inhibited Tlr3, RelA and Sp1 expression in the SVZ following polyI:C administration both *in vivo* and *in vitro*. Furthermore, overexpression of dysbindin-1 (Dtnbp1) gene rescued Tlr3 and RelA expression *in vitro* in neurospheres prepared from Sdy mice. Supporting the notion that dysbindin-1 regulates immune function, SVZ microglial density was higher in Sdy than in WT mice. Also, more leukocytes were found in the postnatal SVZ of Sdy mice following systemic polyI:C injections than in WT mice given saline. Finally, differential cytokine secretion was detected in Sdy neurospheres in comparison to WT neurospheres under baseline and inflammatory conditions. Taken together, I report novel functions of the schizophrenia-relevant dysbinidin-1 in regulating microglial density in the SVZ, and provide evidence for a direct interaction between dysbindin-1 and polyI:C-induced inflammation that is required for maintaining SVZ proliferation, mediating cytokine secretion and restricting leukocyte infiltration into the SVZ. This work provides a novel mechanistic framework for further studying the relationship between genes and environment in the context of schizophrenia.

Acknowledgments

I would like to express my gratitude to everyone who supported me throughout my graduate training. Special thanks and appreciation to my supervisor, Professor Francis Szele, for his constant support from the time I applied to his lab to the final stages of my DPhil training. I am really glad to be a member of his lab and I am thankful to him for creating a lab environment that fosters critical thinking. His exceptional support and encouragement have definitely inspired me to grow as an independent researcher.

I am also grateful to all current and former members of the Szele Group who have truly made my time enjoyable in the lab and who are always keen to offer technical advice related to my project. Many thanks to Dr. Julie Davies, Dr. Istvan Adorjan, Dr. James Hillis, Dr. Bin Sun, Dr. Osama Al Dalahmah, Ms. Mayara Vieira, Mr. Martin Ducker, Ms. Farah Alammari, Ms. Yichen Li, Dr. Anne Wolfes, Mr. Fang Li, Dr. Nick Davies, Dr. Roderick Walker, Dr. Chiara Bardella and Dr. Tracy Lane for being such wonderful lab colleagues!

I am very thankful to the research group in Prof. Richard Wade-martins lab for giving me access to use the ChemiDoc XRS+ system (Bio-Rad) and StepOnePlus Real-Time PCR System (Applied Biosystems), and also to the group in Prof. Matthew Wood lab for allowing me to use the Odyssey Fc Imaging System (LI-COR), their kindness has facilitated the performance of some experiments I used in my thesis.

Many thanks to Dr. Karri Lamsa and Dr. Peter Oliver for the provision of Nrg1 type I overexpressing and Snap25 mutant mice, respectively, which I have used to carry out the initial screening studies. I am indebted to Dr. Sanjeev Bhardwaj and Prof. Lalit Srivastava's lab (McGill University) for designing the initial project related to Sandy mice and from whom we have obtained the Sandy mice in order to carry out the rest of this project. I also would like to thank the staff in the Oxford Biomedical Sciences Building, Ms. Denise Jelfs, Ms. Angela Cooke, Mr. James Ward, Ms. Laura Thomas, Ms. Amy Johnson and Mr. Richard Maxwell for the day-to-day animal care and for the invaluable advice on colony management.

I am privileged to be a member of an ambitious and a fast growing organization, the Qatar Foundation (QF). From the time I have joint the QF Research & Development division I have always been amazed by the exciting and rewarding opportunities offered to me which certainly motivate me to reach my full potential. I would like to especially thank Dr. Ayman Bassil, Dr. Aisha Al-Obaidly, Ms. Maria Estacio, Ms. Nuha Al-Okka, Ms. Hissa Al-Kubaisi and Ms. Omneya Negm for their full support and encouragement during my research career development. Also thanks to the QF Research & Development division for the generous financial support.

Finally, I am very lucky to have great parents, sisters and brothers who have always provided me with unconditional love, support and trust, which encourage me to strive for the best I can achieve. I deeply appreciate the endless patience of my parents during the many years of my study abroad.

Authorship statement

The experimental protocol for *in vivo* polyI:C injections in Sdy mice was designed by Professor Lalit Srivastava's laboratory (McGill University). All other experiments were designed by myself with input from my supervisor, Professor Francis Szele.

In Chapter 3, perfusions of adult $NRG1^{type1\text{-}tg}$ mice were done with kind help from Dr. James Hillis (former DPhil student in Professor Francis Szele's laboratory). Adult $SNAP25^{+/-}$ mice were kindly perfused by Dr. Peter Oliver (DPAG – University of Oxford). PolyI:C injections and perfusions of adult Sdy mice were carried out by Dr. Sanjeev Bhardwaj from Professor Lalit Srivastava's laboratory (McGill University). Behavioural and MRI data as well as body weight measurements at P37-38 and P72-73 were all carried out by Professor Lalit Srivastava's laboratory (McGill University).

I performed all other experimental procedures, quantifications and analysis with generous guidance from members of our laboratory, the University and the greater scientific community.

Table of Contents

List of Figures

Chapter 1:

Chapter 2:

Chapter 3:

Chapter 4:

Chapter 5:

Chapter 6:

List of Tables

Chapter 1:

Chapter 2:

Chapter 3:

Chapter 6:

Abbreviations

BLOC-1	Biogenesis of lysosome-related protein complex-1
CD45	Cluster of differentiation 45 or leukocyte common antigen (LCA)
CD68	Cluster of differentiation 68 or macrosialin
CNS	Central nervous system
CSF	Cerebrospinal fluid
DAPI	4',6-diamidino-2-phenylindole
Dcx	Doublecortin
dsRNA	Double-stranded RNA
GxE	Gene x environment
NF	Nucleofection
NF-κB	Nuclear factor-kappaB
NPC	Neural progenitor cell
Nrg1	Neurgulin-1
NRG1t$^{ypeI\text{-}tg}$ mice	Transgenic mice overexpressing neuregulin-1 type I
NS	Neurosphere
OB	Olfactory bulb
P12	Postnatal day 12
P5-9	Postnatal day 5 to 9
PHi3	Phosphohistone-3
PolyI:C	Polyinosinic-polycytidylic acid
PPI	Prepulse inhibition
RelA	V-rel avian reticuloendotheliosis viral oncogene homolog A

RMS	Rostral migratory stream
RT-qPCR	Real-time quantitative polymerase chain reaction
$Sdy^{-/-}$ or Sdy mice	Sandy mice
$SNAP25^{+/-}$ mice	Snap25 mutant mice
Sp1	Specificity protein-1
SVZ	Subventricular zone
TIR	Toll/IL-1 receptor
Tlr3	Toll-like receptor 3
TRIF	TIR domain-containing adaptor inducing interferon-β
WT	Wild-type

Chapter 1

General introduction

1.1 Overview of schizophrenia

Schizophrenia is the most common mental disorder affecting 1% of the total population. It is a devastating disease that affects perceptions, thoughts, speech and behaviours of the patient with negative consequences on the caregivers or even the wider community (reviewed in (Schultz et al., 2007)). Schizophrenia is characterized by positive and negative symptoms with onset usually during late adolescence and early adulthood. Positive symptoms include hallucinations, delusions, disorganized speech and thoughts and aggressive behaviour, whereas negative symptoms include social withdrawal, loss of motivation and lack of emotions. Overall, patients with schizophrenia have higher mortality rate, due to suicide (10% lifetime risk), than the general public (reviewed in (Schultz et al., 2007)).

Although the exact aetiology of schizophrenia is still unclear, it is widely accepted as a neurodevelopmental disorder influenced by both genetic and environmental factors. As shown in Table 1.1, the prevalence of schizophrenia is higher in individuals with a family history of the disorder than in the general population. Moreover, monozygotic and dizygotic twins from schizophrenic parents are more likely to develop schizophrenia than their second- and third-degree relatives, highlighting an important role of genetic predisposition in disease prevalence (Table 1.1). The heritability of schizophrenia is further emphasized in a recent genome-wide association study (GWAS) that showed significant association of 108 genetic loci with schizophrenia (Schizophrenia Working Group of the Psychiatric Genomics, 2014).

Table 1.1 Family history and schizophrenia

Family history	*Approximate lifetime incidence (%)*
None (e.g., general population)	1
Third-degree relative (e.g., first cousin)	2
Second-degree relative (e.g., niece or nephew)	2 to 6
First-degree relative (e.g., parent, child, sibling)	6 to 17
Dizygotic twin	17
Monozygotic twin	50

Adapted from (Schultz et al., 2007)

Since the incidence of schizophrenia is only 50% in genetically identical monozygotic twins, this may indicate a causative role of the environment (reviewed in (Schultz et al., 2007)). As shown in figure 1.1, various environmental insults during prenatal or early postnatal life may impact brain development and hence increase the chance of developing schizophrenia in adulthood.

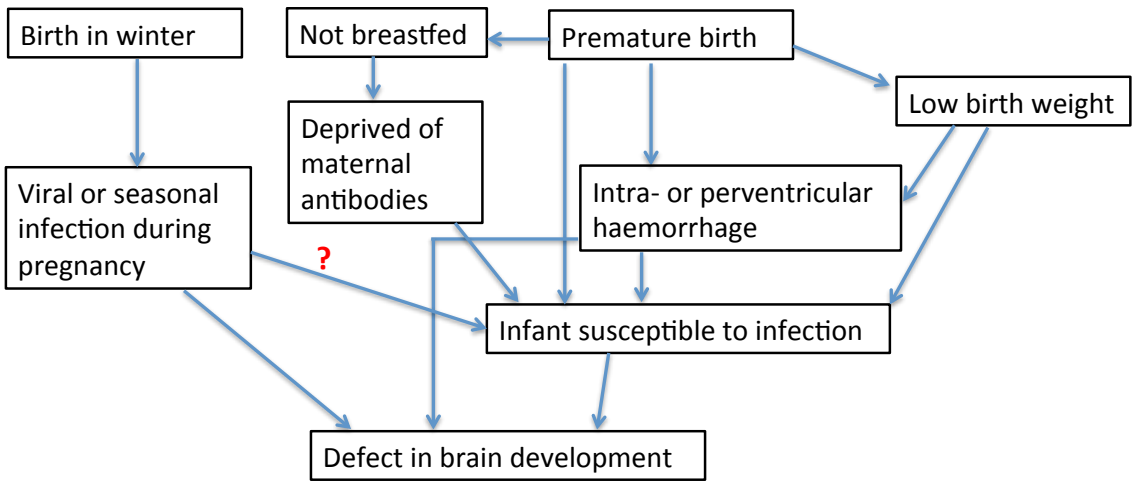

Figure 1.1 Environmental risk factors of schizophrenia

I show a summary of various environmental risk factors of schizophrenia in which all may lead to a defect in neurodevelopment. (?) indicates uncertainty of direct influence.

1.2 Dysbindin-1 (Dtnbp1) as a risk gene for schizophrenia

1.2.1 Dysbindin-1 overview

The dysbindin protein family consists of three paralogs (dysbindin-1, -2 and -3) in which all share a homologous protein region called the dysbindin domain (DD). Each of these paralogs is encoded by a different gene and exists in multiple isoforms. To date, dysbindin-1 is the only paralog shown to associate with schizophrenia (reviewed in (Talbot et al., 2009)). Dysbindin-1 protein is encoded by dystrobrevin binding protein-1 (DTNBP1) gene, which is located in chromosome 6p22.3 in humans and chromosome 13 A5 in mice. Dysbindin-1 is ubiquitously expressed in various tissues, such as brain, skeletal muscle, heart, kidney, liver and more. In the brain, the majority of studies considered dysbindin-1 expression to occur primarily, if not exclusively, in neuronal cell populations (reviewed in (Talbot et al., 2009)). However, evidence from rodent brain showed comparable, if not higher, expression of dysbindin-1 in glial cells (i.e. astrocytes and oligodendrocytes) than in neurons (Ghiani et al., 2010). Moreover, dysbindin-1 was detected in glial cells in *Drosophila*, the majority of which were found in glial processes surrounding neuronal cell bodies with partial distribution in glial cell bodies (Shao et al., 2011). Also, dysbindin-1 expression was identified in astroglia endfeet surrounding blood vessels as well as in capillary endothelial cells in mouse brain tissue (Iijima et al., 2009). However, it is still to be determined if dysbindin-1 is also expressed in microglia.

So far, three isoforms of dysbindin-1 protein are identified in humans (dysbindin-1A, -1B and -1C) and only two isoforms are found in mouse (dysbindin-1A and -1C) (reviewed in (Talbot et al., 2009)). Dysbindin-1A and -1C in humans are

highly homologous to their corresponding isoforms in mouse. The full-length dysbindin-1A protein consists of three basic domains: an amino terminal region (NTR), a coiled-coil domain (CCD) and a carboxy terminal region (CTR) as shown in figure 1.2A. However, dysbindin-1B lacks a fragment of the CTR (i.e. PEST domain), whereas dysbindin-1C lacks the entire NTR (reviewed in (Talbot et al., 2009)). According to Talbot *et al* (2011), human dysbindin-1 isoforms are differentially distributed in subsynaptic compartments. As illustrated in figure 1.2B, dysbindin-1A is predominately localized in postsynaptic densities (PSD) but undetectable in synaptic vesicles (SV) (Talbot et al., 2011). However, dysbindin-1B is abundant in SV and almost absent in PSD. Dysbindin-1C is detected in small amounts in SV but far more abundant in PSD (Talbot et al., 2011). On the other hand, dysbindin-1 isoforms in mouse also have distinctive distributions in subsynaptic regions. In mouse, both dysbindin-1A and -1C are found in PSD, however dysbindin-1A is more enriched in presynaptic membranes whereas dysbindin-1C is mainly localized in SV (Wang et al., 2014). Furthermore, dysbindin-1 isoforms show different temporal expression in mouse brain. From postnatal to adult ages, dysbindin-1A protein levels gradually decrease whereas dysbindin-1C levels gradually increase in the hippocampal formation of mouse brain (Wang et al., 2014). However, it is still to be determined if dysbindin-1 isoforms in human brain are also developmentally regulated.

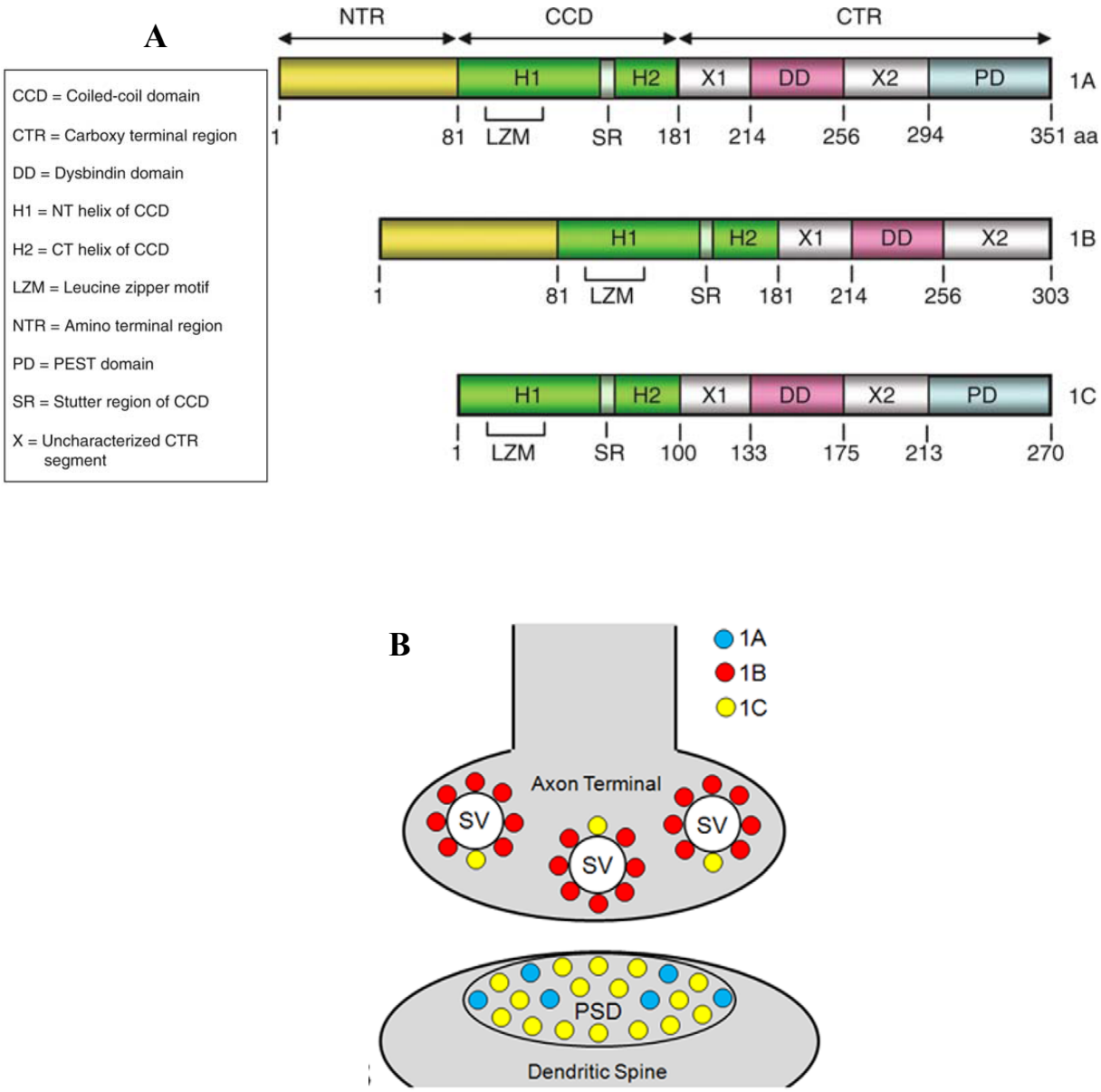

Figure 1.2 Structure and subsynaptic localization of dysbindin-1 isoforms in humans

(A) Structure of human dysbindin-1 isoforms (-1A, -1B & -1C). Dysbindin-1A mainly consists of amino terminal region (NTR), coiled-coil domain (CCD) and a carboxy terminal region (CTR). Dysbindin-1B lacks PEST domain (PD) in CTR, whereas dysbindin-1C lacks the whole NTR. In mouse, only dysbindin-1A and -1C are found and are structurally similar to their corresponding isoforms in humans.

(B) Distribution of dysbindin-1 isoforms in human synaptosomes. Dysbindin-1A is mainly localized in postsynaptic density (PSD) and dysbindin-1B in synaptic vesicles (SV). Dysbindin-1C is identified in both PSD and SV although it is predominately localized in PSD.

Image (A) adapted from (Talbot et al., 2011) and (B) from (Talbot et al., 2009).

1.2.2 Human dysbindin-1 and schizophrenia

Dysbindin-1 was discovered by Benson and colleagues in 2001 (Benson et al., 2001). Soon after that, single nucleotide polymorphisms (SNPs) and/or haplotypes within human DTNBP1 gene were shown to associate with schizophrenia (Straub et al., 2002). This association was further confirmed in various populations (reviewed in (Talbot et al., 2009)). Although it is unclear if risk variants of DTNBP1 gene affect the level of its expression, there are multiple lines of evidence that dysbindin-1 levels are reduced in schizophrenia. Reduction in dysbindin-1 expression was reported in the dorsolateral prefrontal cortex (DLPC) and the hippocampal formation (HF) of schizophrenic patients at both the messenger RNA (mRNA) (Weickert et al., 2008, Weickert et al., 2004) and protein levels (Tang et al., 2009, Talbot et al., 2004). Interestingly, reduction of dysbindin-1 protein was found to occur in isoform-specific manner in schizophrenia. Synaptic dysbindin-1A was shown to decrease in the posterior half of the superior temporal gyrus (pSTG) whereas dysbindin-1B and -1C were decreased in the HF of schizophrenic patients (Talbot et al., 2011). Given the distinctive subcellular distributions of dysbindin-1 isoforms, the authors concluded that the reduction in postsynaptic dysbindin-1A in pSTG of schizophrenic patients might promote dendritic spine loss and hence abnormal auditory processing. However, reduced dysbindin-1B and -1C in HF of both pre- and postsynaptic regions might promote disrupted spatial working memory in schizophrenia (Talbot et al., 2011).

1.2.3 Sandy mouse: Dysbindin-1 mutant

Sandy (Sdy) mice naturally arose at the Jackson Laboratory in 1983. Although these mice are fully viable, they are characterized by diluted pigmentation (albinism) in both eyes and coat (hence the name Sandy) as well as prolonged bleeding times after injury (fig.1.3A-B) (Swank et al., 1991). Genetic tests determined that these phenotypes are due to an autosomal recessive mutation in chromosome 13 (Swank et al., 1991). However, it was not until 2003 in which a genetic and physical mapping study identified a specific mutation in Dtnbp1 gene that causes the observed phenotypes in Sdy mice (Li et al., 2003). As shown in figure 1.3C, Dtnbp1 mutation in Sdy mice is an in-frame deletion from intron 5 to intron 7, which results in the removal of exons 6 and 7 (Li et al., 2003). This Dtnbp1 mutation is not a null mRNA mutation because the mutant Dtnbp1 gene is still transcribed in heterozygous and Sdy mice but the mRNA produced is of shorter length compared to wild-type (WT) mice (fig.1.3D).

In the protein level, Dtnbp1 mutation in Sdy mice results in the deletion of 52 amino acids in the CCD of dysbindin-1 protein (Li et al., 2003). Therefore, it is predicted that absence of intact CCD may lead to a rapid degradation of dysbindin-1 protein in Sdy mice (fig. 3E) due to failure of dysbindin-1 to form stable interactions with its normal binding partners (e.g. BLOC-1, see section 1.2.5 below). As shown in figure 1.3F, expression of both dysbindin-1A and -1C isoforms were reduced in heterozygous brain but completely lost in Sdy brain (reviewed in (Talbot, 2009)). Although the authors referred to bands marked with asterisks in figure 1.F as non-specific, these bands might actually represent dysbindin-1C. Another group also used

the most widely accepted dysbindin-1 antibody to date (PA3111), and they still detected this extra band in Sdy brain (Larimore et al., 2014). Therefore, dysbindin-1A might be completely lost in Sdy brain, however dysbindin-1C may still exist. I have further discussed this in Chapter 6.

1.2.4 Sandy mouse as a model of schizophrenia

Following the discovery of Dtnbp1 mutation in Sdy mice as well as the reported abnormalities of dysbindin-1 in schizophrenic patients, this stimulated the question of whether Sdy mice can be used as a model of schizophrenia. Interestingly, electrophysiological and neurobehavioural characterization of Sdy mice indicated their relevance to the disease. For example, abnormalities in dopaminergic (Nagai et al., 2010, Hattori et al., 2008), glutamatergic (Chen et al., 2008, Jentsch et al., 2009) and GABAergic (Ji et al., 2009) neurotransmission were all reported in the brains of Sdy mice, providing a model of disrupted neural transmission in schizophrenia. Furthermore, schizophrenia-like behaviours such as reduced pre-pulse inhibition (PPI) (Carlson et al., 2011), cognitive deficits (Feng et al., 2008, Bhardwaj et al., 2009) and social withdrawal (Feng et al., 2008, Hattori et al., 2008) were also reported in Sdy mice.

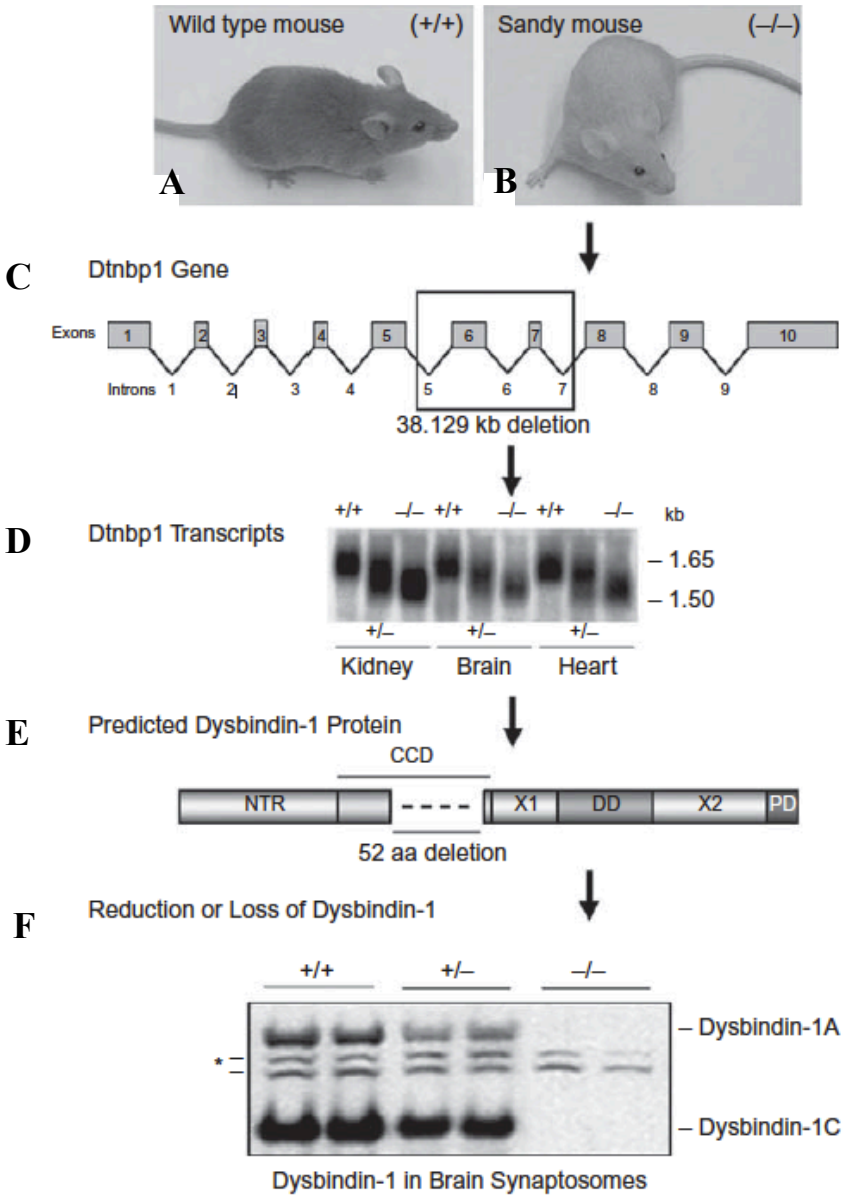

Figure 1.3 Dysbindin-1 (Dtnbp1) gene mutation in Sandy (Sdy) mouse and its effect on gene transcripts and protein expression

(A-B) Sdy mice are characterized by diluted coat colour compared to wild-type mice.

(C) Structure of Dtnbp1 gene in which introns 5-7 (that includes exons 6-7) are deleted in Sdy mice. This results in a large deletion of 38,129kb.

(D) Relative size of Dtnbp1 transcripts in WT (+/+), heterozygous (+/-) and Sdy (-/-) mice as shown with northern blots of kidney, brain and heart tissues.

(E) In Sdy mice, Dtnbp1 mutation results in deletion of 52 amino acids in coiled-coil domain (CCD) of dysbindin-1 protein.

(F) Western blots showing level of dysbindin-1A and -1C proteins in brain synaptosomes of +/+, +/- and -/- mice. Asterisk (*) referred to as non-specific bands by the authors.

Image adapted from (Talbot, 2009).

1.2.5 Sandy mouse: biochemical abnormalities

Dysbindin-1 is a member of the biogenesis of lysosome-related protein complex-1 (BLOC-1). As shown in figure 1.4A, BLOC-1 consists of eight binding partners: muted, snapin, pallidin, cappuccino and BLOC-1 subunits 1-3 (BLOS1-3) in addition to dysbindin-1 (reviewed in (Talbot et al., 2009)). Functionally, BLOC-1 plays crucial roles in the maturation of early endosomes into specialized organelles such as melanosomes, platelet dense granules, lysosomes and synaptic vesicles as illustrated in figure 1.4B. In Sdy mice, loss of dysbindin-1 affects the stability of BLOC-1 components, such as reduced levels of muted, pallidin (Li et al., 2003) and snapin (Feng et al., 2008, Saggu et al., 2013), which together lead to defective maturation of the specialized organelles. This explains the abnormal phenotypes observed in Sdy mice, such as diluted pigmentation due to defective melanosomes and prolonged bleeding due to impaired platelet aggregation (Swank et al., 1991). Furthermore, loss of dysbindin-1 in Sdy mice leads to disrupted neurotransmission due to impaired synaptic vesicle biogenesis, endocytosis and exocytosis (Chen et al., 2008, Saggu et al., 2013). Interestingly, loss of dysbindin-1 also reduces snapin (Feng et al., 2008, Saggu et al., 2013) and Snap25 (Numakawa et al., 2004) levels that are critical for synaptic vesicle fusion with the plasma membrane, providing further explanation for the abnormal synaptic signaling in Sdy brains. Given that lysosomal secretion is reduced in Sdy mice (Swank et al., 1991), it is predicted that this may lead to immune dysfunction. However, no studies to date have studied the effects of immune challenge in Sdy mice. Therefore, one aim of my thesis was to determine the molecular role of dysbindin-1 in regulating immune response following viral-like infection.

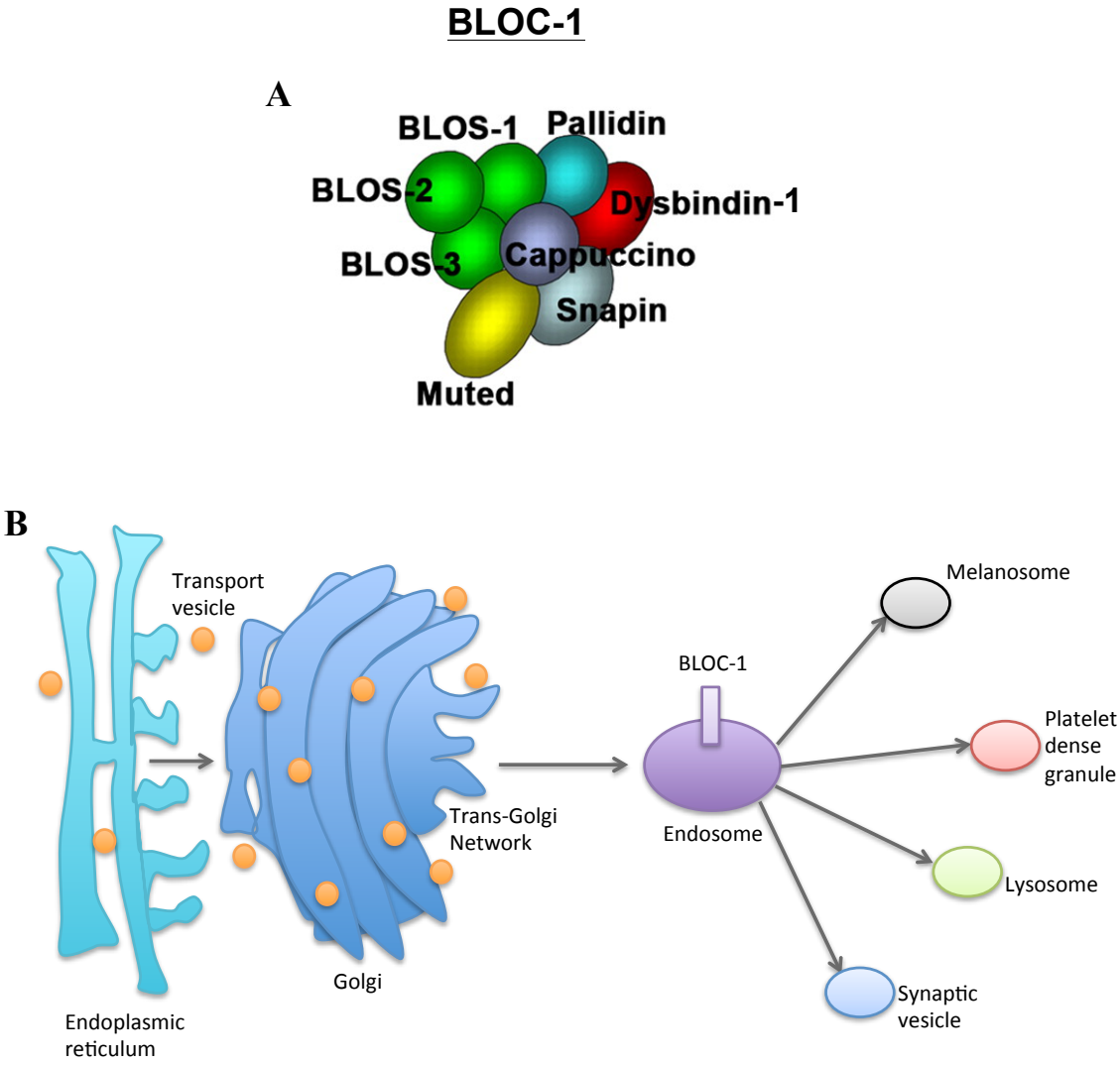

Figure 1.4 Molecular functions of dysbindin-1 and its associated BLOC-1 proteins

(A) Subunit composition of the biogenesis lysosome-related complex-1 (BLOC-1).

(B) BLOC-1 is involved in maturation of endosomal compartments (i.e. melanosome, platelet dense granule, lysosome and synaptic vesicle) that are trafficked from trans-Golgi network.

Image (A) adapted from (Newell-Litwa et al., 2007).

1.3 Viral-like infection as an environmental risk factor for schizophrenia

Various environmental insults such as psychological, epigenetic and immune challenges have been associated with increased risk of developing schizophrenia. For example, a number of epidemiological studies suggested a link between schizophrenia and exposure to viral or bacterial infections during prenatal or early postnatal life (reviewed in (Brown, 2011)). This is further confirmed in recent genome-wide association studies (GWAS) that showed a strong association of immunity with schizophrenia (Network and Pathway Analysis Subgroup of Psychiatric Genomics, 2015, Schizophrenia Working Group of the Psychiatric Genomics, 2014).

In animal models of schizophrenia, two types of molecular immunogens are commonly used to induce inflammation during neurodevelopment such as lipopolysaccharide (LPS) and polyinosinic-polycytidylic acid (polyI:C) (reviewed in (Harvey and Boksa, 2012)). LPS is a component of the outer membrane of Gram-negative bacteria and it is used to mimic bacterial infection. However, polyI:C is a synthetic analog of double-stranded RNA which is used to mimic viral infection. Both LPS and polyI:C bind to toll-like receptors (i.e. LPS to Tlr4 while polyI:C to Tlr3) and induce strong innate immune responses (reviewed in (Harvey and Boksa, 2012)).

In addition to LPS and polyI:C, there are other types of inflammatory stimuli such as cytokines, live viruses and turpentine that are used in neurodevelopmental models. The advantage of direct administration of cytokines, such as interleukin-6

(IL-6), is that the behavioural and neurochemical effects of a specific cytokine can be addressed. Although the intranasal administration of live viruses resembles the naturalistic method of catching an infection, there is difficultly in this method to control the dosage and the window of exposure. Intramuscular injection of turpentine, which is an inflammatory stimulus, remains at the site of the administration and therefore can be useful to study the effect of localized inflammation (reviewed in (Harvey and Boksa, 2012)). Taken together, various inflammatory models are being used in order to study the effects of neonatal immune activation in relation to schizophrenia.

In my thesis, I used the viral immunostimulant polyI:C as an environmental risk factor for schizophrenia because polyI:C mimics viral infections which are widespread such as seasonal flu and common cold. Another reason for using polyI:C is that the dosage and the route of systemic polyI:C administration can be controlled in our model. Also, the downstream signalling pathway from polyI:C is well-described in the literature, and therefore abnormal molecular response to polyI:C can be investigated in our genetic model of schizophrenia. In particular, polyI:C is a specific ligand for toll-like receptor 3 (Tlr3) and activation of Tlr3 triggers downstream signalling pathways that include activation of RelA and Sp1 transcription factors. This Tlr3-RelA-Sp1 signalling pathway is described below.

1.3.1 Toll-like receptors (TLRs) overview

The Toll protein was originally discovered in *Drosophila* as being important for the immune response against fungal infection (Lemaitre et al., 1996). This led to the identification of homologous proteins in humans and mice that were named Toll-like receptors (TLRs) (Medzhitov et al., 1997, Hoshino et al., 1999). TLRs provide the first line of immune defence against invading pathogens ranging from bacteria to viruses to fungi. To date, 12 TLRs have been identified in mice and 10 in humans.

TLRs can be divided into two groups based on their subcellular localization and type of ligands. One group is composed of TLR1, TLR2, TLR4, TLR5 and TLR6, which are expressed on cell membranes and recognize microbial components such as lipids, lipoproteins, lipopolysaccharides (LPS) and proteins. The other group is composed of TLR3, TLR7, TLR8 and TLR9, which are localized in intracellular vesicles such as endosomal and endolysosomal membranes and they recognize microbial nucleic acids (Broz and Monack, 2013). TLR10 is only present in humans and as of yet has no known specific ligand. Recently, it has been shown that human TLR10 mainly acts as a modulatory receptor with anti-inflammatory effects (Oosting et al., 2014). On the other hand, TLR11, TLR12 and TLR13 are only found in mice in which they are expressed in intracellular compartments and are involved in recognition of microbial components (i.e. TLR11 and TLR12) or nucleic acids (i.e. TLR13) (reviewed in (Broz and Monack, 2013)).

1.3.2 Toll-like receptor 3 (TLR3)

TLR3 was discovered in 2001 and was shown to specifically recognize double-stranded RNA (dsRNA) (Alexopoulou et al., 2001), a genetic material that naturally exists in some viruses, such as reovirus, or that is produced by most viruses during replication including West Nile virus, respiratory syncytial virus and encephalomyocarditis virus (reviewed in (Kawai and Akira, 2010)). Furthermore, TLR3 also recognizes a synthetic analog of dsRNA, known as polyI:C as described earlier. Since TLR3 is subcellularly localized in endosomes (Nishiya and DeFranco, 2004), it recognizes dsRNA that directly enters endosomes or following phagocytosis of virally infected cells (Schulz et al., 2005).

In addition to TLR3 expression in immune cells, such as dendritic cells and macrophages, it is also highly expressed in the brain (reviewed in (Kumar et al., 2009)). TLR3 was shown to be expressed in the rodent brain from as early as embryonic day 10.5 (E10.5) (Lathia et al., 2008) and was also detected postnatally at P3-7 (Shi et al., 2013), P9-10 (Stridh et al., 2011) and P13 (Lathia et al., 2008) as well as in the adult mouse brain (Rolls et al., 2007). Similarly, TLR3 is expressed in the foetal (Vontell et al., 2013) and adult human brain (Bsibsi et al., 2002). TLR3 is expressed in several cell types of the mammalian brain. For example, TLR3 was shown to be expressed in neurons and astrocytes in rat brain (Shi et al., 2013) as well as in murine neural stem/progenitor cells (NPCs) (Rolls et al., 2007, Lathia et al., 2008), astrocytes and microglia (Rolls et al., 2007). Also, neurons (Lafon et al., 2006, Vontell et al., 2013), astrocytes (Bsibsi et al., 2002, Vontell et al., 2013), microglia and oligodendrocytes (Bsibsi et al., 2002) were all shown to express TLR3 in the

human brain. Studies have shown that TLR3 deficiency in humans is associated with herpes simplex virus type 1 (HSV-1) encephalitis (Zhang et al., 2007) and that TLR3 deficient mice are vulnerable to lethal infection with murine cytomegalovirus (Tabeta et al., 2004).

1.3.2.1 TLR3 structure

As shown in figure 1.5A, TLR3 is a type I transmembrane glycoprotein composed of an N-terminal extracellular domain (ECD), a single transmembrane helix and a C-terminal cytoplasmic tail. The ECD of TLR3 is located in the inside of endosomes and can be described as a horseshoe-shaped structure formed by 23 leucine-rich repeats (LRRs) (fig. 1.5A). The surface of LRRs is heavily glycosylated with 15 N-linked glycans, however one side is devoid of glycans allowing for free interaction with dsRNA (Bell et al., 2005, Choe et al., 2005). This localization of TLR3-ECD inside endosomes is critical to prevent contact with "self" nucleic acids and therefore avoid the risk of autoimmunity. On the other hand, the C-terminal cytoplasmic tail is the signalling domain that contains three homologous regions (Box 1, 2 and 3) to IL-1 receptor (IL-1R), which is also named TIR (Toll/IL-1R) domain as illustrated in figure 1.5A (reviewed in (O'Neill, 2000)).

1.3.2.2 TLR3 signalling

Although TLR3-ECD exists as a monomer in solution, it binds as a single homodimer to dsRNA with a minimal length of 40-50bp as shown in figure 1.5B. Multiple homodimers of TLR3-ECD bind to longer lengths of dsRNA and form a stable complex (Leonard et al., 2008). Upon dimerization of Tlr3-ECD, the two cytoplasmic TIR domains are brought into contact (Liu et al., 2008), thereby inducing the recruitment of its adapter protein that initiates downstream signalling pathway (fig. 1.5B). In particular, TIR domain-containing adaptor inducing interferon-β (TRIF), which is also named TIR-containing adaptor molecule-1 (TICAM-1), was shown to be an essential adapter protein for TLR3-mediated signalling (Oshiumi et al., 2003, Yamamoto et al., 2002, Yamamoto et al., 2003). As illustrated in figure 1.5B, TLR3-activation of TRIF-dependent pathway induces two transcription factors: nuclear factor-kappaB (NF-κB) and interferon regulatory factor-3 (IRF3), which lead to the production of inflammatory cytokines and type 1 interferon (IFN), respectively (reviewed in (Kawai and Akira, 2010)).

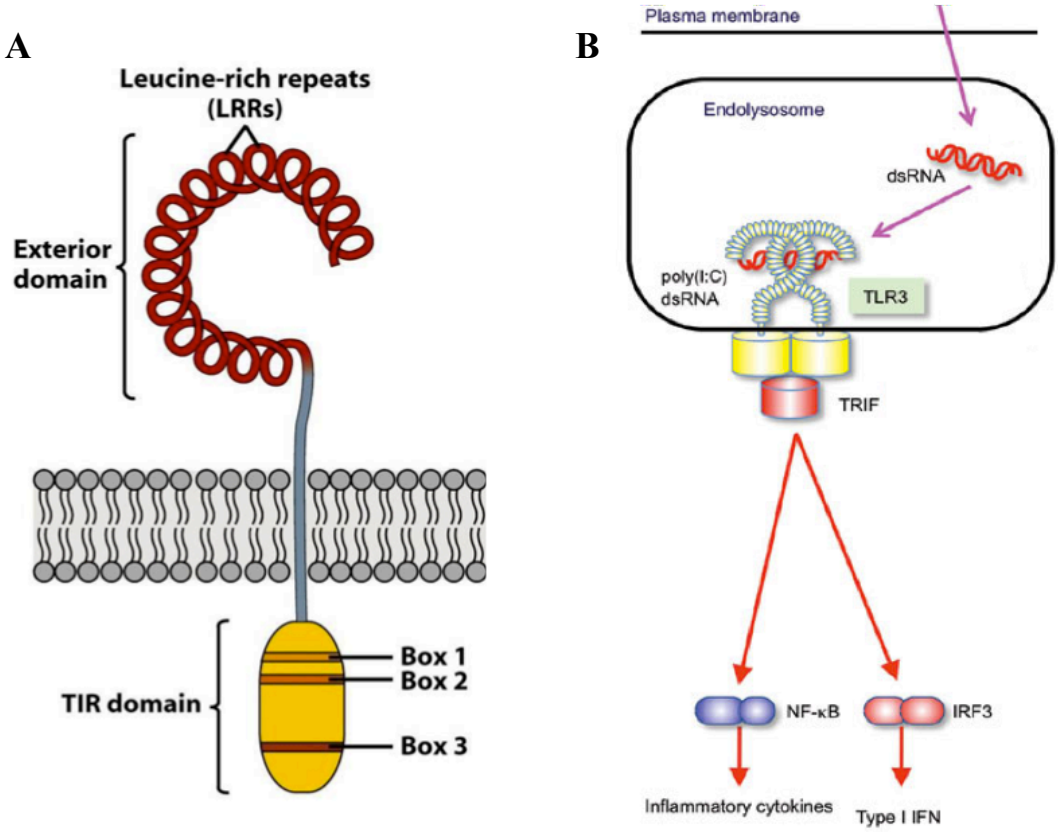

Figure 1.5 Structure of Toll-like receptor 3 (TLR3) and its downstream signaling pathway

(A) TLR3 is primarily composed of an extracellular domain (ECD), a single trasmembrane helix and a cytoplasmic tail. The ECD contains leucine-rich repeats (LRRs) and is located inside endosomes whereas the cytoplasmic tail contains the TIR domain with three homologous regions (Box 1-3) located in cellular cytoplasm.

(B) Following entry of double-stranded (dsRNA), such as polyI:C, into the endolysosomal compartment, it is recognized by TLR3-ECD homodimers that become dimerized and activate its cytoplasmic TRIF* mediator. This induces downstream nuclear factor-kappaB (NF-κB) and interferon regulatory factor-3 (IRF3) leading to the production of inflammatory cytokines and type 1 interferon (IFN), respectively.

* TRIF stands for TIR domain-containing adaptor inducing interferon-β.

Image (A) adapted from
https://classconnection.s3.amazonaws.com/817/flashcards/995817/jpg/tlr1323553992098.jpg
Image (B) adapted with amendments from (Kawai and Akira, 2010).

1.3.2.3 RelA

RelA, which stands for v-rel avian reticuloendotheliosis viral oncogene homolog A, is a member of the NF-κB family. RelA becomes activated upon TLR3 stimulation with polyI:C as described earlier. NF-κB is short for nuclear factor kappa-light-chain-enhancer of activated B cells which was discovered almost 30 years ago (Sen and Baltimore, 1986). NF-κB is a family of transcription factors that consists of five members in mammalian cells: RelA (p65), RelB and c-Rel as well as precursor proteins NF-κB1 (p105) and NF-κB2 (p100) that undergo processing and generate p50 and p52, respectively. NF-κB plays important roles in various cellular functions such as cell survival and proliferation, differentiation, migration, apoptosis and immunity (reviewed in (Bortolotto et al., 2014)).

In the CNS, NF-κB is present as a heterodimer consisting of RelA and p50 subunits, which is the most abundant form. In baseline conditions, NF-κB (RelA/p50 heterodimer) is bound by inhibitory protein IκB that keeps the heterodimer in the inactive form in the cytoplasm. NF-κB can be activated by various stimuli such as viral and bacterial infection, oxidative stress and cytokines. Upon NF-κB activation, IκB is dissociated and the NF-κB (RelA/p50 heterodimer) is translocated to the nucleus where it binds to target genes and induces transcription (reviewed in (Bortolotto et al., 2014)). Interestingly, RelA and another transcription factor, specificity protein-1 (Sp1), were shown to transactivate each other during viral infections (Doyle et al., 2013, Gu et al., 2002, Perkins et al., 1994, Yurochko et al., 1997). In particular, polyI:C was shown to induce RelA binding to the promoter region of Sp1 and activates its transcription (Doyle et al., 2013).

1.3.2.4 Specificity protein-1 (Sp1)

Sp1 belongs to the Sp/KLF (specificity protein/Krüppel-like factor) family of transcription factors, which all contain Cys_2His_2-type zinc fingers that are required for DNA binding at the promoter/regulatory regions. Sp1 is the founding member of the Sp subfamily that to date consists of nine members (Sp1-9) (reviewed in (Beishline and Azizkhan-Clifford, 2015)). Historically, Sp1 was the first mammalian transcription factor to be cloned (Kadonaga et al., 1987). It was first identified as an important factor that binds to Simian Virus 40 (SV40) early promoter and regulates its transcription (Dynan and Tjian, 1983). Sp1 binds to GC-rich motifs that are found in the promoter regions of many housekeeping genes, and therefore Sp1 was initially regarded as a general transcription inducer of housekeeping genes. However, it has later become clear that Sp1 undergoes various posttranslational modifications and found to regulate the expression of many genes involved in various processes such as cell growth/proliferation, apoptosis, angiogenesis, differentiation and immune responses (reviewed in (Tan and Khachigian, 2009)).

1.4 Gene x environment (GxE) interaction in schizophrenia: focusing on the subventricular zone (SVZ)

As discussed earlier, multiple genetic and environmental risk factors may contribute to the susceptibility to schizophrenia. However, it has become increasingly apparent from epidemiological studies that the combined effect of gene mutations and environmental challenges may increase the likelihood of developing schizophrenia compared to a single factor alone. For example, individuals exposed to neonatal infection who already had a family history of schizophrenia were five times more likely to develop schizophrenia than those who did not (Clarke et al., 2009). This was also illustrated in transgenic mouse models of schizophrenia in which a combination of both genetic and neonatal immune challenge gave rise to worse histological and behavioural phenotypes relevant to the disease than a single risk factor alone (Ibi et al., 2010). Taken together, gene x environment (GxE) interaction may play a significant role in the aetiology of schizophrenia, and therefore GxE animal models may provide fundamental insights into the underlying mechanisms. Here, the subventricular zone (SVZ) was used as a neurodevelopmental model for dissecting the molecular mechanisms of GxE interaction in schizophrenia. The SVZ provides an excellent model for studying these interactions since it continuously generates neural stem cells that undergo the full developmental process into mature neurons. In addition, the SVZ is in close proximity to the choroid plexus which is the major route of substance exchange between the systemic blood and the brain through the cerebrospinal fluid (CSF) (reviewed in (Falcao et al., 2012)). Therefore, the SVZ is ideally located to study the impact of systemic immune activation on neurodevelopmental cells.

1.4.1 Adult SVZ neurogenesis

The mammalian brain contains two sites which continuously produce new neurons into adulthood; the subventricular zone (SVZ) lining the lateral ventricle and the subgranular zone (SGZ) of the hippocampal dentate gyrus (fig. 1.6A, reviewed in (Alvarez-Buylla and Lim, 2004)). Neuroblasts generated in the SGZ only move a short distance to the granular cell layer where they differentiate into dentate granular cells (Cameron et al., 1993). However, newborn cells in the SVZ travel long distances via the rostral migratory stream (RMS) into the olfactory bulb (OB) where they differentiate into periglomerular or granule cells, both of which are local interneurons (fig.1.6A) (Doetsch and Alvarez-Buylla, 1996). As shown in figure 1.6B, the SVZ is a neurogenic layer that lines the lateral ventricle and multiciliated ependymal cells (E) separate the SVZ from the circulating cerebrospinal fluid (CSF). The SVZ niche contains multiple cell types (type B, C and A-cells), which also include microglia, the primary immune cells of the brain. Type B cells have astrocytic characteristics and are subdivided into type B1 and B2 cells. Type B1 cells have direct contact with the lateral ventricle (LV) and act as self-renewing neural stem cells whereas type B2 cells do not maintain direct contact with the LV and act as niche astrocytes. Type B1 cells give rise to progenitor or type C-cells that actively divide and give rise to immature neuroblasts (i.e. type-A cells) that migrate to the OB (reviewed in (Ihrie and Alvarez-Buylla, 2011, Ihrie and Alvarez-Buylla, 2008)).

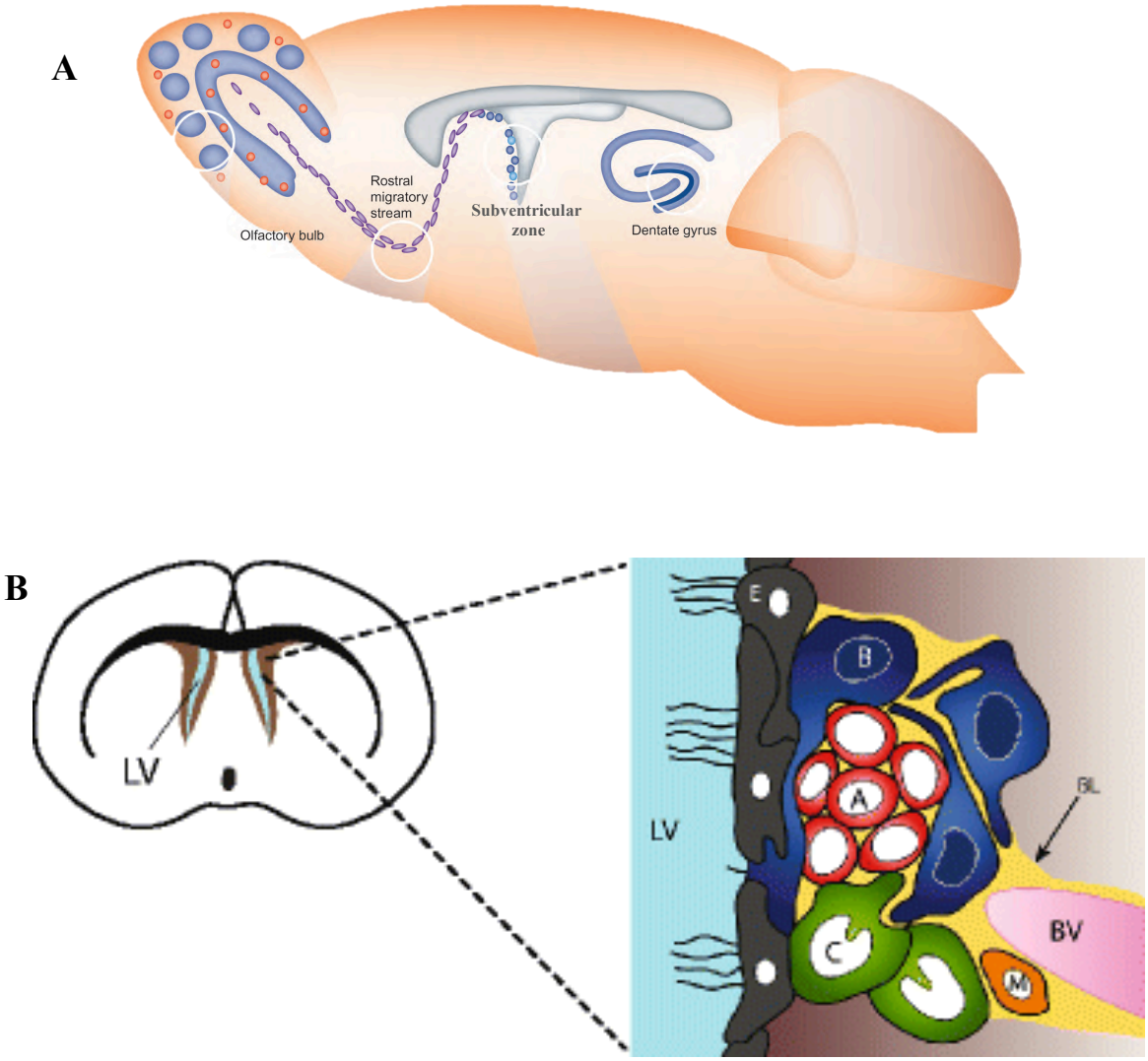

Figure 1.6 Morphology of the subventricular zone (SVZ) in adult mouse brain

(A) Sagittal view of mouse brain illustrating the SVZ, rostral migratory stream and olfactory bulb.

(B) The SVZ lines the lateral ventricle (LV) as shown in the coronal section (left). The SVZ neurogenic niche (right) is made up of astrocyte-like neural stem cells (type B-cells) that give rise to rapidly dividing type C-cells which then give rise to immature neuroblasts or type A-cells. The SVZ cells make contact with microglia (M), blood vessels (BV) and basal lamina (BL). The multiciliated ependymal cells (E) separate the SVZ region from the cerebrospinal fluid (CSF).

Image (A) adapted from Gerd Kempermann and Abcam; http://docs.abcam.com/pdf/neuroscience/adult_neurogenesis.pdf. Image (B) adapted from (Ihrie and Alvarez-Buylla, 2008).

1.4.2 Relevance of SVZ neurogenesis to schizophrenia

Current work on adult neurogenesis has either: 1) studied SVZ neurogenesis in neurological but not neuropsychiatric disease; or 2) studied hippocampal but not SVZ neurogenesis in neuropsychiatric disease. For example, Alzheimer's disease, Huntington's disease and multiple sclerosis were all found to activate SVZ stem cells and enhance neurogenesis and migration towards lesions (Curtis et al., 2003, Jin et al., 2004, Nait-Oumesmar et al., 2007). On the other hand, hippocampal neurogenesis was shown to decrease in schizophrenic patients (Reif et al., 2006) and mice that were deficient in hippocampal neurogenesis were more susceptible to depression (Snyder et al., 2011).

Therefore, no study has looked directly at the SVZ neurogenesis in neuropsychiatric disease. As listed below, there are several reasons the SVZ is relevant to schizophrenia.

1) <u>Antipsychotic drugs enhance adult neurogenesis in the SVZ.</u>

SVZ neurogenesis was shown to be enhanced in adult rats when treated with either typical (i.e. haloperidol) (Kippin et al., 2005) or atypical (i.e. olanzapine or risperidone) (Wakade et al., 2002) antipsychotic drugs. Moreover, an increased number of newly generated cells were also detected in the prefrontal cortex (PFC) in animals treated with olanzapine (Wang et al., 2004). This is interesting because it suggests that these new cells in the PFC might have migrated from the neurogenic SVZ and hence suggests a role of the SVZ in mediating cognitive function in schizophrenia.

2) Specific SVZ-cell types express dopamine receptors that are involved in schizophrenia.

The dopaminergic system becomes hyperactivated in schizophrenia and antipsychotic drugs act to lower this hyperactivation by antagonizing dopamine receptors. Interestingly, dopamine receptors are also expressed by the neural stem cells (NSCs) in the SVZ, which suggests a direct link between neural activity and NSC proliferation. Interestingly, a study showed this link by specific antagonism of dopamine 2 receptor (D2R) and found increased NSCs proliferation (Kippin et al., 2005). Furthermore, another study found that *in vivo* antagonism of dopamine 3 receptor (D3R) decreased proliferation of progenitor cells in the SVZ and also decreased the number of neuroblasts reaching the OB (Kim et al., 2010). Together, these studies illustrate how SVZ neurogenesis can be modulated by the dopaminergic system, and this system is dysregulated in schizophrenia.

3) The size of the lateral ventricle changes in the brain of schizophrenic patients.

Since the SVZ is a neurogenic layer that lines the lateral ventricle, abnormal changes in the lateral ventricle would be expected to cause cytoarchitectural or neurogenic abnormalities in the SVZ. Surprisingly, only one study to date has examined the SVZ cytoarchitecture in schizophrenia, although no apparent differences were detected in their cohorts (Comte et al., 2012). Studies have extensively characterized the changes in the size of the lateral ventricle before and after antipsychotic treatment. Drug-naïve schizophrenic patients show an increase in the size of the lateral ventricles (Rais et al., 2012) but a decrease in the striatal (Shihabuddin et al., 1998), caudate (Keshavan et al., 1998, Corson et al., 1999),

whole-brain and cortical volumes (Joyal et al., 2002, Rais et al., 2012) (also reviewed in (Torrey, 2002)). Interestingly, these morphological changes are abolished after chronic treatment with antipsychotic drugs which induce less ventricular enlargement (DeLisi et al., 1997, Lieberman et al., 2001) but an increase in the striatal (Shihabuddin et al., 1998, Chakos et al., 1998), subcortical (i.e. putamen, caudate and thalamic) (Gur et al., 1998) and cortical volumes (DeLisi et al., 1985). A number of studies have suggested that these reversible effects of antipsychotic drugs in brain morphology might be due to the increase in neuronal size (Kerns et al., 1992, Benes et al., 1985) and synapse numbers (Meshul and Casey, 1989, Uranova et al., 1991) or might be due to the induction of NSC proliferation in the SVZ (Kippin et al., 2005, Wakade et al., 2002) and striatum (Wang et al., 2004). Taken together, ventricular enlargement in schizophrenia prior to treatment might lead to a decrease in SVZ neurogenesis; and the latter has not yet been shown.

4) The number of immature neurons is increased in the olfactory epithelium of schizophrenic patients.

Independent of medication, schizophrenic patients exhibit functional olfactory deficit (Moberg et al., 1999) that is correlated with a significant reduction in the size of the OB (Turetsky et al., 2000). This reduction in OB size might be due to decreased generation or migration of neuroblasts from the SVZ during development. However, in the peripheral olfactory epithelium (OE) the number of immature neurons was shown to increase in schizophrenia (Arnold et al., 2001) which might be due to the loss of healthy synaptic connections with the OB and hence resulting in accelerated OE turnover (Arnold et al., 2001, Arnold et al.,

1998). Taken together, structural or neurogenic abnormalities observed in peripheral (i.e. OE) and central (i.e. OB) olfactory systems might be due to disrupted SVZ neurogenesis.

1.5 Overall aims of the thesis

In my thesis, dysbindin-1 mutant (Sdy) mice were postnatally challenged with systemic polyI:C injections and were used as a model of GxE interaction in schizophrenia. For simplicity, the term "GxE" was used in the next chapters to refer to "dysbindin-1 mutation x polyI:C administration". As discussed earlier, polyI:C is an immune stimulant that induces Tlr3-RelA-Sp1 signalling pathway. Given that both Tlr3 and dysbindin-1 are subcellularly localized in endosomes, this might suggest possible functional interactions between the two proteins. Therefore, one aim of this thesis was to address whether genetic mutation in schizophrenia-related dysbindin-1 might directly influence Tlr3-RelA-Sp1 signalling pathway. This would provide insights into how genetic and environmental risk factors of schizophrenia may interact with each other at the molecular level. Also, another aim of this thesis was to investigate the impact of the GxE interaction on SVZ proliferation, microglia/macrophages, cytokine release as well as behavioural outcomes in adulthood. Together, these aims would provide a link for how GxE interaction at the molecular level might be reflected at the cellular level, and also more broadly at the behavioural level. A summary of the aims of this thesis is shown below in figure 1.7.

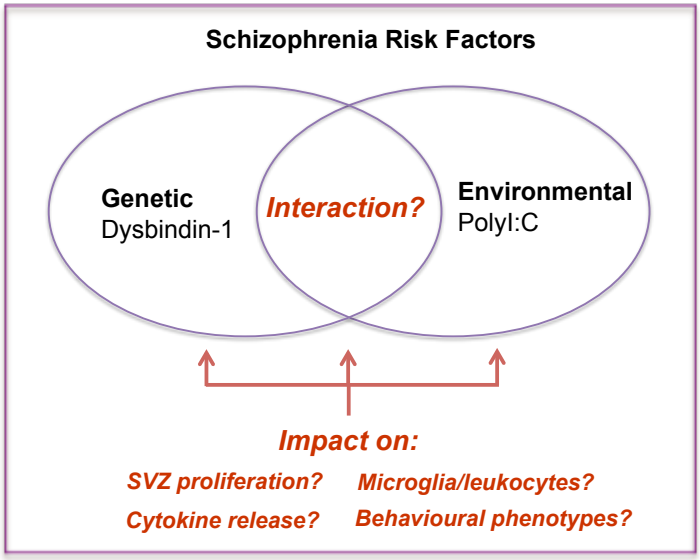

Figure 1.7 Summary of overall aims of my thesis

Chapter 2

Materials and Methods

2.1. Animals

Three mouse models of schizophrenia were studied: 1) Transgenic mice overexpressing Nrg1 type I ($NRG1^{typeI\text{-}tg}$), 2) Snap25 mutant ($SNAP25^{+/-}$) mice and 3) Dysbindin-1 mutant or Sandy (Sdy) mice. Adult $NRG1^{typeI\text{-}tg}$ and wild-type (WT) mice were obtained from Dr. Karri Lamsa's laboratory (Oxford University - Department of Pharmacology). All $NRG1^{typeI\text{-}tg}$ and WT mice (N=4 per group) were at postnatal day 60 (P60) with mixed gender in the background strain C57BL/6. Adult $SNAP25^{+/-}$ and WT mice (N=3 per group) were obtained from the laboratory of Prof. Kay Davies (Oxford University - DPAG) in which all mice were females at P60 in the background strain C3H.

For postnatal Sdy experiments, heterozygous breeding mice in the C57BL/6J background strain were obtained from Professor Lalit Srivastava's Laboratory (McGill University). For colony maintenance, heterozygotes were crossed to generate WT, Sdy and heterozygous mice. In order to obtain enough number of pups for *in vivo* and *in vitro* experiments, (WT x WT) and (Sdy x Sdy) breeding pairs were set up in which all these breeding pairs were direct progeny from heterozygotes. All animals were maintained in individually ventilated cages at the University of Oxford animal housing facility on 12-hour light/dark cycle with unlimited access to chow and water. Procedures were carried out with University of Oxford Research Ethics Committee approval, in accordance with the Animals (Scientific Procedures) Act of 1986 (UK). All efforts were made to minimize animal suffering and distress.

2.2. PolyI:C administration

Postnatal Sdy and WT pups were intraperitoneally (i.p.) injected with normal saline (0.9% NaCl, Aqupharm 01300101) or polyI:C (Invivogen tlrl-pic, 1mg/ml stock solution in supplied 0.9% NaCl) from P5 to P9 (five injections, once daily) in a dose of 5mg/kg. All i.p. injections for postnatal Sdy and WT mice that were used in adulthood experiments were carried out by Dr. Sanjeev Bhardwaj from Professor Srivastava's lab (McGill University). I have carried out all i.p. injections for postnatal Sdy and WT mice that were used in postnatal experiments.

2.3 Genotyping

The genotype of WT, heterozygous and Sdy mice from heterozygous breeding pairs was determined by analyzing DNA samples from mouse earclips. For DNA extraction, E.Z.N.A Tissue DNA Kit (Omega Bio-tek D3396-02) was used and eluted DNA samples (50µl) were stored at -20°C until use.

For polymerase chain reaction (PCR) amplification, 4µl DNA sample was added to 21µl reaction mixture (table 2.1) to make a final reaction volume of 25µl. The primers for WT gene were as follows: forward-WT (50-TGAGCCATTAGGAGATAAGAGCA-30) and reverse-WT (50-AGCTCCACCTGCTGAACATT-30) yielding a PCR product of 472 base pairs (bp). The primers for Sdy gene were: forward-Sdy (50-TCCTTGCTTCGTTCTCTGCT-30) and reverse-Sdy (50-CTTGCCAGCCTTCGTATTGT-30) yielding a PCR product of 274bp. The reaction mixture was run in the following PCR programme: 95°C for 5

min followed by 35 cycles of denaturation at 95°C for 20 sec, annealing at 56°C for 20 sec and elongation at 72°C for 30 sec, then a final elongation at 72°C for 5 min and the reaction was stopped at 4°C. The amplified PCR products were stored at -20°C until separated by gel electrophoresis.

Table 2.1 Components of PCR reaction mixture for genotyping

Component	Amount	Final concentration	Catalog number
10X PCR buffer	2.5µl	1X	Invitrogen 10966-026
10mM 2'-deoxynucleoside 5'-triphosphate (dNTP) mix	0.5µl	0.2mM	Invitrogen 18427-013
50mM magnesium chloride ($MgCl_2$)	1.04µl	2.08mM	Invitrogen 10966-026
Platinum *Taq* DNA polymerase	0.2µl	---	Invitrogen 10966-026
Nuclease-free water (H_2O)	16µl	---	Qiagen 129114
10µM of each of four primers (forward-WT, reverse-WT, forward-Sdy and reverse-Sdy)	4 x 0.25µl	100nM	Custom designed primers from Invitrogen

For gel electrophoresis, a gel was made which consisted of 100ml of 1X TAE (Tris-acetate-EDTA) buffer (recipe in Appendix), 2g agarose (Sigma A9539) to make 2% agarose and 5µl of 10mg/ml ethidium bromide (Sigma E1510) for a final concentration 0.5µg/ml. In order to determine size of PCR products, 8µl of 100bp DNA ladder (Bio-labs N0467S) was loaded into the solidified gel submerged in 1X TAE running buffer. The 25µl PCR products were mixed with 5µl of 6X Gel Loading Dye (Bio-labs B7021S) and 20µl of total mixture was loaded into the gel. Samples were run at 120V for about 30 minutes using PowerPac Basic power supply (Bio-rad

1645050). Under ultraviolet light, a single band is detected in WT (size 472bp) and Sdy (size 274bp) mice whereas two bands are detected in heterozygous (HET) mice (sizes 472 and 274bp). An example is shown below in figure 2.1.

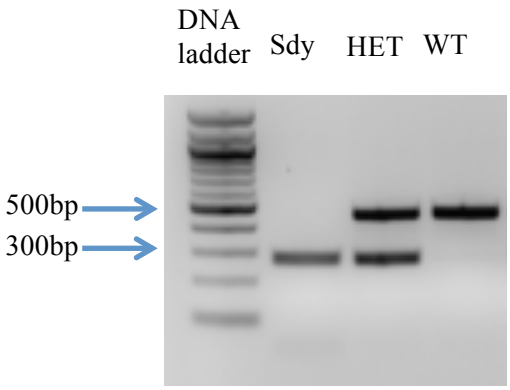

Figure 2.1 Example of a genomic PCR result for mice in Sdy colony

2.4 Perfusion and tissue preparation

Mice were deeply anaesthetized with an overdose of 0.1ml i.p, injection of pentobarbitone (200mg, Oxford University Veterinary Services 12122457) and transcardially perfused with ice cold 0.9% normal saline via 27G Winged Needle Infusion Set (BD Biosciences 12349189) followed by ice-cold 4% paraformaldehyde (PFA, recipe in Appendix). Brains were carefully dissected out of the skull and post-fixed for 24 hours in 4% PFA at 4°C followed by cryoprotection for 3-4 days in 30% sucrose at 4°C (Recipe in Appendix). Brains were snap-frozen using dry ice and then kept at -80°C until use. Perfusions of adult NRG1$^{typeI\text{-}tg}$ and WT mice (N=4 per group) were done with a kind help from Dr. James Hillis (former member of Szele Group). Adult SNAP25$^{+/-}$ and WT mice (N=3 per group) were kindly perfused by Dr. Peter Oliver (Oxford University - DPAG). Adult Sdy and WT mice that were postnatally

injected with saline or polyI:C (four groups, N=6 per group) were perfused by Dr. Sanjeev Bhardwaj from Professor Srivastava's lab (McGill University). All Sdy and WT mice were adult males at the age of ~12-14 weeks when perfused.

2.5 Microtome sectioning

Sliding microtome (Leica SM2000R) was used to cut frozen brains into 30μm coronal sections. Frozen brains were first mounted onto a frozen stage with 0.1M phosphate buffer (PB, pH7.2) then serially cut and placed as free-floating sections in cryoprotectant in 48-well plates and stored at -20°C (Recipe for PB and cryoprotectant in Appendix). The mouse brain stereotaxic atlas by Franklin & Paxinos (2001) was used as a reference for determining the coronal coordinates of the brain regions (Franklin and Paxinos, 2001). The sections collected from the OB correspond to figures 1-9 of the atlas, which are 4.28 to 2.58mm relative to bregma. The RMS sections correspond to figures 10-15 (2.46 to 1.94mm to bregma), SVZ (figures 22-38, 1.10 to -0.82mm to bregma) and hippocampus (figures 39-53, -0.94 to -2.70mm to bregma). For postnatal brains, sections were collected from the OB, RMS and SVZ, and for each region they were placed in a serial order into 6-wells of 48-well plate. This was also done for adult brains, however sections per region were serially placed into 8-wells of 48-well plate and hippocampal regions were also collected. This sectioning method resulted in a minimum of three sections per well for each brain region. Identification of stereotaxic coordinates was confirmed under a dissecting microscope.

2.6 Fluorescent immunohistochemistry

In all immunohistochemistry, a minimum of three animals was used per experimental group. Also, a minimum of three sections per animal was used in which all sections were within same Bregma regions (see section 2.5). Immunohistochemistry was carried out in two days in which all room temperature washes and incubations were performed on a shaking platform whereas overnight incubations on an orbital shaker. On day one, free-floating sections were placed within porous well inserts (Sigma CLS3477) in 12-well plates and were washed 3 times for 10 min in 0.1M phosphate buffer saline (PBS pH7.4, recipe in Appendix). This was followed by 15 min incubation in 50mM glycine in PBS to minimize auto-fluorescence and then sections washed again in PBS (3 times, 10min) before blocking for 1 hour in PBS+ (i.e. 10% donkey serum (Bio-Rad C06SBZ) and 0.1% Triton (Sigma X-100) diluted in PBS). Primary antibodies from different species (table 2.2) were diluted in PBS+ and sections were incubated in the diluent overnight at 4°C on a constant rocker.

On day two, sections were washed in PBS (3 times, 10 min) and were incubated for 1 hour in secondary antibodies (table 2.2) diluted in PBS+ (all 1:500 dilution) that matched the host species of the primary antibodies. This was followed with PBS washes (3 times, 10 min) and sections were then incubated in DAPI (1:1000 dilution in PBS) for 10 min for nuclear staining (DAPI: 4′,6-diamidino-2-phenylindole dihydrochloride, MP Biomedicals 0215757450, stock 10mg/ml). Finally, sections were rinsed 3 times, 10 min in PB and were mounted with FluorSave reagent (Calbiochem-Merck 345789) and coverslipped. No primary control was performed in all immunohistochemistry experiments.

Table 2.2 List of primary and secondary antibodies for immunohistochemistry

Primary antibodies	**Dilution of primary antibodies**	**Manufacturer and catalogue number of primary antibodies**	**Secondary antibodies**
Rabbit anti-Phosophistone-3 **(PHi3)**	1:400	Millipore 09-797	Donkey anti-Rabbit Alexa Fluor 488 (life technologies A21206)
Goat anti-Doublecortin **(Dcx)**	1:100	Santa-Cruz sc-8066	Donkey anti-Goat Alexa Fluor 568 (life technologies A11057)
Goat anti-Ionized calcium-binding adapter molecule 1 **(Iba1)**	1:200	Abcam ab5076	Donkey anti-Goat Alexa Fluor 568 (life technologies A11057)
Rat anti-Cluster of differentiation 45 **(CD45)** Also known as leukocyte common antigen (LCA).	1:200	Millipore 05-1416 (clone IBL5/25)	Donkey anti-Rat Alexa Fluor 647 (Abcam ab150155)
Rabbit anti-Cluster of differentiation 68 **(CD68)** Also known as macrosialin	1:400	Abcam ab125212	Donkey anti-Rabbit Alexa Fluor 488 (life technologies A21206)
Rabbit anti-Toll-like receptor 3 **(Tlr3)**	1:400	Abcam ab62566	Donkey anti-Rabbit Alexa Fluor 568 (life technologies A10042)

2.7 Microscopy and quantification

In all experiments, slides were coded and were quantitatively or qualitatively analyzed by a blinded investigator. A minimum of three sections per animal was used in all immunohistochemical analysis and all sections were within same Bregma regions (see section 2.5). In all experiments, only cells that showed clear nuclear DAPI+ staining were included for analysis. In adult SVZ and RMS, quantification of PHi3+ cells was performed straight under the epifluorescence microscope (Leica

DMIRB) using 40X objective lens. For quantifying Dcx+ cells in adult RMS, images were acquired using Openlab software (Improvision) with a digital camera (Hamamatsu C4742-95) and the surface area occupied by a population of Dcx+ cells was measured using the lasso selection tool. Representative images for analyzed PHi3+ cells in adult SVZ as well as Dcx+ cells in adult RMS were obtained using Zeiss LSM 710 laser scanning confocal microscope.

In postnatal SVZ, co-localization analysis of PHi3+/Dcx+ cells as well as Iba1+/CD68+/CD45+ cells was performed by taking 20X tile-scan confocal images that covers whole SVZ region. By using ImageJ programme, total PHi3+ cells as well as co-labelled PHi3+/Dcx+ cells were quantified in whole SVZ (fig. 2.2) whereas quantification of total Iba1+ cells and Iba1+/CD68+/CD45+ co-labelled cells was only done in dorsal SVZ (fig. 2.2). For postnatal Tlr3 immunohistochemistry, confocal images were taken of dorsal SVZ using 40X oil immersion objective lens and images were qualitatively analyzed using ImageJ. Figures for immunohistochemitry experiments was generated using ImageJ (version 2.0.0) or Adope Photoshop Elements Organizer (version 12.0).

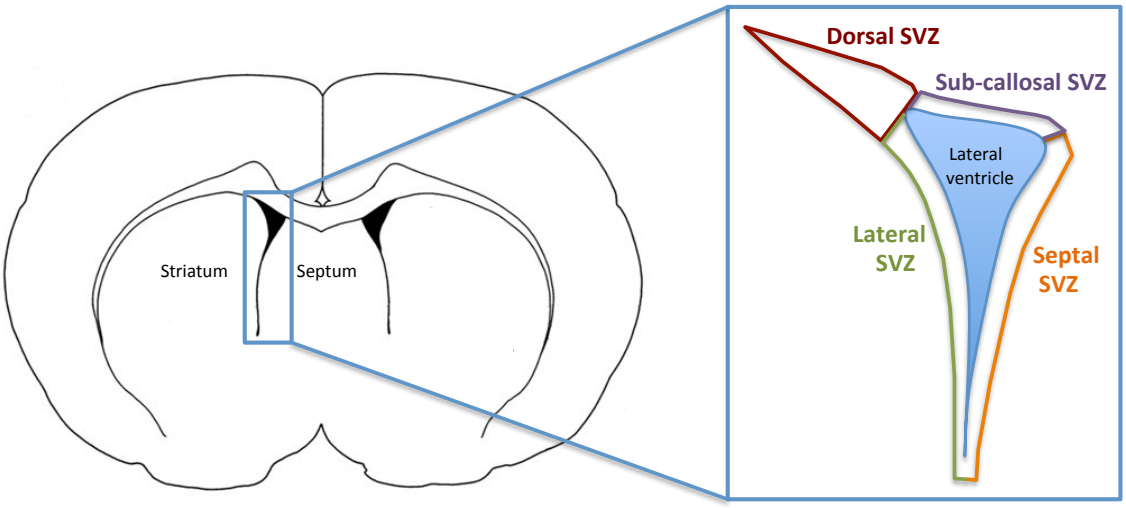

Figure 2.2 Subventricular zone (SVZ) subdivisions

Coronal slices of mouse brains were used for immunohistochemistry (IHC), neurosphere culture and *in vivo* RT-qPCR, *left.* For IHC, cells were quantified either in dorsal SVZ only or in whole SVZ subregions, *right.* For neurosphere culture and *in vivo* RT-qPCR, lateral and septal SVZ were microdissected, *right.*

2.8 Neurospheres culture

Postnatal 5 days old pups were anaesthetized by cooling followed by decapitation and whole brains were dissected out and sectioned into 0.5mm coronal slices using neonatal mouse brain slicer matrix (Zivic instruments BSMNS005-1). Under sterile laminar flow hood, both lateral and septal SVZ were microdissected (fig. 2.2) in ice-cold Advanced DMEM (Dulbecco's Modified Eagle Medium, Gibco) and were pooled together from N=2-5 per group. SVZ tissues were briefly centrifuged; aspirated supernatant and tissues were dissociated into single cells by incubation in 1ml accutase solution (Sigma A6964) for about 10 min with gentle pipetting up and down. This was followed with two washes in neurobasal A+ (table 2.3),

centrifugation and supernatant aspiration before resuspending cell pellets in neurobasal A+ with growth factors as listed in table 2.4. Cells were counted using haemocytometer, plated at a density of 100,000 cells/ml in 6-well plates (2ml/well) and incubated at 37°C and 5% CO_2. In order to avoid neurospheres adhesion to the wells, the 6-well-plates were coated with 1.2mg/ml poly-HEMA (poly(2-hydroxyethyl methacrylate), Sigma P3932) in 95% ethanol and were allowed to air dry inside sterile laminar hood before use. The poly-HEMA stock solution (12mg/ml) was prepared by dissolving 3g of poly-HEMA in 250ml of 95% ethanol. Neurospheres were dissociated with fresh media every fourth day. Tertiary passaged neurospheres were used for real-time quantitative PCR (RT-qPCR) whereas quaternary passaged cells were used for nucleofection or proteome array.

Table 2.3 Components of neurobasal A+

Component	Amount	Final concentration	Catalog number
Neurobasal A media 1X	480mL	1X	Gibco 10888-022
B27 supplement 50X	10mL	1X	Gibco 17504
Glutamax 100X	5mL	1X	Gibco 35050-038
Penicillin/Streptomycin 100X	5mL	1X	Gibco 15070-063

Table 2.4 Components of neurobasal A+ with growth factors

Component	Amount	Final concentration	Catalog number
Neurobasal A+ (see table 2.3)	25mL		
Basic Fibroblast growth factor (bFGF) (100µg/ml)	5µl	20ng/ml	R&D Systems 3139-FB-025
Epidermal growth factor (EGF) (100µg/ml)	5µl	20ng/ml	Sigma E4127

2.9 Nucleofection

Sdy neurospheres after quaternary passage were nucleofected with either sterile H_2O (mock) or Dtnbp1 gene in sterile H_2O (OriGene MR205351, distrubutor AMSBIO, fig. 2.3) according to the protocol of Nucleofector Kit for Moue Neural Stem Cells (LONZA VPG-1004). A total of $1x10^6$ dissociated cells were mixed with nucleofector solution plus supplement and were nucleofected with either 2µg Dtnbp1 gene in 4µl sterile H_2O or only 4µl sterile H_2O (Mock) using Nucleofector Device (LONZA). Nucleofected cells were immediately transferred into one-well in poly-HEMA coated 12-well plates (i.e. separate well per condition) that contained culture medium (final volume 1ml/well) and incubated at 37°C and 5% CO_2.

After 24 hours, neurospheres were suspended in fresh culture medium and each sample (Dtnbp1 or Mock nucleofected) was split into two wells (0.5ml/well) in poly-HEMA coated 24-well plates in which either pre-warmed saline or polyI:C (50µg/ml) was added. This experimental design worked as "within wells control" and therefore any detected response is likely due to treatment itself and not due to variation in cell populations. Neurospheres were incubated at 37°C and 5% CO_2 for 3 hours before use in RT-qPCR.

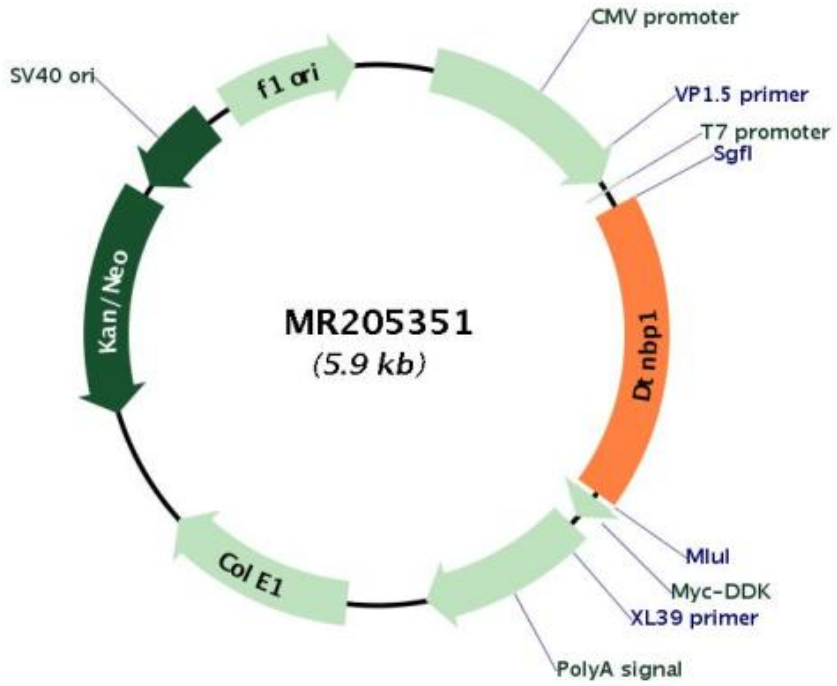

Figure 2.3 Plasmid map for Dtnbp1 mouse cDNA clone that was use for nucleofection experiments

2.10 Real-time quantitative PCR (RT-qPCR)

For *in vivo* experiments, postnatal littermates (N=3 per group) were repeatedly i.p. injected with saline or polyI:C (as described in section 2.2). At P12, they were deeply anesthetized with an overdose of pentobarbitone (0.05ml, i.p.) and brains were dissected out and coronally sliced into 0.5mm slices using young mouse brain slicer matrix (Zivic instruments BSMYS005-1). Both lateral and septal SVZ were microdissected and SVZ tissues (N=3 per group) were pooled together and snap-frozen in dry ice and kept at -80°C until use. According to manufacturer instructions,

total RNA samples were purified using RNeasy Mini Kit (Qiagen 74104) in which tissues were disrupted using Eppendorf micropestle (Sigma Z317314), lysates were homogenized using QIAshredder spin columns (Qiagen 79654) and DNA was removed with on-column DNase digestion set (Qiagen 79254). Equal amount of RNA samples per experiment were reverse transcribed into cDNA using High-Capacity RNA-to-cDNA Kit (Applied Biosystems 4387406). For RT-qPCR, cDNA samples were mixed with TaqMan gene expression master mix (Applied Biosystems 4369016) and TaqMan gene expression assays listed below. In all experimental groups, 100ng cDNA was used for all genes (except the highly abundant Rn18S in which only 10ng cDNA was used). For *in vitro* experiments, neurosphere samples (see section 2.8 and 2.9) were processed using Cells-to-CT 1-Step TaqMan Kit (Ambion A25603) in which 1.5µl cell lysates was used for all genes.

The following inventoried TaqMan gene expression assays (Applied Biosystems) were used for both *in vivo* and *in vitro* experiments: Target genes Dtnbp1 (Mm00458743_m1), Tlr3 (Mm01207404_m1), RelA (Mm00501346_m1) and Sp1 (Mm00489039_m1) whereas housekeeping genes β-actin (Mm00607939_s1) and ribosomal 18S (Rn18S) (Mm03928990_g1). All experiments were run in 20µl reaction volumes in 96-well plates (Applied Biosystems 4346906) that were carefully sealed with adhesive film (Applied Biosystems 4311971) before using StepOnePlus Real-Time PCR System (Applied Biosystems 4376600). Standard cycling conditions were run according to manufacture's protocol for each reagent (i.e. here used Applied Biosystems protocol number (4371134) for *in vivo* experiments and Ambion protocol number (MAN0010751) for *in vitro* experiments). All measurements were performed

in duplicates in which mean values of mRNA levels of the target genes were normalized to the geometric mean of β-actin and Rn18S (Vandesompele et al., 2002) and relative gene expression of treated to non-treated controls per experiment was calculated using the $2^{-\Delta\Delta Ct}$ method (Livak and Schmittgen, 2001). No-template control was also run for each gene tested in all experiments to ensure no contamination of the RT-qPCR reactions.

2.11 Mouse cytokine proteome array

WT and Sdy neurospheres were used after quaternary passage (as described in section 2.8). Each sample (e.g. WT) was divided into five wells in two separate poly-HEMA coated 6-well plates (i.e. total ten wells) at a density of 100,000 cells/ml (2ml/well) and incubated at 37°C and 5% CO_2. After 3 days, pre-warmed saline or polyI:C (50μg/ml) was added per sample (e.g. saline to five wells of WT saline group) and were incubated for 24 hours. Because saline or polyI:C treated neurospheres were originally derived from the same sample, this experimental design is to ensure that any detected response is likely due to the treatment itself and not due to variation in cell populations.

After 24 hours, supernatants (10ml per group) were harvested and concentrated in less volume (~260μl) using centrifugal filter unit of 3kDa molecular weight cut-off (Amicon UFC900324) to ensure maximal retention of even the smallest protein size. Recovered samples were then analyzed using Proteome Profiler Mouse Cytokine Array Kit, Panel A (R&D Systems ARY006) according to the manufacture's protocol. This immunoassay allows for simultaneous detection of 40

cytokines that include chemokines, interleukins and acute phase proteins. Capture antibodies to these target proteins are spotted in duplicates in a single array membrane. Briefly, supernatant samples were mixed with a cocktail of antibodies and incubated with array membranes overnight at 4°C on an orbital shaker. Membrane-bound proteins were then incubated with chemiluminescent reagents and were visualized using Odyssey Fc Imaging System (LI-COR) after 10 min exposure time. Captured images were analyzed using Image Studio Lite (Version 5.0.21) in which pixel intensity of each detected spot was subtracted from background pixel intensity, and the mean pixel intensity was then measured of each duplicate spots.

2.12 Behavioural tests

2.12.1 Spontaneous locomotor activity

The spontaneous locomotion tests were carried out in 20 Acrylic chambers (AccuScan Instruments, Columbus, OH, USA) with the following dimensions (L×W×H= 17.5×10×26 cm). The activity chambers were equipped with infrared sensors in order to assess locomotion and the data were collected using the Versamax Software (version 4.0, AccuScan Instruments). On the test day between 9:00am to 11:00am, mice were placed in the activity chambers in a dimly lit room and their activities were monitored for two hours. The total horizontal distance (cm) traveled per mouse in 10 min intervals was used for analysis.

2.12.2 Prepulse inhibition (PPI)

The PPI test was measured using the startle response system (SR-LAB, San Diego Instruments) consisting of multiple sound-attenuating cabinets, each equipped with a cylindrical animal enclosure and a small electric fan to provide ventilation and a background noise of 70 decibels (dB).

Animals were familiarized to the enclosure for 5 min before starting the tests. Animals were presented with noise pulses presented via a speaker placed directly above the animal. The animal motion in response to the noise was detected via an accelerometer attached to the frame of the animal enclosure. The SR-LAB software was used to record the animal responses and also to control the noise pulse parameters.

Animals were first habituated to a startle (main) pulse of 120 dB in two trials (not included in analysis) followed by subsequent 40 trials in which the startle response to the main pulse was measured and analyzed. The main pulse was either presented alone or 100 milliseconds (ms) following prepulses of 30 ms duration with intensities of 3, 6, 9, 12 and 15 dB above the background noise. These prepulse intensities varied randomly between trials and each prepulse was presented five times. The average interval between trials was 15 seconds (s) (range 5-30 s). Animals were also presented with a startle pulse alone in another 10 trials. The startle responses were automatically determined by SR-LAB software. The percent PPI was calculated in the following formula: %PPI = [100 - (startle response to prepulse and pulse trials) ÷ (startle response to pulse alone trials) * 100].

2.12.3 Object recognition

An open-field chamber made of dark Plexiglas was used for the test. In a quiet room, mice were individually placed in this chamber (L×W×H: 45×45×45 cm) for 20 min each day for 3 days with two identical objects (toys, Dollar Store) in order to acclimatize them with the test environment. On the test day, the mice were placed in the chamber and allowed to explore two new identical objects for 5 min (familiarization phase), and were then placed back into their home cage for 5 min (retention time). During this time, the objects in the chamber were replaced with two new objects in which one of them had an identical shape to the objects used during the familiarization phase while the other had a novel shape. Finally, the mice were placed in the chamber and were allowed to explore the objects for 3 min (testing phase).

The behavioural activities of mice were videotaped during both the familiarization and testing phases and were and analyzed by investigators blinded to the genotype. The time was only calculated if a mouse was involved in object exploration based on the following criteria: 1) the mouse head was leaning towards the object and only within 2-3 cm away from it; 2) the mouse had at least one forepaw on the object and/or was sniffing or licking the object. Rodents naturally tend to explore novel than familiar objects in their environment. Therefore, object recognition memory was evaluated based on the increased time a mouse spent to explore a novel (TN) than a familiar (TF) object. This was determined using the following formula [Exploration ratio = TN ÷ (TF + TN)], in which a value significantly different from 0.5 (chance level) reveals the level of the recognition memory.

2.13 Statistics

Data were analyzed using GraphPad Prism (version 7.0a). Student's t-test was used to analyze differences between two groups. Two-way analysis of variance (ANOVA) was used to analyze two or more groups with two independent variables, and was followed by Tukey's multiple comparisons test where appropriate. Data were presented as mean ± standard error of the mean (SEM).

Chapter 3

Adult SVZ proliferation, migratory neuroblasts and behavioural abnormalities in GxE model of schizophrenia

3.1 Introduction

Schizophrenia has been widely associated with abnormality in neurochemical function (reviewed in (Harrison, 1999)). A number of neurotransmitters such as dopamine, glutamate and GABA have been shown to directly affect SVZ neurogenesis, and SVZ cells express receptors to these neurotransmitters (reviewed in (Young et al., 2011)). Schizophrenia related genes such as neuregulin-1 (Nrg1), Snap25 and dysbindin-1 (Dtnbp1) are functionally involved in regulating neurotransmission, suggesting that dysregulated expression of these genes may impact SVZ neurogenesis. Therefore, the aim of this chapter was to screen adult SVZ neurogenesis in three mouse models of schizophrenia: 1) Transgenic mice overexpressing Nrg1 type I ($NRG1^{typeI\text{-}tg}$), 2) Snap25 mutant ($SNAP25^{+/-}$) mice and 3) Dysbindin-1 mutant or Sandy (Sdy) mice (table 3.1). Specifically, I sought to address whether adult SVZ proliferation as well as RMS proliferation and migratory neuroblasts were affected in these three mouse models. In addition, I sought to find whether exposing one mouse model (here Sdy mice) to postnatal polyI:C injections (gene x environment (GxE) model) may further impact adult SVZ neurogenesis and the behaviour of these mice in adulthood.

3.1.1 Schizophrenia-related genetic models and adult SVZ neurogenesis

Since no perfect animal model exists for schizophrenia, I started my project by screening adult SVZ neurogenesis in three mouse models of the disease that are described below in table 3.1.

Table 3.1 Overview of three genetic mouse models of schizophrenia

	NRG1$^{typeI\text{-}tg}$ mice	**SNAP25$^{+/-}$ mice**	**Sdy mice**
Description	Neuregulin-1 (Nrg1) is a growth factor involved in neuronal migration (Flames et al., 2004), myelination (Brinkmann et al., 2008, Michailov et al., 2004) and neurotransmission (Stefansson et al., 2002). Nrg1 has many isoforms that are grouped into six different types (I-VI) (Mei and Xiong, 2008, Harrison and Law, 2006).	Snap25 is a presynaptic protein (25kDa) encoded by Snap25 gene. Snap25 protein belongs to the SNARE complex that is essential for synaptic release by fusing synaptic vesicles to plasma membranes (Jeans et al., 2007, Oliver and Davies, 2009). Two Snap25 isoforms (A & B) have been identified (Bark et al., 1995).	Dysbindin-1 protein (40-50kDa) is encoded by Dtnbp1 gene. Dysbindin-1 protein is involved in vesicle trafficking (Li et al., 2003), exocytosis (Chen et al., 2008) and synaptic signaling (Benson et al., 2001). Two isoforms (A & C) exist for murine dysbindin-1 protein (Talbot, 2009).
Mutation	Heterozygous overexpression of Nrg1-type I (β1a-isoform) under the control of murine Thy1.2 promoter (Michailov et al., 2004) with robust overexpression in various brain regions (Brinkmann et al., 2008, Deakin et al., 2009).	Dominant, missense mutation resulting in a single amino acid isoleucine-to-threonine substitution in codon 67 (I67T) in isoform-b of Snap25 protein. This impairs synaptic function although no reduction in Snap25 expression (Jeans et al., 2007, Oliver and Davies, 2009).	Autosomal recessive mutation (loss of amino acids 119–172) that abolishes expression of isoforms (A & C) of dysbindin-1 protein. Arose spontaneously in Jackson laboratory in 1983 (Swank et al., 1991).

Behaviour	Tremor or shaking behaviour, reduced prepulse inhibition (PPI), impaired on rotarod (Deakin et al., 2009) and working-memory deficit (Deakin et al., 2012).	Disrupted circadian rhythms (Oliver et al., 2012), reduced PPI, impaired sensorimotor gating and ataxia (Jeans et al., 2007). These endophenotypes are modulated by stress (Oliver and Davies, 2009).	Object-recognition deficit (Feng et al., 2008, Bhardwaj et al., 2009), impaired long-term memory (Takao et al., 2008), reduced PPI (Carlson et al., 2011), decreased locomotor activity (Hattori et al., 2008), reduced habituation to novelty (Bhardwaj et al., 2009, Cox et al., 2009) and social withdrawal (Feng et al., 2008, Hattori et al., 2008).
Relevance to schizophrenia	Expression of NRG1 type I isoform is elevated in the hippocampus (Law et al., 2006) and dorsolateral prefrontal cortex (DLPFC) (Hashimoto et al., 2004) of schizophrenic patients.	In humans, SNAP25 mutation is linked to schizophrenia (Lewis et al., 2003). Snap25 expression is decreased in the hippocampus (Thompson et al., 2003, Young et al., 1998) and frontal lobe (Thompson et al., 1998) of schizophrenic patients.	Dysbindin-1 expression is reduced in the hippocampus (Weickert et al., 2008) and DLPFC (Weickert et al., 2004) of schizophrenic patients.

Although mice deficient in dysbindin-1 are fully viable (Swank et al., 1991), knockout of Nrg1 type I is embryonic lethal (Kramer et al., 1996). Therefore, Sdy mice were used in order to model the loss of dysbindin-1 in schizophrenia whereas $NRG1^{typeI\text{-}tg}$ overexpressing mice were used to model the increase in Nrg1 type I expression in the disease.

On the other hand, Snap25 expression is unaltered in $SNAP25^{+/-}$ mice, although the Snap25 function is disrupted in this mouse model (Jeans et al., 2007). In addition to $SNAP25^{+/-}$ mice, there is a list of other Snap25 mutants such as homozygous and heterozygous Snap25 knockout mice (Washbourne et al., 2002),

Snap25^{Tkneo} mice (Bark et al., 2004) and SNAP-25 knock-in mice (Kataoka et al., 2011). The homozygous Snap25$^{-/-}$ knockout mice die embryonically (Washbourne et al., 2002) whereas a targeted homozygous mutation in Snap25^{Tkneo} mice that impairs the shift of Snap25 isoform A to isoform B results in premature mortality at around P21 to P35 (Bark et al., 2004). Although the heterozygous Snap25$^{+/-}$ mice are viable (Washbourne et al., 2002), studies are inconsistent in regards to the relevance of this model to schizophrenia at the neurochemical and behavioural level (Washbourne et al., 2002, Oliver and Davies, 2009, Corradini et al., 2014, Braida et al., 2016). In the SNAP-25 knock-in mice, a single amino acid Ser187 is replaced with Ala in Snap25 protein resulting in disrupted Snap25 phosphorylation (Kataoka et al., 2011). These SNAP-25 knock-in mice show behavioural and neurochemical deficits relevant to schizophrenia (Kataoka et al., 2011, Ohira et al., 2013).

In this study, SNAP25$^{+/-}$ mice were selected due to the limitation of studying homozygous Snap25 mutants in adulthood. The SNAP25$^{+/-}$ mice are fully viable and display phenotypic abnormalities relevant to schizophrenia as described in Table 3.1. In addition, SNAP25$^{+/-}$ mice carry a point mutation that affects the function of Snap25 isoform-b (Jeans et al., 2007), an isoform that is developmentally regulated and becomes predominantly expressed in the adult mouse brain (Bark et al., 1995). Therefore, SNAP25$^{+/-}$ mice were used to study the impact of disrupted Snap25 isoform-b in adulthood.

Adult SVZ neurogenesis *in vivo* has not been previously characterized in NRG1$^{typeI\text{-}tg}$, SNAP25$^{+/-}$ and Sdy mice. However, receptor tyrosine kinase (ErbB4) and its ligand Nrg1 were detected in PSA-NCAM+ immature neuroblasts in the SVZ and RMS, indicating they may mediate neuroblast migration (Ghashghaei et al., 2006, Anton et al., 2004). Nrg1 type I was demonstrated *in vitro* to regulate migration of SVZ cells in explant migration assays, and ErbB4-deficient mice showed disrupted neuroblasts migration to the RMS (Anton et al., 2004).

3.1.2 GxE model of schizophrenia and adult SVZ neurogenesis

In addition to the schizophrenia risk genes described above, environmental stimuli during early brain development may also increase the risk of developing schizophrenia in adulthood. For example, postnatal polyI:C injections in mice (i.e. inflammatory stimuli) was demonstrated to induce schizophrenia-like behaviours in adulthood (Ibi et al., 2009). Moreover, combining a mutation in DISC1 risk gene of schizophrenia with postnatal polyI:C injections further amplified behavioural abnormalities in adulthood (Ibi et al., 2010). Interestingly, polyI:C administration during embryonic development was previously shown to affect SVZ neurogenesis in adulthood (Liu et al., 2013). Therefore, I aimed here to characterize adult SVZ neurogenesis in response to a combination of postnatal polyI:C injections and dysbindin-1 mutation, and whether this GxE model may exhibit worsened behavioural phenotypes in adulthood.

3.1.3 Schizophrenia-related behavioural phenotypes in mice

Prepulse inhibition (PPI), novel object recognition and locomotor activity were tested in our GxE model of schizophrenia. The PPI test is commonly used to evaluate sensorimotor gating in both humans and mice (reviewed in (Braff and Geyer, 1990)). In schizophrenia, reduced PPI is a well-established endophenotype of the disease in which introduction to an auditory pre-pulse of variable intensities fails to inhibit the startle response when introduced to a subsequent pulse at a stronger intensity (reviewed in (Braff and Geyer, 1990)). Hence, PPI test was used to assess sensorimotor gating in our GxE model.

On the other hand, cognitive impairment is common in schizophrenia ((Elvevag and Goldberg, 2000)). In order to evaluate the cognitive function in our GxE model, a novel object recognition test was used. Mice have a natural tendency to explore novel objects in their surroundings. Therefore, mice were first familiarized with objects and then introduced to a novel and a familiar object, and the longer time they spent preferentially exploring novel rather than familiar objects was indicative of their cognitive ability in recognizing novel objects.

In schizophrenia, social isolation and depression represent the negative symptoms of the disease (Hafner et al., 1999). In mice, locomotor activity can be used as a sign of motivation and therefore reduced locomotion might indicate depressive-like behaviour (reviewed in (Maes et al., 2012)). Since polyI:C was given to our postnatal pups, it may induce sickness behaviour which is characterized by various symptoms that include reduced locomotion and weight loss (Cunningham et al., 2007). Therefore, locomotor activity and body weight were used as a measure of depressive-like and sickness behaviours in our GxE model of schizophrenia.

3.1.4 Research questions

Adult SVZ neurogenesis has not been previously studied in genetic mouse models of schizophrenia. Furthermore, adult neurogenesis in the SVZ, and even in the DG, has not been investigated in response to a combination of both postnatal inflammation and a risk gene for schizophrenia. Here, I focused on the adult SVZ to address the following questions:

1) Do mutations in genes relevant to schizophrenia affect proliferation in the SVZ and RMS?

2) Do mutations in genes relevant to schizophrenia affect migratory neuroblasts in the RMS?

3) Does a combination of both gene mutation and postnatal inflammation have a stronger effect than gene mutation alone in each of the following:

- SVZ and RMS proliferation.
- Migratory neuroblasts in the RMS.
- Behavioural outcomes.*

* These experiments were performed by our collaborator, Professor Lalit Srivastava's laboratory (McGill University).

In this study, I used the mitotic marker phosophistone-3 (PHi3) as a read-out for proliferation, whereas doublecortin (Dcx) was used as a marker for immature neuroblasts.

3.2 Results

3.2.1 Adult SVZ neurogenesis, RMS proliferation and migratory neuroblasts were not changed in NRG1$^{typeI\text{-}tg}$ overexpressing mice

Adult NRG1$^{typeI\text{-}tg}$ overexpressing mice were used in order to determine the effect of Nrg1 type I mutation in adult SVZ neurogenesis. There was no significant change in the number of proliferative (PHi3+) cells in the adult SVZ of NRG1$^{typeI\text{-}tg}$ overexpressing mice (Mean ± SEM= 31.73 ± 1.639) in comparison to WT mice (30.85 ± 2.654) as analysed using Student's two-tailed t-test ($t(6)= 0.2805$; N=4 per group; $P>0.05$; fig.3.1A). Similarly, the number of proliferative neuroblasts (PHi3+/Dcx+) cells in the adult SVZ was not significantly different between NRG1$^{typeI\text{-}tg}$ overexpressing mice (25.52 ± 1.310) and WT mice (24.02 ± 1.908) as determined using Student's two-tailed t-test ($t(6)= 0.6482$; N=4 per group; $P>0.05$; fig. 3.1B). Representative images are illustrated in figure 3.1 (C-D) showing PHi3+/Dcx+ cells in the SVZ of WT mice (fig.3.1C) and NRG1$^{typeI\text{-}tg}$ overexpressing mice (fig.3.1D). Taken together, adult SVZ neurogenesis was unaffected in NRG1$^{typeI\text{-}tg}$ overexpressing mice.

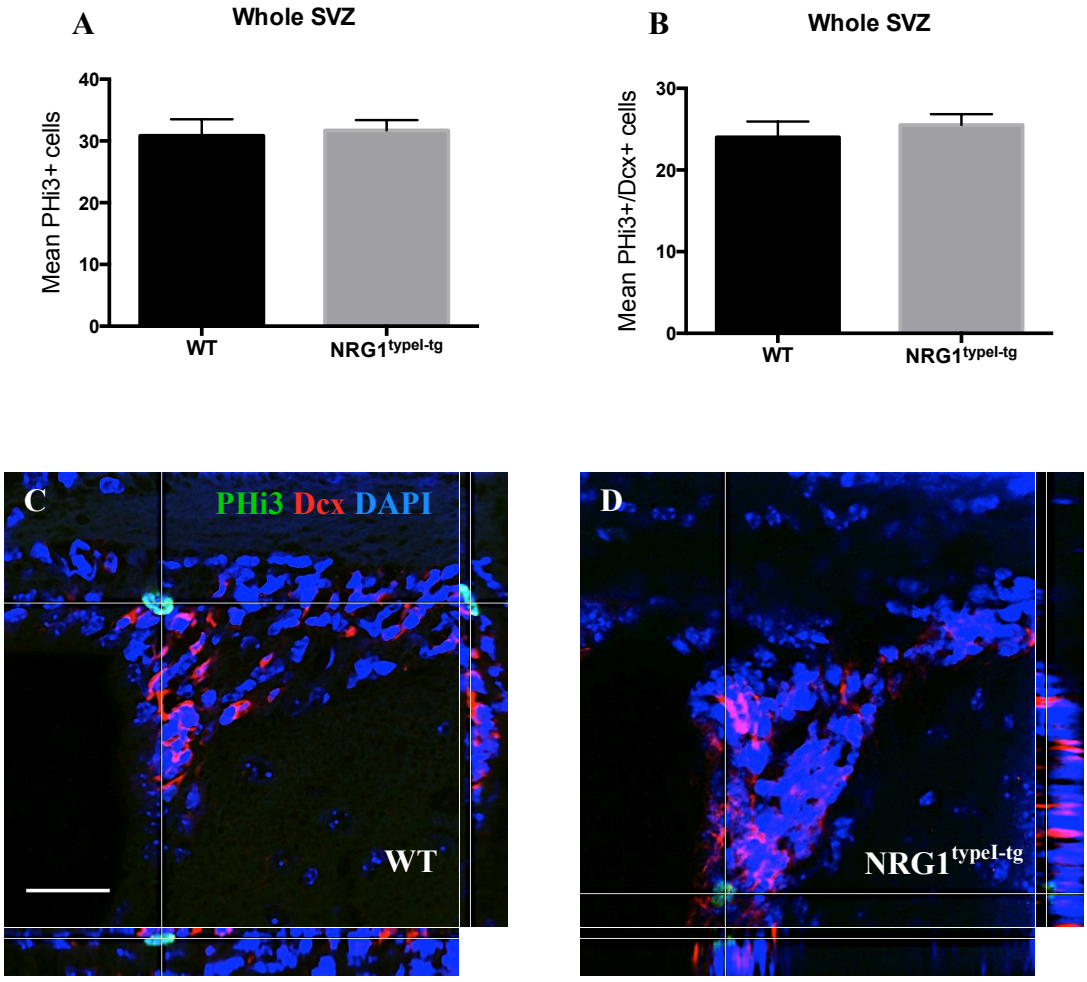

Figure 3.1 Adult SVZ neurogenesis in neuregulin-1 type I (NRG1$^{typeI-tg}$) overexpressing mice

(A-B) In the SVZ, there was no significant change in the number of proliferative (PHi3+) cells (A) or proliferative neuroblasts (PHi3+/Dcx+) cells (B) in NRG1$^{typeI-tg}$ overexpressing mice compared to WT mice.

(C-D) Representative orthogonal views showing PHi3+/Dcx+ cells in the SVZ of WT and NRG1$^{typeI-tg}$ overexpressing mice. Scale bar 25µm.

Mean ± SEM. N=4 per group. Data were analyzed using Student's two-tailed t-test. P>0.05.

Also, NRG1$^{typeI\text{-}tg}$ overexpressing mice were used in order to determine the impact of Nrg1 type I mutation on proliferation and migratory neuroblasts in the RMS. The number of proliferative (PHi3+) cells was not statistically different between NRG1$^{typeI\text{-}tg}$ overexpressing mice (Mean ± SEM= 7.678 ± 0.4741) and WT mice (6.940 ± 0.1957) in adulthood (Student's two-tailed t-test; t(6)= 1.438; N=4 per group; P>0.05; fig. 3.2C). In addition, the surface area occupied by the population of migratory Dcx+ neuroblasts was not significantly different in NRG1$^{typeI\text{-}tg}$ overexpressing mice (13,551 ± 361.7 μm^2) compared to WT mice (13,033 ± 1,234 μm^2) (Student's two-tailed t-test; t(6)= 0.4027; N=4 per group; P>0.05; fig. 3.2D). Representative images are shown in figure 3.2 (C-F') illustrating comparable migratory neuroblasts and proliferation in the RMS of WT mice (C-C'; E-E') and NRG1$^{typeI\text{-}tg}$ overexpressing mice (D-D'; F-F'). Hence, Nrg1 type I mutation did not impact proliferation and neuroblast population in the adult RMS.

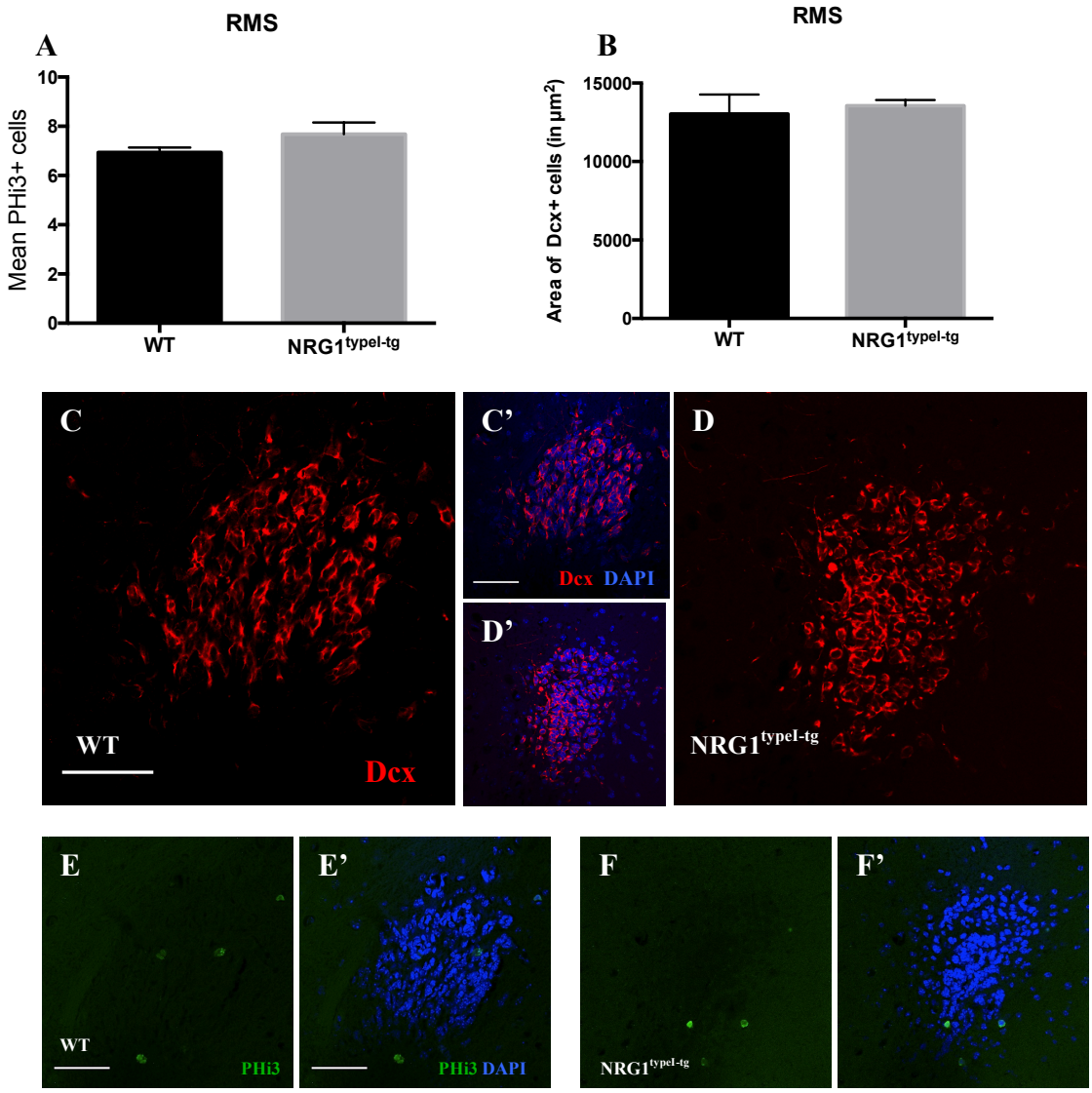

Figure 3.2 Adult RMS proliferation and migratory neuroblasts in neuregulin-1 type I (NRG1$^{typeI-tg}$) overexpressing mice

(A-B) In the RMS, no significant change was found in proliferation (A) or the average area of migratory neuroblasts (B) in NRG1$^{typeI-tg}$ overexpressing mice in comparison to WT mice.

(C-D') Representative images illustrating comparable populations of Dcx+ cells in the RMS of WT (C-C') and NRG1$^{typeI-tg}$ overexpressing (D-D') mice. Scale bar 25µm.

(E-F') Representative images showing similar number of proliferative (PHi3+) cells in the RMS of WT (E-E') and NRG1$^{typeI-tg}$ overexpressing (F-F') mice. Scale bar 25µm.

Mean ± SEM. N=4 per group. Data were analyzed using Student's two-tailed t-test. P>0.05.

3.2.2 SNAP25$^{+/-}$ mice were comparable to WT mice in adult SVZ proliferation, RMS proliferation and migratory neuroblasts

SNAP25$^{+/-}$ mice were used to find if the Snap25 mutation might affect adult SVZ proliferation. The number of proliferative (PHi3+) cells in the adult SVZ was not significantly different between SNAP25$^{+/-}$ mice (Mean ± SEM= 25.75 ± 2.222) and WT mice (21.50 ± 3.881) as analysed using Student's two-tailed t-test ($t(4)= 0.9503$; N=3 per group; $P>0.05$; fig. 3.3A). This suggested that adult SVZ proliferation was normal in SNAP25$^{+/-}$ mice.

Similarly, adult SNAP25$^{+/-}$ mice were used in order to determine the effect of Snap25 mutation in proliferation and migratory neuroblasts in the RMS. There was no statistical difference in the number of proliferative (PHi3+) cells in the adult RMS of SNAP25$^{+/-}$ mice (Mean ± SEM= 10.06 ± 1.399) compared to WT mice (7.867 ± 0.8293) as determined using Student's two-tailed t-test ($t(4)= 1.348$; N=3 per group; $P>0.05$; fig. 3.3B). Additionally, the surface area occupied by the population of migratory Dcx+ neuroblasts was comparable between SNAP25$^{+/-}$ mice (13,328 ± 2,332 μm^2) and WT mice (12,165 ± 967.7 μm^2) in adulthood (Student's two-tailed t-test; $t(4)= 0.4608$; N=3 per group; $P>0.05$; fig. 3.3C). Together, these data may indicate that proliferation and neuroblast population in the RMS were unaffected in adult SNAP25$^{+/-}$ mice.

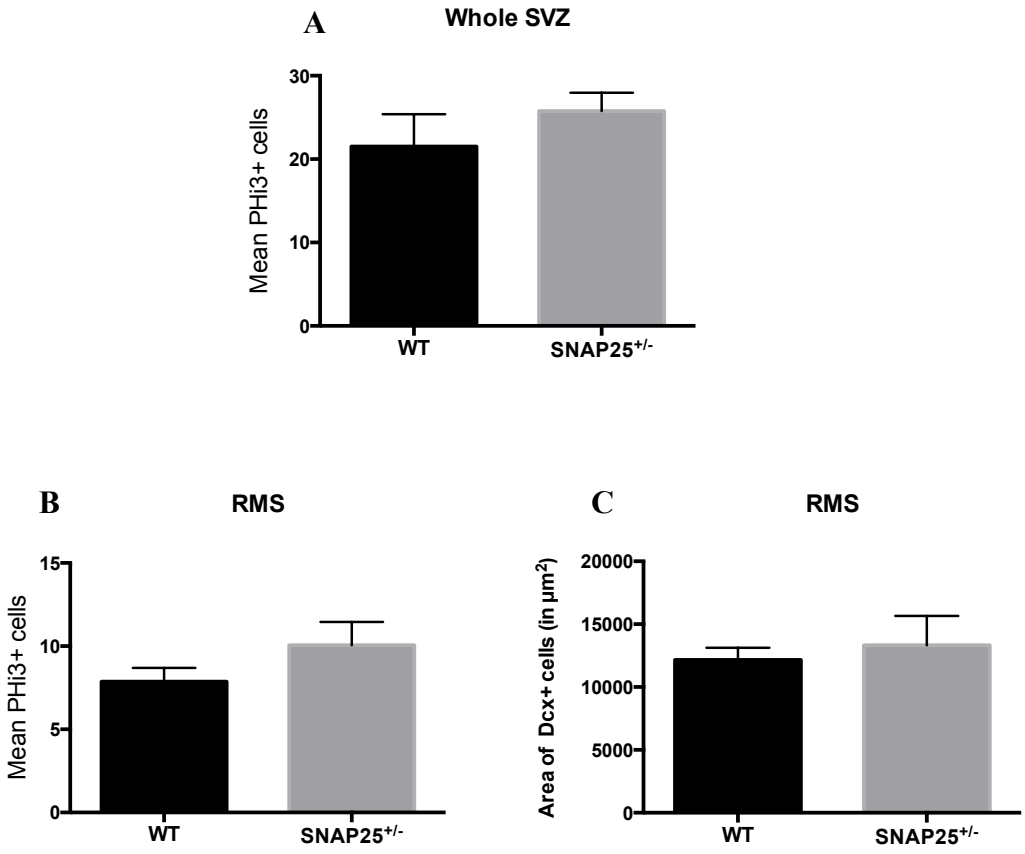

Figure 3.3 Proliferation and migratory neuroblasts in adult Snap-25 mutant (SNAP25$^{+/-}$) mice

(A) No significant change was found in the number of proliferative (PHi3+) cells in the SVZ of SNAP25$^{+/-}$ mice compared to WT mice.

(B-C) In the RMS, there was no significant change in proliferation (C) or the average area of migratory neuroblasts (D) in SNAP25$^{+/-}$ mice compared to WT mice.

Mean ± SEM. N=3 per group. Data were analyzed using Student's two-tailed t-test. P>0.05.

3.2.3 Reduced adult SVZ proliferation in Sdy mice given postnatal polyI:C

In order to determine the impact of GxE interaction in adult SVZ proliferation, dysbindin-1 mutant Sdy mice were given multiple saline or polyI:C injections during early postnatal ages as illustrated in figure 3.4A. Interestingly, there was a significant decrease in proliferation (PHi3+ cells) in adult Sdy mice given postnatal polyI:C injections (GxE model) in comparison to adult WT saline group (two-way ANOVA with Tukey's post-hoc test; $P<0.05$; N=6 per group; fig.3.4B). Representative images are illustrated in figure 3.4 (C-D") showing the decrease in PHi3+ cells in Sdy polyI:C group (fig.3.4D-D") compared to WT saline group (fig.3.4C-C"). These images were taken from similar anatomical coordinates (0.26mm to bregma) in both WT saline (fig.3.4C') and Sdy polyI:C (fig.3.4D') groups according to the mouse brain atlas by (Franklin and Paxinos, 2001). Hence, the interaction between GxE factors caused a reduction in adult SVZ proliferation.

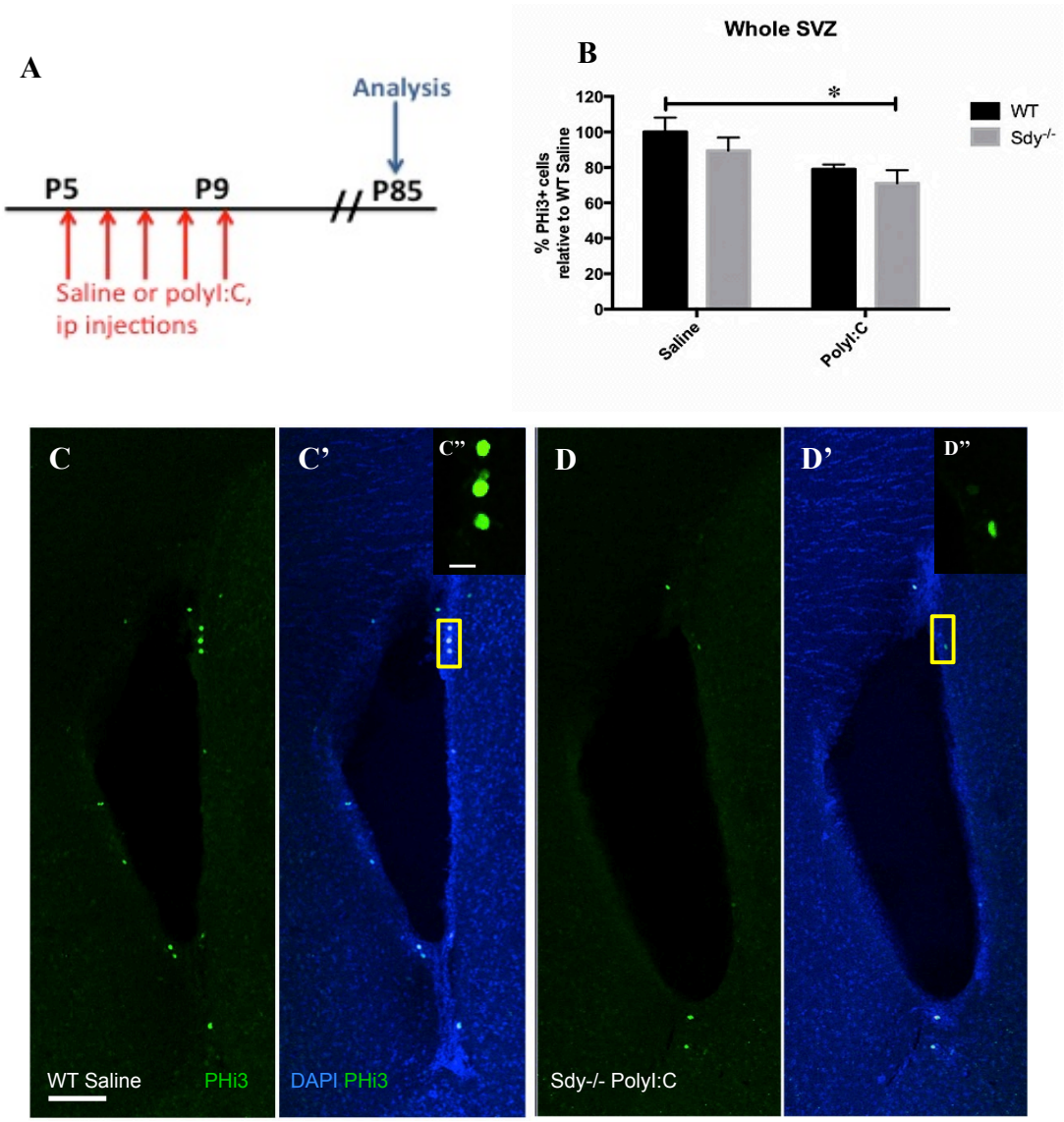

Figure 3.4 Proliferation in the adult SVZ of GxE model

(A) Experimental design of postnatal saline or polyI:C injections in WT and Sdy mice. Brains were collected for analysis at around postnatal 85 (P85).

(B) There was a significant reduction in the proliferative (PHi3+) cells in the adult SVZ of Sdy mice injected with polyI:C compared to WT saline group. Mean ± SEM. Data were analyzed using two-way ANOVA with Tukey's post-hoc test. N=6 per group. *P<0.05.

(C-D') Representative images showing reduced PHi3+ cells in the SVZ of Sdy polyI:C group (D) compared to WT saline group (C) that were taken from similar stereotaxic coordinates (0.26mm to bregma) as illustrated with DAPI staining in WT saline (C') and Sdy polyI:C (D') groups. Scale bar 100µm.

(C"-D") Higher magnification images of the yellow-boxed areas in (C'-D') showing PHi3+ cells in the WT saline (C") and Sdy polyI:C (D") groups. Scale bar 15µm.

3.2.4 Total population of migratory neuroblasts, but not proliferation, was decreased in the RMS of adult Sdy mice given postnatal polyI:C

Similar to the experimental design in figure 3.4A, WT and Sdy mice were repeatedly given saline or polyI:C and proliferation and migratory neuroblasts in the RMS were studied. The number of proliferative (PHi3+) cells was not significantly different between adult WT and Sdy mice that were postnatally injected with saline or polyI:C (two-way ANOVA with Tukey's post-hoc test; $P>0.05$; N=3 per group; fig.3.5A). However, there was a significant decrease in the surface area covered by migratory (Dcx+) neuroblasts in Sdy polyI:C group in comparison to both WT and Sdy saline groups in adulthood (two-way ANOVA with Tukey's multiple comparisons test; $P<0.01$; N=3 per group; fig.3.5B). Representative images are shown in figure 3.5(C-D'') illustrating the decrease in Dcx+ surface area in Sdy polyI:C group (fig.3.5D) compared to Sdy saline group (fig.3.5C). In reference to the atlas by (Franklin and Paxinos, 2001), these images were taken from similar stereotaxic coordinates (2.10mm to bregma) in both Sdy saline (fig.3.5C'-C") and Sdy polyI:C (fig.3.5D'-D") groups. Together, GxE interaction may negatively affect neuroblast migration, but not proliferation, in the adult RMS.

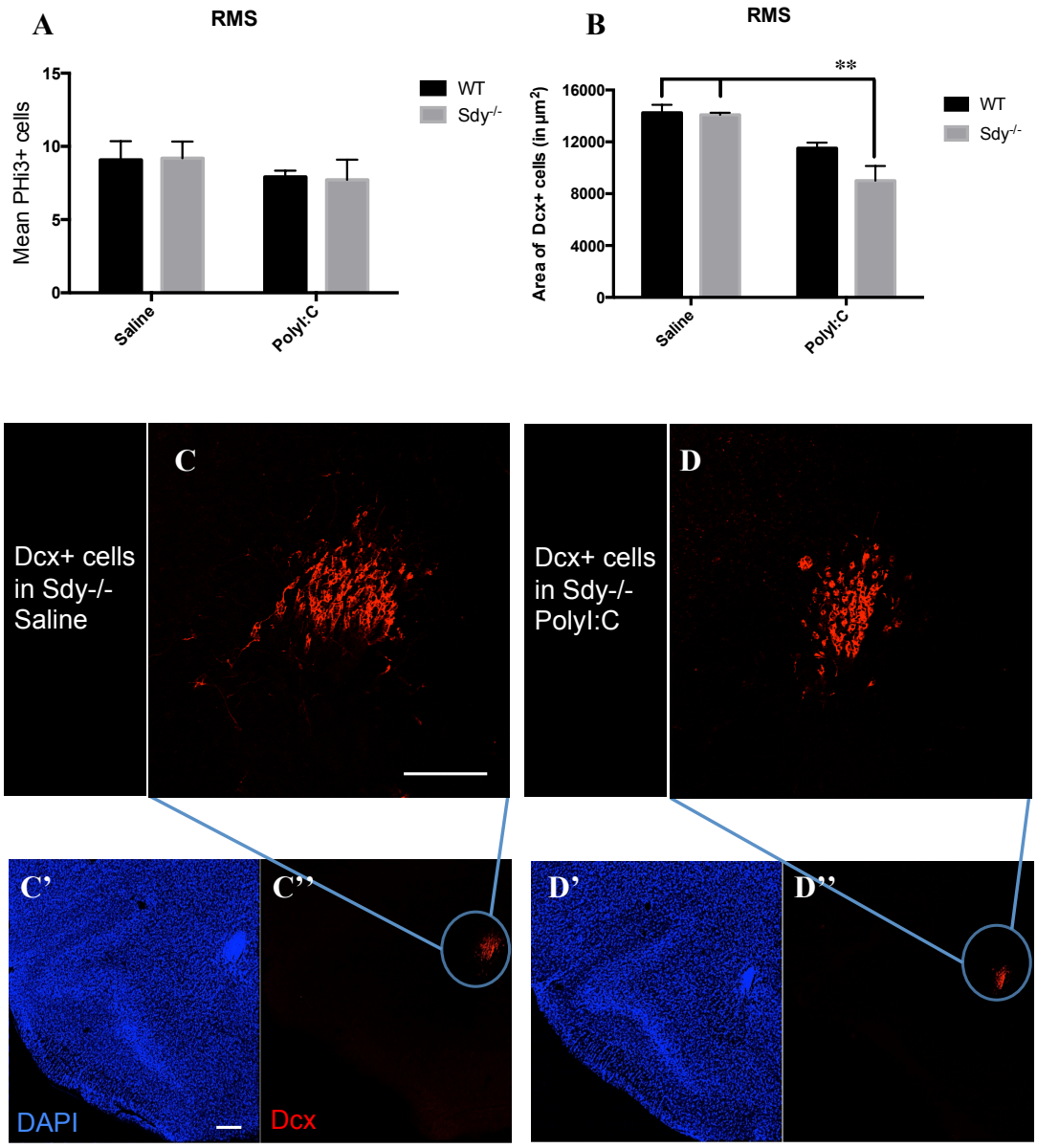

Figure 3.5 Proliferation and migratory neuroblasts in the RMS of adult GxE model

(A) No significant change was found in the number of proliferative PHi3+ cells in the RMS of GxE model. Mean ± SEM. Data were analyzed using two-way ANOVA with Tukey's post-hoc test. N=3 per group. P>0.05.

(B) In the RMS, surface area of total Dcx+ migratory neuroblasts was significantly reduced in adult Sdy mice given postnatal polyI:C compared to adult WT and Sdy mice postnatally injected with saline. Mean ± SEM. Data were analyzed using two-way ANOVA with Tukey's post-hoc test. N=3 per group. **P<0.01.

(C-D") Representative images illustrating the decrease in the RMS area of migratory neuroblasts in Sdy polyI:C group (D) in comparison to Sdy saline group (C). DAPI staining in (C' & D') showing that both images were taken from the same anatomical coordinates (2.10mm to bregma) according to the atlas by (Franklin and Paxinos, 2001). Dcx staining in (C" & D") were magnified in (C & D) for clarity. Scale bars 100 µm.

3.2.5 Postnatal polyI:C injections caused a long-lasting decrease in body weight that was associated with reduced locomotion in adult GxE model

The following data were collected by our collaborator, Professor Lalit Srivastava's laboratory (McGill University), and I have run the statistical analysis. As shown in figure 3.6A, body weights of WT polyI:C and Sdy polyI:C groups were significantly reduced in young adulthood at postnatal day 37-38 (P37-38) in comparison to WT saline group (two-way ANOVA with Tukey's multiple comparisons test; $P<0.0001$; N=6 per group; fig.3.6A). Likewise, body weights of WT polyI:C and Sdy polyI:C groups were significantly reduced compared to Sdy saline group in young adulthood at P37-38 (two-way ANOVA with Tukey's post-hoc test; $P<0.01$; N=6 per group; fig. 3.6A). This decrease in the body weights of WT polyI:C and Sdy polyI:C groups continued to later adulthood at P72-73 and showed significant reduction in WT polyI:C group ($P<0.01$) and Sdy polyI:C group ($P<0.001$) in comparison to WT saline group (two-way ANOVA with Tukey's post-hoc test; N=6 per group; fig. 3.6B). Together, postnatal polyI:C injections caused long-lasting decreases in the body weights of WT and Sdy mice in adulthood.

Locomotor activity was assessed at P70 in all four groups. Interestingly, locomotion was significantly reduced in Sdy polyI:C group in comparison to WT saline group (two-way ANOVA with Bonferroni's multiple comparisons test; WT saline N=17; Sdy saline N=14; WT polyI:C N=13 ; Sdy polyI:C N= 12; $P<0.05$; fig. 3.6C). In contrast, WT polyI:C group did not show statistically significant reductions in locomotion compared to the WT saline group (fig.3.6C). Hence, GxE factors negatively affected locomotor activity in adulthood suggesting that GxE interaction in our model might mimic some of the negative symptoms in schizophrenia.

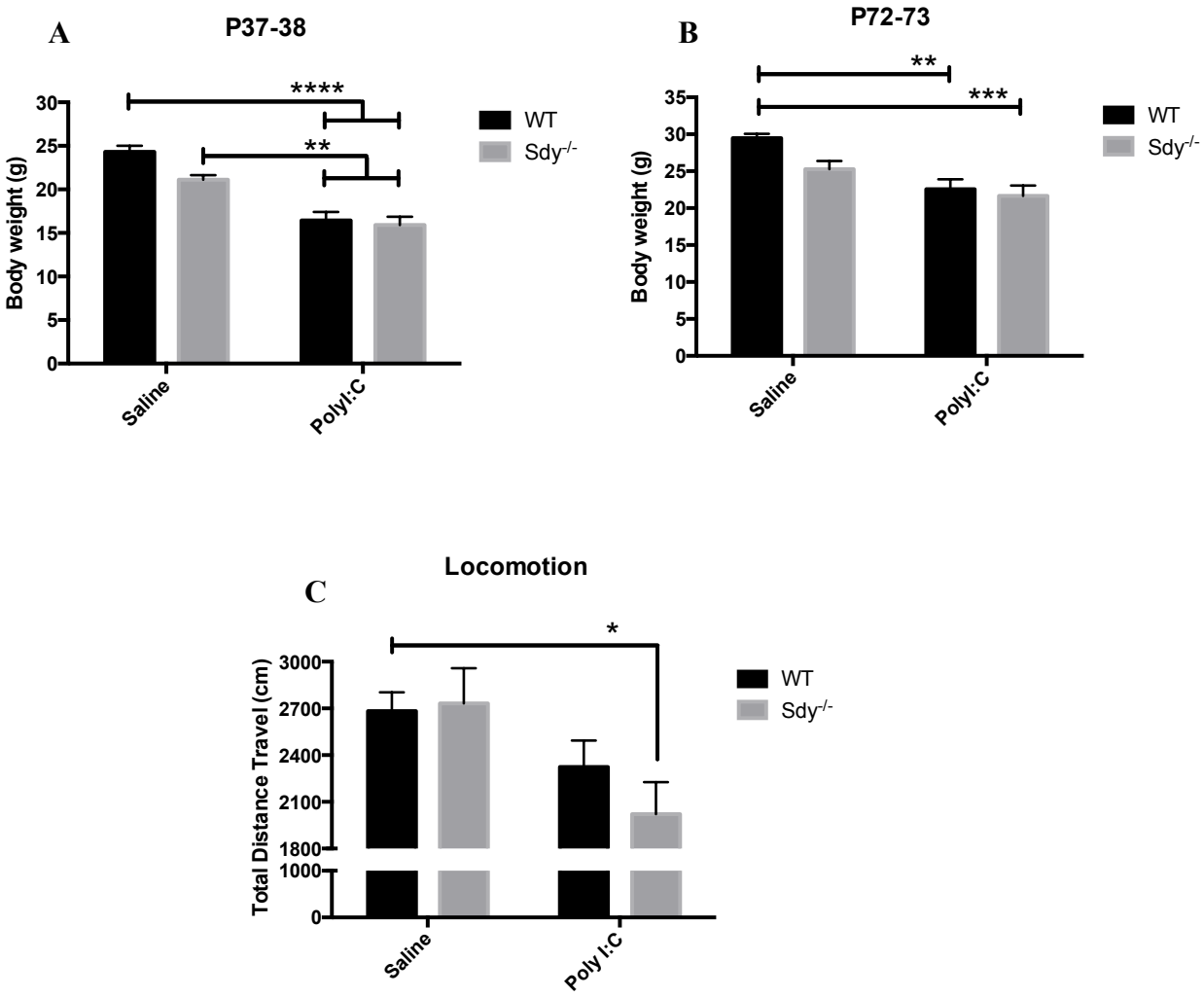

Figure 3.6 Body weight and locomotion in the adult GxE model

(A-B) Following repeated saline or polyI:C injections from postnatal day 5 (P5) to P9, there was a significant decrease in body weight of WT and Sdy mice at P37-38 (A) and P72-73 (B). Mean ± SEM. Data were analyzed using two-way ANOVA with Tukey's post-hoc test. N=6 per group. **P<0.01, ***P<0.001, ****P<0.0001.

(C) Spontaneous locomotor activity was significantly reduced in adult GxE model at P70 in comparison to WT saline group. Mean ± SEM. Data were analyzed using two-way ANOVA with Bonferroni's post-hoc test. WT saline N=17; Sdy saline N=14; WT polyI:C N=13 ; Sdy polyI:C N= 12. *P<0.05.

These data were collected by our collaborator, Professor Lalit Srivastava's laboratory (McGill University), and statistical analysis was run by myself.

3.2.6 GxE model showed reduced prepulse inhibition (PPI) and cognitive deficits in adulthood

The following data were collected and statistically analyzed by our collaborator, Professor Lalit Srivastava's laboratory (McGill University). Here, adult mice were presented with an auditory prepulse (PP) of 3, 6, 9, 12 or 15 decibels (PP3-15), and their responses to a main pulse of 120 decibels were recorded (fig.3.7A). Interestingly, Sdy mice showed a slight reduction in PPI, however this only reached statistical significance when Sdy mice were postnatally injected with polyI:C (N=6 per group; $P<0.05$; fig.3.7A-B). The PPI test showed normal response in adult WT mice regardless of postnatal injections (fig.3.7A-B). Together, these data may indicate sensorimotor deficits in our GxE model as demonstrated with the PPI test.

In order to assess cognitive memory in our GxE model, a novel object recognition test was used. As shown in figure 3.7C, WT saline mice spent longer time exploring a novel object than a familiar object (a value significantly different from 0.5 (chance level); $P<0.05$; N=6; fig.3.7C). However, the other three groups did not show preference to a novel object over a familiar object, suggesting deficits in novel object recognition ($P>0.05$; N=6 per group; fig.3.7C). It should be noted that during the familiarization phase, there was no difference in the total time that mice spent in exploring objects in all the four groups (data not shown). Taken together, postnatal inflammation and/or dysbindin-1 mutation may negatively impact cognitive function in adulthood.

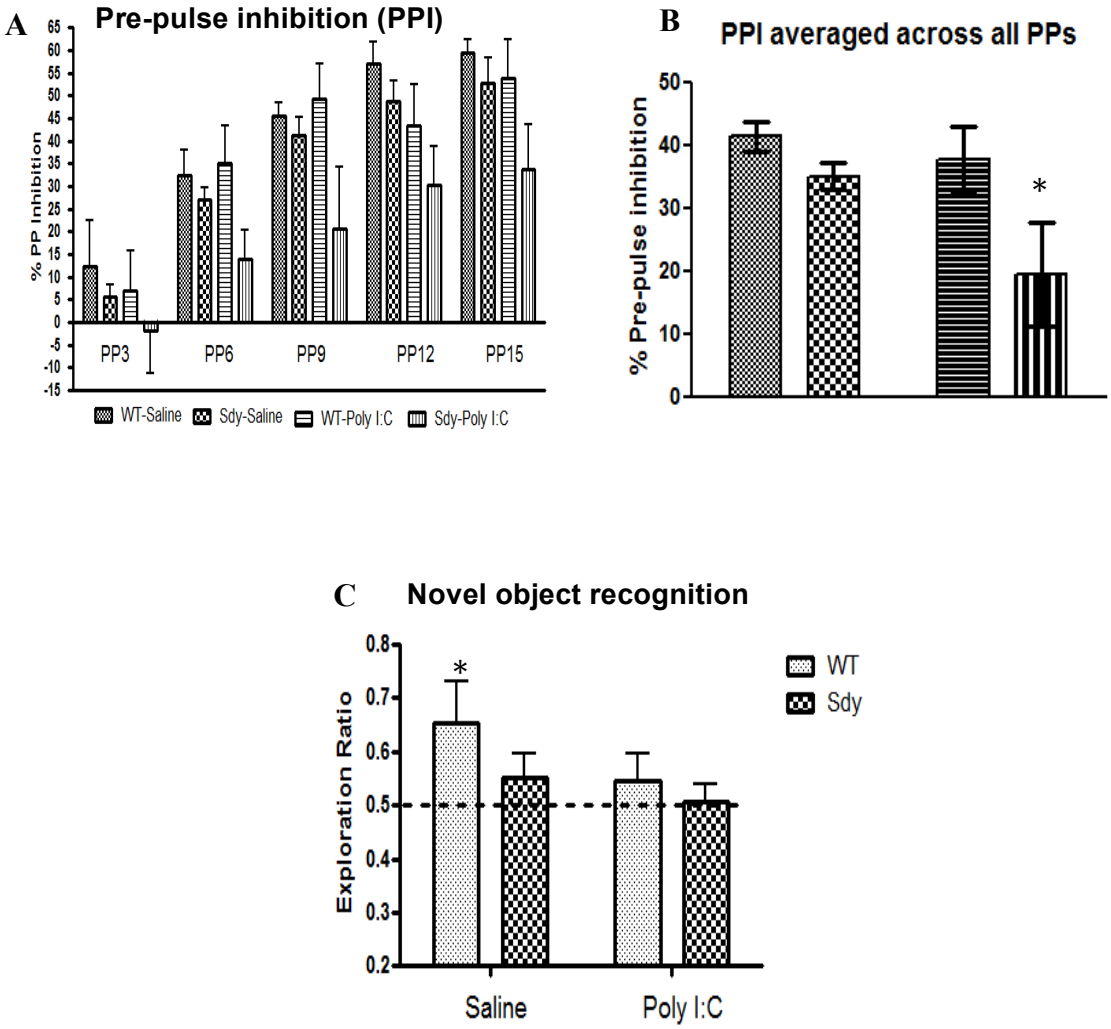

Figure 3.7 Reduced prepulse inhibition and cognitive dysfunction in GxE model

(A-B) At P74, prepulse (PP) intensities of 3, 6, 9, 12 or 15 decibels (PP3-15) caused a reduced inhibitory response in GxE model when exposed to a subsequent main pulse of 120 decibels. The average of prepulse inhibition (PPI) across all prepulses (PPs) is illustrated in (B) showing significant reduction in PPI in GxE model. N=6 per group. *P<0.05.

(C) In comparison to WT saline group, Sdy mice as well as WT mice given postnatal polyI:C showed cognitive deficits in novel object recognition at P74. N=6 per group. *P<0.05.

These data were collected and statistically analyzed by our collaborator, Professor Lalit Srivastava's laboratory (McGill University).

3.3 Discussion

I found that mutations in Nrg1 type I, Snap-25 or dysbindin-1 genes relevant to schizophrenia did not affect SVZ proliferation or RMS proliferation and migratory neuroblasts in adulthood. However, combining postnatal inflammation with dysbindin-1 mutation in Sdy mice (GxE model) resulted in reduced SVZ proliferation as well as decreased neuroblast population, but not proliferation, in the RMS in adulthood. Interestingly, these observations in the GxE model were also correlated with behavioural deficits relevant to schizophrenia as demonstrated by our collaborators.

3.3.1 GxE model of schizophrenia, but not genetic mutation alone, decreased SVZ proliferation in adulthood

I found that GxE model of schizophrenia showed a significant decrease in adult SVZ proliferation. This was demonstrated using dysbindin-1 mutant Sdy mice that were postnatally injected with polyI:C. Interestingly, increased physical activity was previously reported to associate with increased SVZ proliferation (Lee et al., 2016). Here, the GxE model showed reduced locomotor activity which might explain the decrease in SVZ proliferation. On the other hand, I found normal proliferation in the SVZ of adult Sdy mice that were postnatally unchallenged. This is consistent with other studies that reported normal proliferation in the dentate gyrus of adult Sdy mice following BrdU injections (Wang et al., 2014, Nihonmatsu-Kikuchi et al., 2011). Postnatal polyI:C injections caused a slight but non significant decrease in proliferative PHi3+ cells in the adult SVZ of WT mice. Conversely, another study showed that prenatal exposure to polyI:C in WT mice resulted in significantly

decreased number of mitotic (PHi3+) cells in the adult SVZ (Liu et al., 2013). This discrepancy might be due to the variation in the selected neurodevelopmental period for administering polyI:C.

On the other hand, I found no change in SVZ proliferation in adult NRG1$^{typeI-tg}$ overexpressing mice. So far, no studies have addressed the role of Nrg1 type I in SVZ proliferation although it was reported to be expressed in the SVZ and RMS (Anton et al., 2004). Previous studies showed that Nrg1, but not specifically type I, did not affect SVZ proliferation in adult mice in which Nrg1 was administered either subcutaneously (Mahar et al., 2011) or through direct infusion into the lateral ventricle (Ghashghaei et al., 2006).

Adult neurogenesis was not previously characterized in SNAP25$^{+/-}$ mice. Here, I showed that adult SVZ proliferation was unaffected in SNAP25$^{+/-}$ mice. In addition, adult hippocampal neurogenesis was unchanged in SNAP25$^{+/-}$ mice (data not shown). However, adult hippocampal neurogenesis was previously studied in SNAP-25 knock-in mice, which carry a different type of Snap25 mutation (as described in section 3.1.1). In adult SNAP-25 knock-in mice, hippocampal proliferation was reduced as demonstrated with Ki67 marker as well as with multiple BrdU injections (Ohira et al., 2013). In addition, the number of Dcx+ cells in the dentate gyrus was decreased in adult SNAP-25 knock-in mice indicating reduced hippocampal neurogenesis (Ohira et al., 2013). The inconsistency in adult neurogenesis between SNAP25$^{+/-}$ and SNAP-25 knock-in mice might be due to the variation in the type of mutation in Snap25 gene, which may differentially affect Snap25 protein function. Our SNAP25$^{+/-}$ mice show normal expression of Snap25

protein although the protein function is disrupted (Jeans et al., 2007, Oliver and Davies, 2009), however there is 50% reduction in Snap25 protein expression in SNAP-25 knock-in mice (Kataoka et al., 2011). Therefore, the normal expression of Snap25 protein in our $SNAP25^{+/-}$ mice might be sufficient to maintain adult neurogenesis.

3.3.2 Evidence for reduced neuroblast migration in the RMS of adult GxE model, but not in genetic mutation models

I found that the surface area occupied by migratory neuroblasts in the RMS was significantly reduced in adult Sdy mice given postnatal polyI:C injections, which may indicate reduced number of neuroblasts in the RMS due to decreased neuroblast migration from the SVZ. Since proliferation in the RMS was unaffected in the GxE model, this may exclude the effect of RMS proliferation in the observed reduction in surface area of Dcx+ cells in the RMS, but may rather indicate reduced levels of neuroblast migration from the SVZ. This is further supported since SVZ proliferation was reduced in the GxE model, which probably resulted in fewer neuroblasts being available to migrate in the RMS. However, this proposed reduction in neuroblast migration in the GxE model is still to be confirmed using other techniques such as RMS explant migration assay or time-lapse imaging of neuroblast migration in brain slices.

Interestingly, dysbindin-1 regulated transcriptional activity of RelA, which promoted matrix metalloproteinase-9 (MMP-9) expression (Fu et al., 2015) and MMP-9 was shown to be important in the migration of SVZ neuroblasts (Lee et al.,

2006). Since I found that dysbindin-1 loss in Sdy mice resulted in inhibited RelA expression after inflammation (Chapter 4), this may indicate that Sdy polyI:C mice also have inhibited MMP-9 expression and therefore decreased neuroblast migration in the RMS. Also, Sp1 expression was inhibited in Sdy polyI:C mice (Chapter 4) and Sp1 was shown to regulate MMP-9 expression in migratory and invasive cancer (Hung et al., 2010). Taken together, inhibited RelA and Sp1 expression in the Sdy polyI:C mice (GxE model) may dysregulate MMP-9 expression which together may support the proposed reduction in neuroblast migration in the RMS of the GxE model.

On the other hand, I found that the area of migratory neuroblasts was unaffected in adult $SNAP25^{+/-}$ and $NRG1^{typeI\text{-}tg}$ overexpressing mice. The role of Snap25 in cell migration has not been previously characterized. However, another study reported that short-term (24 hours) infusion of Nrg1 into the lateral ventricle induced aggregation of neuronal progenitors into clusters in the SVZ, and that continuous infusion of Nrg1 for 3- or 7-days into the lateral ventricle inhibited the migration of neuroblasts from the SVZ to the RMS (Ghashghaei et al., 2006). This discrepancy between my work and their work might be because they exogenously infused Nrg1 specifically into the lateral ventricle, which may attract and retain neuroblasts in the SVZ resulting in reduced migration to the RMS (Ghashghaei et al., 2006). This is especially since Nrg1 was previously shown *in vitro* to act as a chemoattractant for SVZ cells (Anton et al., 2004). However, in our transgenic mouse model only type I of Nrg1, and not all six types, was overexpressed in various brain regions and not specifically in the SVZ. Therefore, variations in experimental design between our transgenic model and the previous publications probably caused the differential effects of Nrg1 in migratory neuroblasts.

3.3.3 GxE model showed schizophrenia-relevant behaviours in adulthood

In order to characterize the behavioural phenotypes of our GxE model, prepluse inhibition (PPI), novel object recognition and locomotor activity were tested. Here, our adult GxE model showed a significant reduction in PPI, suggesting sensorimotor gating deficits. Although adult Sdy mice were previously reported to show a significant decrease in PPI (Carlson et al., 2011), this did not reach a statistical significance in the current study. Interestingly, postnatal polyI:C injections reduced the ability of our adult WT mice to recognize novel objects and this is consistent with a previous study (Ibi et al., 2009). In addition, object recognition memory was also disrupted in our adult Sdy mice supporting previous reports (Feng et al., 2008, Bhardwaj et al., 2009). In our GxE model, object recognition memory was also disrupted and this is consistent with another study that showed this effect in adult DISC1 mutant mice that were postnatally injected with polyI:C (Ibi et al., 2010). Taken together, our adult GxE model showed behavioural deficits relevant to schizophrenia.

Furthermore, repeated polyI:C injections in postnatal WT and Sdy pups caused a significant decrease in body weights in young (P37-38) and later (72-73) adulthood. This detrimental effect of polyI:C in reducing body weight was also evident in early postnatal pups (P5-9) and P12 of both genotypes, although the effect seemed more severe in Sdy pups (data not shown). Interestingly, locomotor activity was significantly reduced in adult Sdy, but not WT, mice that were postnatally given polyI:C (GxE model). The normal locomotion in adult WT mice given postnatal polyI:C is also consistent with another study (Ibi et al., 2009). Although locomotion

was previously reported to decrease in adult Sdy mice that were not postnatally immune challenged (Hattori et al., 2008), this was not noticed in the current study. The decrease in locomotion in our adult GxE model, but not in adult Sdy saline group, suggests a deleterious effect of polyI:C in mutant mice during postnatal development that might be long-lasting. Another study showed that a single systemic injection of polyI:C in adult WT mice caused a dose-dependent decrease in body weight and locomotor activity that was fully recovered 24-96 hours post injection (Cunningham et al., 2007). This supports previous reports that the impact of immune challenge during early postnatal life is more severe and persists for longer period of time than in adulthood (reviewed in (Holladay and Smialowicz, 2000)). Together, depressive-like and sickness behaviours were induced in our GxE model, suggesting that neonatal inflammation in combination with a genetic vulnerability to schizophrenia may amplify the likelihood of developing the negative symptoms in adulthood.

3.4 Conclusions

I report novel evidence for a gene (dysbindin-1 mutation) x environment (postnatal polyI:C) interaction in schizophrenia that negatively affected adult SVZ proliferation and the population of migratory neuroblasts in the RMS. Moreover, these observations were correlated with behavioural abnormalities relevant to schizophrenia in adulthood. Since postnatal immune challenge in dysbindin-1 mutant mice impacted SVZ proliferation in adulthood, this may suggest a critical requirement for dysbindin-1 during postnatal development in order to maintain SVZ proliferation as well as to mediate the inflammatory response. These aims were addressed in the next chapter (Chapter 4).

Chapter 4

Postnatal SVZ proliferation and immune signalling pathway in GxE model of schizophrenia

4.1 Introduction

It has become increasingly clear that genetic or environmental risk factors alone may not be sufficient to give rise to schizophrenia. For example, a study showed that developing schizophrenia was five times greater in individuals exposed to infection during early brain development and who also had a family history of psychosis than those who did not (Clarke et al., 2009). To date, the majority of schizophrenia-related studies have either investigated the effects of genes or environments separately, or only described the outcome of multiple risk factors. To the best of my knowledge, only one study described an underlying mechanism for the gene x environment (GxE) interactions in schizophrenia in which an environmental stressor epigenetically regulated dopaminergic neurons via glucocorticoids, and this was only observed in a genetic model of schizophrenia (Niwa et al., 2013). However, the authors did not describe why the environmental factor affected only the genetic model of the disease. Therefore, the aim of this chapter was to investigate how the GxE risk factors of schizophrenia might functionally interact and regulate each other, and the impact of this interaction on neurodevelopment. I demonstrated this using dysbindin-1 mutant (i.e. Sdy) mice as a genetic risk factor in combination with polyI:C as an environmental risk factor, and SVZ proliferation was analysed at postnatal day 12 (P12).

4.1.1 Genes upregulated following polyI:C-induced inflammation

In order to determine whether dysbindin-1 might functionally affect polyI:C induced inflammation, it is important to consider the genes that are induced in response to polyI:C, and any possible interactions they may have between each other.

PolyI:C is a double-stranded (dsRNA) which is a by-product of a wide range of replicating viruses (Jacobs and Langland, 1996). Therefore, using polyI:C mimics viral infections, and it is one of the major tools that immunologists use to study inflammation-related mechanisms. Upon polyI:C administration, it activates its specific receptor toll-like receptor 3 (Tlr3). RelA is a transcription factor downstream from Tlr3 (reviewed in (Kawai and Akira, 2010)). Several studies demonstrated that Sp1 transcription factor and RelA transactivate each other during various types of viral infections (Doyle et al., 2013, Gu et al., 2002, Perkins et al., 1994, Yurochko et al., 1997). Specifically, polyI:C was shown to induce RelA binding to the Sp1 promoter and to activate its transcription (Doyle et al., 2013). Interestingly, both RelA (Song et al., 2009) and Sp1 (Ben-Shachar and Karry, 2007, Pinacho et al., 2014) have been implicated in schizophrenia.

4.1.2 Function of polyI:C-induced genes in CNS proliferation

A second aim of this chapter was to determine possible correlations between polyI:C-induced genes (i.e. Tlr3, RelA and Sp1) and postnatal SVZ proliferation, and whether loss of dysbindin-1 in Sdy mice may alter the observed effects.

Several studies have suggested a possible role of Tlr3 in regulating CNS proliferation. For example, Tlr3 expression in the neuroepithelium (ventricular zone) was shown to be highest during early embryonic development when neural progenitor cells (NPCs) were highly proliferative, however Tlr3 expression declined when neurogenesis and gliogenesis commenced, indicating a role of Tlr3 in proliferation (Lathia et al., 2008). Moreover, embryonic-derived NPCs cultured as free-floating neurospheres highly expressed Tlr3 but its expression sharply decreased when these neurospheres were induced to differentiate (Lathia et al., 2008), providing further evidence for the role of Tlr3 in proliferation. Since Tlr3 expression in the CNS gradually declines with age (reviewed in (Barak et al., 2014)), this highlights the important role of Tlr3 during early brain development when proliferative potential is highest, and that Tlr3 dysregulation during early neurodevelopment may have long-lasting effects.

Similarly, RelA (a subunit of NF-κB) also has proliferative functions in the CNS. This was reported in adult SVZ neurospheres in which RelA activation was essential for neurosphere proliferation via upregulation of its target gene cyclin D1. Inhibiting RelA activity reduced cyclin D1 expression and resulted in significantly decreased proliferation (Widera et al., 2006). This was the first study to report the role of NF-κB activation in adult neurosphere proliferation (Widera et al., 2006). In embryonically derived neurospheres, loss of RelA and p50 subunits of NF-κB was also shown to significantly inhibit proliferation (Young et al., 2006). A functional role of RelA in inducing proliferation and inhibiting myogenic differentiation was also demonstrated in non-CNS cell lines (Guttridge et al., 1999). Taken together, induction

of Tlr3 and RelA following polyI:C-induced inflammation may also affect proliferation in the SVZ.

Sp1 has been extensively studied in various cancers due to its role in promoting cell proliferation. Sp1 plays key functions in mediating cell-cycle progression by regulating the expression of cell-cycle regulatory genes such as cyclin B1, cyclin D1 and cyclin E1 as well as thymidine kinase (reviewed in (Mao et al., 2009)). Also, Sp1 promotes the expression of various growth factors and their receptors, such as FGF, IGF1/R and EGF/R (reviewed in (Beishline and Azizkhan-Clifford, 2015)). Sp1 knockdown was shown to block mitosis; highlighting the essential role of Sp1 in inducing cell proliferation (reviewed in (Mao et al., 2009)). In the CNS, Sp1 expression dramatically decreased during neuronal differentiation (Mao et al., 2009, Mao et al., 2007), suggesting its role in cell proliferation. Also, overexpression of Sp1 was associated with increased proliferation of glioma cells in brain cancer (Guan et al., 2012, Luo et al., 2015, Xu and Shu, 2007, Yan et al., 2000). Sp1 was also reported to mediate the function of nerve growth factor (NGF) (Miura et al., 2012, Sobue et al., 2005), and NGF was shown to induce SVZ proliferation (Scardigli et al., 2014). Hence, Sp1 may also regulate SVZ proliferation during inflammation.

4.1.3 Research questions

To date, no studies have examined the combined effect of GxE risk factors for schizophrenia on proliferation in neurogenic niches during early brain development. Despite the well-described genetic and environmental risk factors for schizophrenia, direct functional interactions between these two factors have remained elusive. Therefore, I sought to address the following questions:

1) What is the impact of combined dysbindin-1 mutation x postnatal polyI:C injections on postnatal SVZ proliferation?

2) Does the dysbindin-1 mutation affect the response of postnatal SVZ cells to polyI:C induced inflammation *in vivo* and/or *in vitro*?

3) Is there a correlation between postnatal SVZ proliferation and the expression of Tlr3, RelA and Sp1 genes following polyI:C administration?

4) Does the dysbindin-1 (Dtnbp1) gene play a functional role in mediating the expression of Tlr3, RelA and Sp1 genes?

4.2 Results

4.2.1 Postnatal SVZ proliferation was reduced in the GxE model

In order to determine the effect of GxE factors on SVZ proliferation, repeated saline or polyI:C injections (fig.4.1A) were given to WT and Sdy mice and the total number of SVZ mitotic (PHi3+) cells were quantified in all four groups as illustrated in figure 4.1B. There was a significant decrease in the number of SVZ proliferative cells in Sdy mice given polyI:C in comparison to WT saline group as determined using two-way ANOVA followed by Tukey's multiple comparisons test ($P<0.05$; N=3 per group; fig.4.1B). Although the significant difference detected in this experiment was based on three mice per group, a post hoc power analysis was conducted in order to determine the statistical power of the results. This was performed using GPower Software (version 3.1.9.2) which showed that a total sample size of 12 mice in four groups with an effect size of ($f=0.938$) from my data and the alpha set at 0.05 was sufficient to reach a power of 0.811 (>80% chance) for detecting differences between groups. This indicates that the reduced number of PHi3+ cells in the SVZ of Sdy polyI:C group was likely due to the significant effect of the combination of polyI:C injections and dysbindin-1 mutation which was not limited by the small sample size.

In addition, the number of mitotic neuroblasts (PHi3+/Dcx+) was quantified in the postnatal SVZ (fig. 4.1C). Although there was a significant main effect of polyI:C injections in the number of PHi3+/Dcx+ cells (two-way ANOVA; $F(1,8)=5.763$; $P<0.05$; N=3 per group; fig.4.1C), Tukey's multiple comparisons test did not reveal a specific difference among all four groups. Therefore, a priori power analysis was

conducted using GPower Software in order to determine the number of mice that are needed to reach a statistical significance between the groups. Based on the following parameters (effect size f=0.258, alpha=0.05, power=0.80), a total of 25 mice are required in order to reach >80% chance for detecting differences between groups in the number of PHi3+/Dcx+ SVZ cells.

Representative images for the co-localization of PHi3+/Dcx+ are shown in figure 4.1 for WT saline group (D-D") versus Sdy polyI:C group (E-E"). Taken together, these results indicated that the genetic or environmental risk factors alone were not sufficient to affect postnatal SVZ proliferation. However a combination of GxE factors significantly reduced postnatal SVZ proliferation.

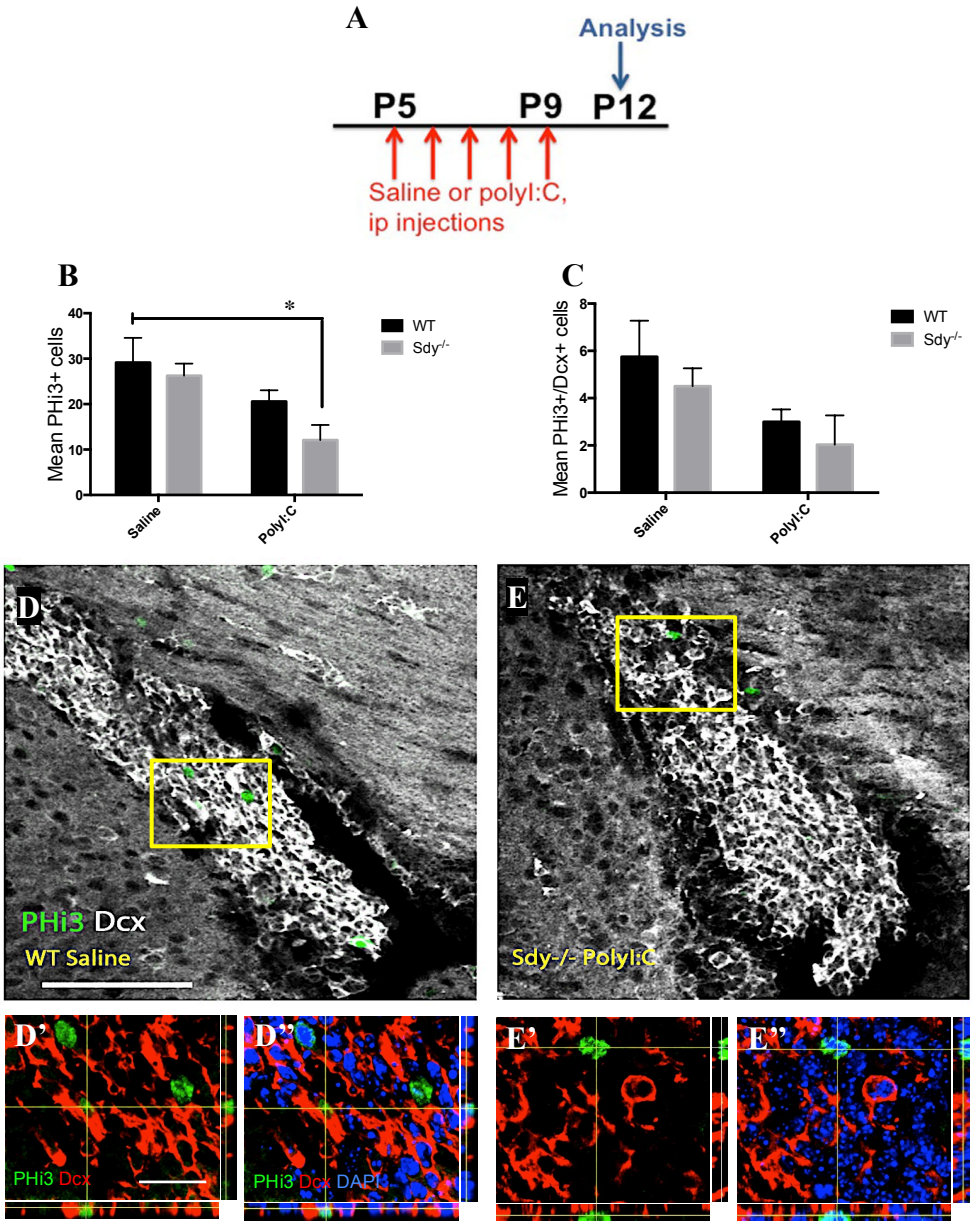

Figure 4.1 Postnatal polyI:C injections reduced SVZ proliferation in Sdy but not WT mice at P12

(A) Experimental design of postnatal saline or polyI:C injections in WT and Sdy mice. Brains were collected for analysis at postnatal day 12 (P12).

(B) Mean number of mitotic (PHi3+) cells in the SVZ at P12. Mean ± SEM. Data were analyzed using two-way ANOVA with Tukey's post-hoc test. N=3 per group. *P<0.05.

(C) Mean number of SVZ proliferative neuroblasts (PHi3+/Dcx+). Mean ± SEM. Data were analyzed using two-way ANOVA with Tukey's post-hoc test. N=3 per group.

(D-E) Representative images of double-labeled PHi3+/Dcx+ cells in the SVZ showing reduced number of PHi3+ cells in Sdy polyI:C group (E) compared to WT saline group (D). Scale bar 100µm.

(D'-E") Orthogonal views of PHi3+/Dcx+ cells in WT saline (D'-D") and Sdy polyI:C (E'-E") groups magnified from the yellow-boxed areas in D and E, respectively. Scale bar 20µm.

4.2.2 Postnatal inflammatory response in the SVZ was induced in WT but not Sdy mice following *in vivo* and *in vitro* polyI:C administration

Saline or polyI:C was administered to WT and Sdy mice (fig.4.2A) and to their SVZ-derived neurospheres (fig.4.3A), and the expression of dysbindin-1 (Dtnbp1), Tlr3, RelA and Sp1 genes in the SVZ was normalized to the geometric mean of two housekeeping genes (Vandesompele et al., 2002); β-actin and ribosomal 18S. Within each separate experiment, the arbitrary unit for all genes in WT saline and Sdy saline groups were set to 1. Gene expression in WT polyI:C group was calculated relative to their WT saline littermates; whereas gene expression in Sdy polyI:C group was relative to their Sdy saline littermates.

Following repeated ip injections of saline or polyI:C to WT and Sdy mice (fig.4.2A), *in vivo* expression of dysbindin-1 (Dtnbp1) gene was significantly induced in WT polyI:C group (~1.6 fold increase) in comparison to the WT saline group (Student's two-tailed t-test ($t(4)= 9.721$; $N=3$; $P<0.001$; fig. 4.2B). Also, increased gene expression of Tlr3 (~1.9 fold), RelA (~1.6 fold) and Sp1 (~1.7 fold) was detected in the *in vivo* WT polyI:C group compared to the WT saline group as analyzed using Student's two-tailed t-test (N=3; fig.4.2B). However, *in vivo* polyI:C injections to Sdy mice did not cause a significant difference in Tlr3, RelA and Sp1 gene expression in comparison to the Sdy saline group (Student's two-tailed t-test; $N=3$; $P>0.05$; fig.4.2B).

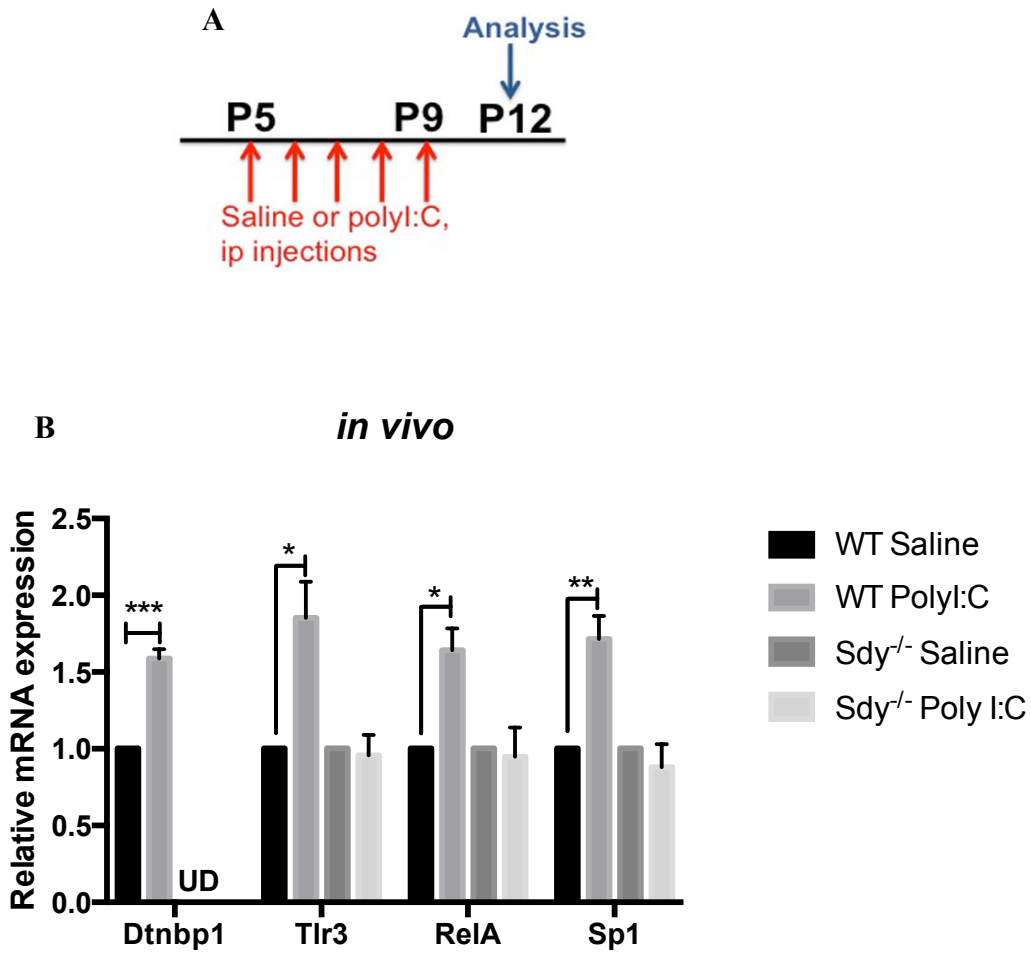

Figure 4.2 Inflammatory response was induced in WT but not Sdy mice following polyI:C injections *in vivo*

A) Experimental design of *in vivo* saline or polyI:C ip injections to WT and Sdy mice from postnatal day 5 (P5) to P9. SVZ was dissected at P12 and used in RT-qPCR (B).

(B) Expression of dysbindin-1 (Dtnbp1) gene was undetermined (UD) in Sdy neurospheres. Relative to the WT saline group, gene expression of Dtnbp1, Tlr3, RelA and Sp1, was all significantly increased in WT polyI:C group. However, gene expression of Tlr3, RelA and Sp1 was not statistically different between Sdy saline and Sdy polyI:C groups. Mean ± SEM from three independent experiments. Data were analyzed using Student's two-tailed t-test.
*P<0.05; **P<0.01; ***P<0.001.

In vitro polyI:C administration to WT neurospheres significantly increased dysbindin-1 (Dtnbp1) gene expression (~1.8 fold increase) in comparison to the WT saline group as analysed using Student's two-tailed t-test ($t(4)=6.632$; N=3; $P<0.01$; fig. 4.3B). Similarly, increased gene expression of Tlr3 (~1.5 fold), RelA (~2 fold) and Sp1 (~1.6 fold) was all found in the *in vitro* WT polyI:C group compared to the WT saline group (Student's two-tailed t-test; N=3; fig.4.3B). However, *in vitro* polyI:C administration to Sdy neurospheres significantly reduced gene expression of RelA (~0.5 fold) and Sp1 (~0.6 fold), but not Tlr3 (~0.8 fold), in comparison to Sdy saline group (Student's two-tailed t-test; N=3; fig.4.3B). Taken together, WT (but not Sdy) mice responded to the inflammatory stimuli, polyI:C, and induced the expression of Tlr3, RelA and Sp1 in the SVZ both *in vivo* and *in vitro*. Unpredictably, polyI:C also induced the expression of dysbindin-1 in the SVZ of WT mice and neurospheres, indicating a potential role for dysbindin-1 in regulating inflammation.

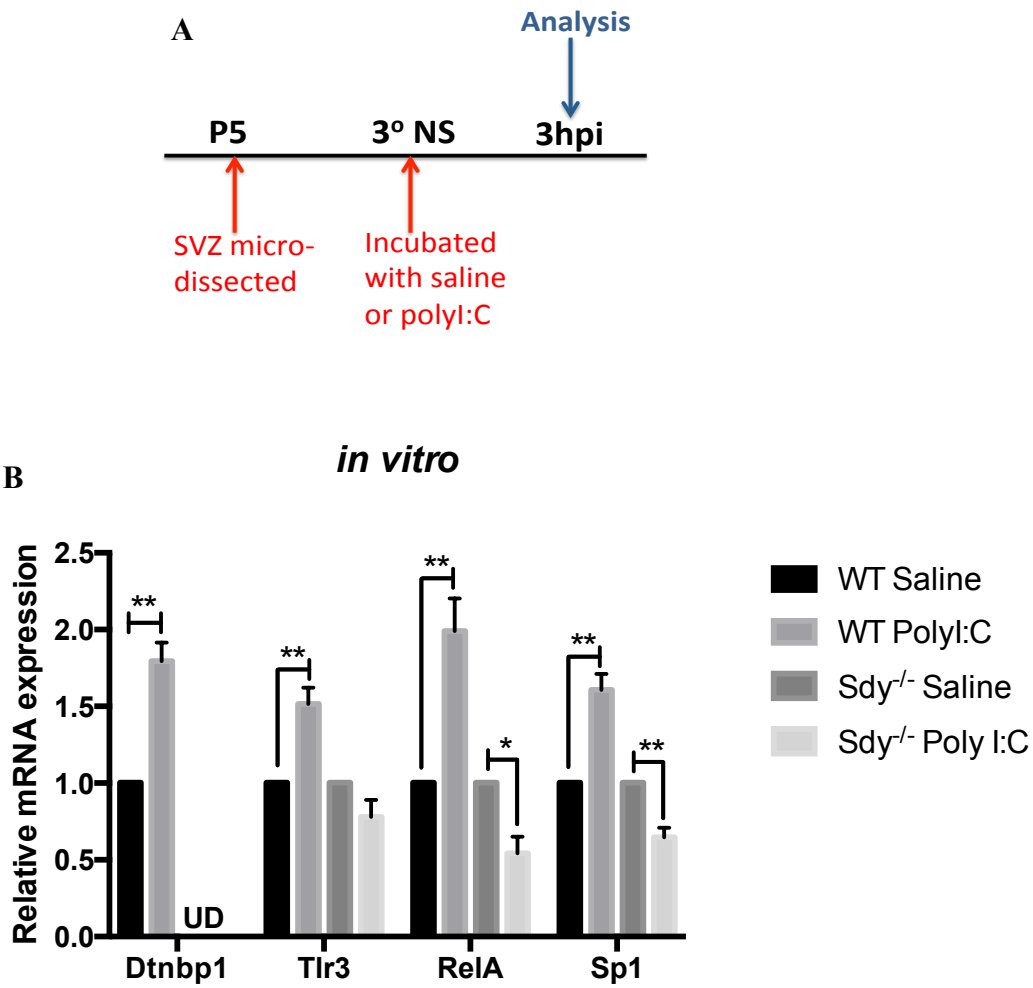

Figure 4.3 PolyI:C induced inflammatory response in WT but not Sdy mice *in vitro*

(A) Experimental design of SVZ-derived neurospheres (NS) used in RT-qPCR (B). **3°** denotes tertiary; **hpi** means hours post-incubation.

(B) Dysbindin-1 (Dtnbp1) gene expression was undetermined (UD) in Sdy neurospheres. Gene expression of Dtnbp1, Tlr3, RelA and Sp1 was all significantly induced in WT polyI:C group relative to the WT saline group. However, gene expression of RelA and Sp1, but not Tlr3, was significantly reduced in Sdy polyI:C group compared to the Sdy saline group. Mean ± SEM from three independent experiments. Data were analyzed using Student's two-tailed t-test.
*P<0.05; **P<0.01.

4.2.3 Tlr3 immunohistochemical expression was increased in postnatal WT but not Sdy mice following *in vivo* polyI:C injections

To further confirm my RT-qPCR data, Tlr3 immunohistochemistry in the dorsal SVZ was qualitatively analyzed in the postnatal WT and Sdy mice following repeated saline or polyI:C injections (fig.4.4A). Images were captured in the dorsal SVZ (fig.4.4B) using the same exact settings and slides were coded in order to avoid any biased comparisons. As shown in figure 4.4(C), I confirmed the expression of Tlr3 protein in the dorsal SVZ of WT saline group. Interestingly, polyI:C injections in WT mice enhanced Tlr3 protein expression in the dorsal SVZ (fig.4.4D) in comparison to WT saline group (fig.4.4C). Baseline expression of Tlr3 protein in Sdy saline group (fig.4.4E) seemed slightly reduced compared to WT saline group (fig.4.4C). Postnatal polyI:C injections in Sdy mice seemed to further reduce Tlr3 protein expression (fig.4.4F) compared to Sdy saline group (fig.4.4E). Together, my Tlr3 immunohistochemistry confirmed my RT-qPCR data and showed that protein expression of Tlr3 was increased in the postnatal SVZ of WT, but not Sdy, mice given polyI:C.

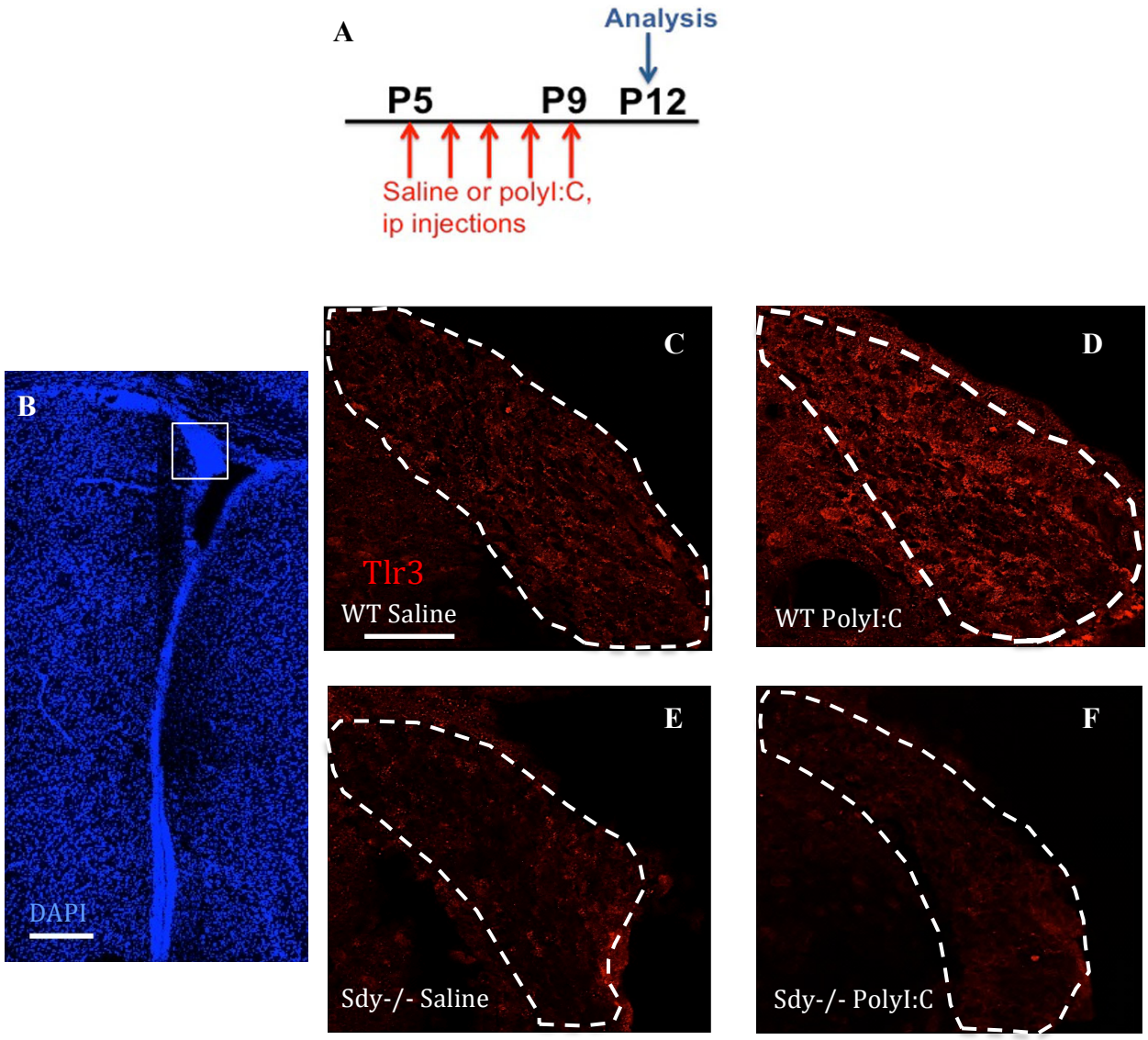

Figure 4.4 Postnatal polyI:C induced Tlr3 protein expression in WT mice but reduced its expression in Sdy mice

(A) Experimental design of postnatal saline or polyI:C injections in WT and Sdy mice. Brains were collected for analysis at postnatal day 12 (P12).

(B) Anatomical location of the dorsal SVZ (white-boxed area) in which all images in (C-F) were taken. Scale bar 200µm.

(C-F) Representative images of Tlr3 staining in the dorsal SVZ of WT saline (C), WT polyI:C (D), Sdy saline (E) and Sdy polyI:C (F) groups. These were representative of N=2-3 per group. Scale bar 50µm.

4.2.4 Nucleofection with dysbindin-1 (Dtnbp1) gene rescued the expression of Tlr3 and RelA in postnatal Sdy neurospheres

In order to confirm whether Tlr3, RelA and Sp1 were directly regulated by dysbindin-1, I carried out a rescue experiment in which mock or murine dysbindin-1 (Dtnbp1) gene was nucleofected into neurospheres derived from Sdy mice (fig.4.5A). Following 24 hours post nucleofection, neurospheres were incubated with saline or polyI:C for three hours (fig.4.5A). As shown in figure 4.5(B), dysbindin-1 (Dtnbp1) gene started to be expressed in Sdy neurospheres nucleofected with Dtnbp1 gene (positive control), however Dtnbp1 gene was not expressed in mock nucleofected Sdy neurospheres (negative control). In Dtnbp1 nucleofected neurospheres, polyI:C caused a slight but non-significant increase in Dtnbp1 gene expression compared to saline incubated neurospheres (Student's two-tailed t-test; $P>0.05$; N=3; fig.4.5B), suggesting that nucleofected neurospheres were also responsive to polyI:C. In comparison to mock nucleofected neurospheres, Dtnbp1 gene caused an approximately four-fold increase in Tlr3 expression in Sdy neurospheres regardless of the treatment (two-way ANOVA followed by Tukey's multiple comparisons test; $P<0.0001$; N=3; fig.4.5B). Similarly, RelA expression was significantly induced in Dtnbp1 nucleofected neurospheres that were incubated with saline compared to mock nucleofected neurospheres that were incubated with saline ($P<0.05$) or polyI:C ($P<0.01$) (two-way ANOVA with Tukey's multiple comparisons test; N=3; fig.4.5B). Although there was a slight increase in Sp1 expression following Dtnbp1 nucleofection, this did not reach statistical significance (two-way ANOVA with Tukey's post-hoc test; $P>0.05$; N=3; fig.4.5B). Taken together, dysbindin-1 intrinsically regulated the expression of Tlr3 and RelA in the SVZ cells.

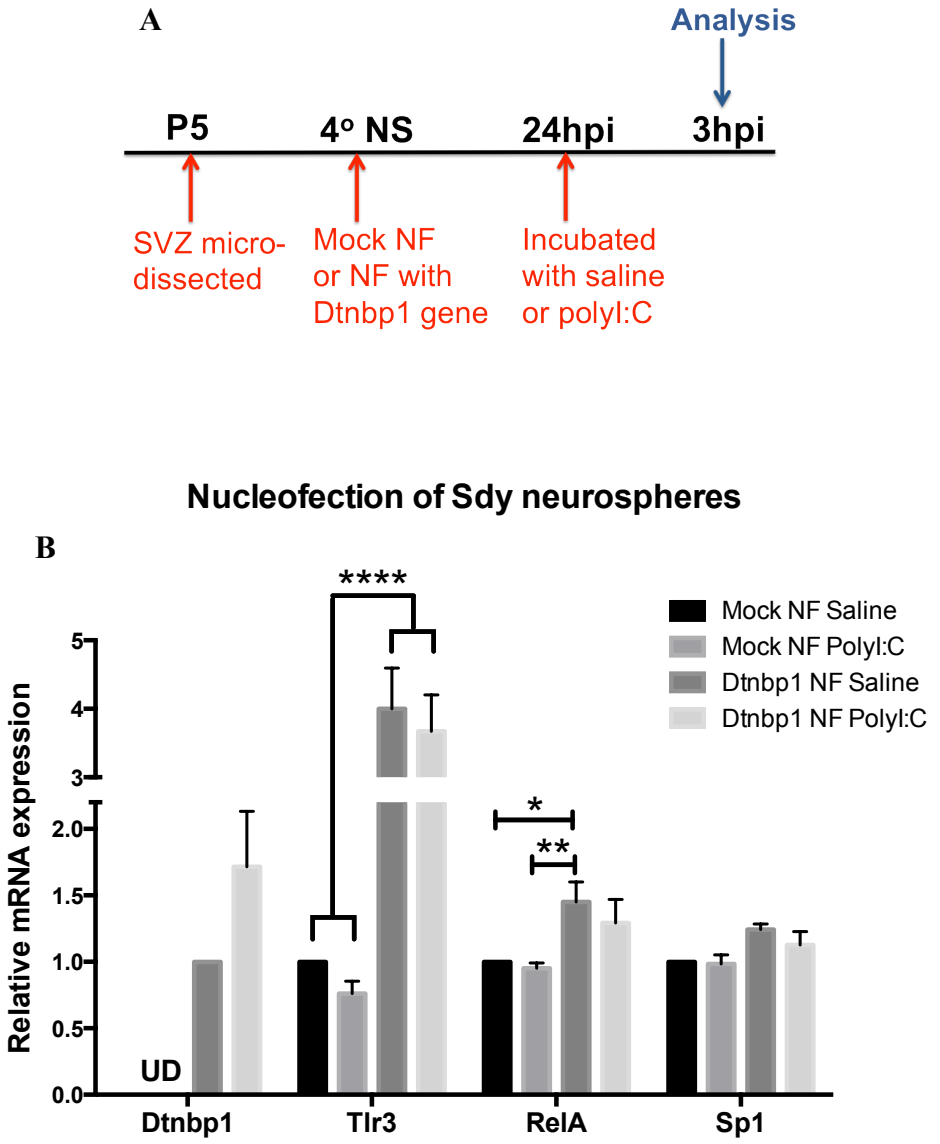

Figure 4.5 Nucleofecting Sdy neurospheres with dysbindin-1 (Dtnbp1) gene rescued expression of Tlr3 and RelA genes

(A) Design of nucleofection (NF) experiment in which SVZ-derived neurospheres (NS) were used in RT-qPCR (B). **4°** denotes quaternary; **hpi** means hours post-incubation.

(B) Expression of dysbindin-1 (Dtnbp1) gene was undetermined (UD) in mock NF Sdy neurospheres that were incubated with saline or polyI:C. However, expression of Dtnbp1 gene was induced in Sdy NS following nucleofection with Dtnbp1 gene. Relative to mock NF neurospheres, gene expression of Tlr3 and RelA, but not Sp1, was significantly induced following nucleofection with Dtnbp1 gene in Sdy neurospheres. Mean ± SEM from three independent experiments. Data were analyzed using two-way ANOVA with Tukey's post-hoc test.
*P<0.05; **P<0.01; ****P<0.0001.

4.2.5 Proposed (dysbindin-1)-Tlr3-RelA-Sp1 signalling pathway during polyI:C-induced inflammation

Based on my results described above, I propose a novel functional role for dysbindin-1 in mediating Tlr3-RelA-Sp1 signalling pathway (fig.4.6). Previously, Tlr3, RelA and Sp1 were all shown to mediate cell proliferation. Since our GxE model showed an inhibited expression of Tlr3, RelA and Sp1 (i.e. disrupted inflammatory response), this might explain the reduction in SVZ proliferation.

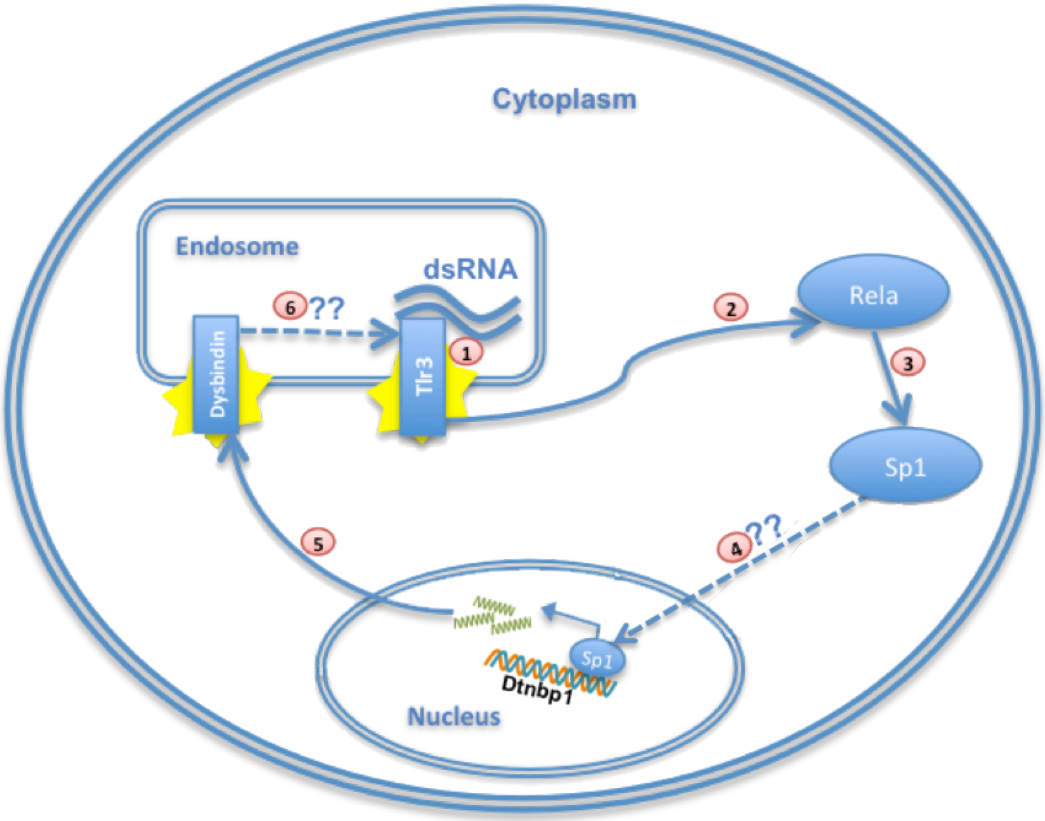

Figure 4.6 Mechanistic role of dysbindin-1 in regulating inflammatory response and maintaining SVZ proliferation during inflammation

Following polyI:C (dsRNA) recognition by Tlr3, it becomes activated (1) and induces RelA (2) which transactivates Sp1 (3). Sp1 is predicted to bind to the promoter region in dysbindin-1 (Dtnbp1) gene (4) and this might explain the increase in dysbindin-1 (Dtnbp1) gene expression that I found (5). I predict dysbindin-1 protein binds directly to Tlr3 protein and mediates its function (6). Together, these genes maintain SVZ proliferation during inflammation.
Note: for simplicity, RelA-Sp1 transcriptional regulation is drawn in the cytoplasm. References for numbers 1 to 4 in the diagram are as follows: 1&2(Alexopoulou et al., 2001); 3(Doyle et al., 2013) and 4(Liao and Chen, 2004).

4.3 Discussion

In this chapter, I showed novel data that repeated polyI:C injections resulted in a significant reduction of SVZ proliferation in Sdy, but not WT mice at P12. This might be due to the inhibited inflammatory response in the GxE model that I have confirmed both *in vivo* and *in vitro*. Unexpectedly, polyI:C induced dysbindin-1 expression suggesting a role for dysbindin-1 in mediating inflammation. I have confirmed this by nucleofecting Sdy neurospheres with Dtnbp1 gene that rescued the gene expression of Tlr3 and RelA.

4.3.1 Decreased SVZ proliferation in the postnatal GxE model

Proliferation in the postnatal SVZ has not been previously characterized in response to systemic inflammation. Here, I showed that SVZ proliferation was slightly but non significantly reduced in postnatal WT mice given polyI:C. However, loss of dysbindin-1 in Sdy mice resulted in a significant reduction in postnatal SVZ proliferation following polyI:C injections. These results suggested a role of dysbindin-1 in maintaining proliferation post inflammation.

Current studies have primarily administered polyI:C during embryonic development, and studied proliferation at various stages of development. However, the time-point of inducing inflammation is critical and may result in confounding differences between studies. To the best of my knowledge, studies were consistent in showing that polyI:C administration during embryonic development resulted in significant reductions in CNS proliferation. For example, polyI:C injection in

pregnant mice reduced proliferation of embryonic cortical progenitors (Soumiya et al., 2011) as well as cerebral cortical cells in P8 pups (De Miranda et al., 2010). Similarly, proliferation was significantly reduced in embryonic cortical neurospheres cultured with polyI:C (Lathia et al., 2008, Yaddanapudi et al., 2011). Since the expression of polyI:C specific ligand, Tlr3, was shown to be higher during embryonic than postnatal development (Lathia et al., 2008), this may indicate that activating Tlr3 embryonically may cause stronger detrimental effect than postnatal activation.

4.3.2 Inhibited immune response in the postnatal GxE model

I have shown that Tlr3, RelA and Sp1 genes were expressed both *in vivo* and *in vitro* in the postnatal SVZ of WT and Sdy mice. Following polyI:C administration, WT mice increased the expression of these genes. However, Sdy mice showed an inhibited expression of Tlr3, RelA and Sp1 following polyI:C administration, indicating a role of dysbindin-1 in regulating the inflammatory response. I have further confirmed this at the protein level that showed reduced expression of Tlr3 in Sdy mice given polyI:C compared to increased expression of Tlr3 immunofluorescence in WT polyI:C group. Furthermore, the baseline expression of Tlr3 protein in Sdy mice looked slightly reduced than in WT mice, which may suggest disrupted expression of Tlr3 protein in Sdy mice under normal conditions. The further reduction in Tlr3 protein expression in Sdy mice given polyI:C might be due to the increased cellular consumption of the available Tlr3 proteins, and that loss of dysbindin-1 may disrupt the ability of Sdy cells to generate more Tlr3 proteins in order to meet the increased cellular demand during inflammation. Therefore, this may have resulted in decreased Tlr3 expression in our GxE model. Interestingly, this was

also consistent with another study that showed reduced Tlr3 expression following polyI:C administration to monocytes derived from schizophrenic patients (Muller et al., 2012).

4.3.3 Decreased SVZ proliferation was correlated with inhibited immune response in the postnatal GxE model

As described in the introduction of this chapter, Tlr3, RelA and Sp1 all play important functions in CNS proliferation. Here, I showed that polyI:C induced the expression of these genes in WT mice and was associated with maintained SVZ proliferation. However, Sdy mice given polyI:C showed inhibited expression of these genes, which was correlated with reduced SVZ proliferation. Together, these may suggest novel roles for dysbindin-1 in regulating immune response and maintaining SVZ proliferation during inflammation.

4.3.4 PolyI:C increased dysbindin-1 expression in the postnatal SVZ

The role of dysbindin-1 in immunity has not previously been reported. Unexpectedly, I found increased expression of dysbindin-1 in the SVZ after polyI:C administration in WT mice and also in WT neurospheres incubated with polyI:C. Since polyI:C induced Sp1 expression in WT mice and neurospheres, this may suggest transcriptional upregulation of dysbindin-1 expression via Sp1 transcription factor. Sp1 is predicted to directly bind to the promoter region in dysbindin-1 gene (Liao and Chen, 2004), therefore it would be interesting to confirm this in the SVZ (fig.4.6). However, this does not exclude the possibility that RelA itself may also directly bind

to dysbindin-1 gene and promote its transcription, although this needs to be verified. This is especially since dysbindin-1 and RelA proteins were shown to interact in the nucleus, and since dysbindin-1 protein regulated RelA transcriptional activity (Fu et al., 2015). Therefore, it would be interesting to confirm whether Sp1 and/or RelA directly bind to the promoter region in dysbindin-1 gene and regulate its expression in the SVZ. Since both dysbindin-1 and Tlr3 are subcellularly localized in endosomes, it would be interesting to determine through co-immunoprecipitation whether dysbindin-1 protein directly binds to Tlr3 protein specifically to the TRIF-domain, which is an essential adapter protein for mediating Tlr3 signalling as described in Chapter 1. This would clarify whether dysbindin-1 regulates Tlr3 function directly or indirectly (fig.4.6). Also, it is still an open question to determine if dysbindin-1 mediates signalling of other toll-like receptors that are involved in innate immunity.

In addition to the abovementioned novel roles of dysbindin-1 in immune function, dysbindin-1 upregulation during inflammation may have proliferative functions. I have already provided evidence here showing that loss of dysbindin-1 in Sdy mice disrupted SVZ proliferation after polyI:C induced inflammation. Also, dysbindin-1 overexpression was shown to induce cardiac hypertrophy (Rangrez et al., 2013), suggesting a role in proliferation. Moreover, a study reported amplification of chromosome 6p22.3 in aggressive cancer cells (Shen et al., 2013) and dysbindin-1 gene is localized in this region of the chromosome (Straub et al., 2002). Together, dysbindin-1 itself may also mediate SVZ proliferation during inflammation.

4.3.5 Dysbindin-1 (Dtnbp1) gene rescued the expression of immune-related genes in Sdy neurospheres

In order to further confirm the functional association of dysbindin-1 to Tlr3, RelA and Sp1, I have nucleofected Sdy neurospheres with the dysbindin-1 (Dtnbp1) gene and analyzed the expression of these genes. Interestingly, expression of dysbindin-1 as well as Tlr3 and RelA, but not Sp1, was upregulated post nucleofection. This supports my proposed feedback loop from dysbindin-1 to Tlr3-RelA-Sp1 (fig.4.6). Additionally, it confirms a functional role of dysbindin-1 in regulating the expression of immune-related Tlr3 and RelA genes. Since Tlr3 expression was more strongly upregulated than RelA expression following dysbindin-1 overexpression, this may provide further evidence for the potential direct interaction between dysbindin-1 and Tlr3 proteins as discussed above in section 4.3.4. This notion is also supported since Tlr3 immunofluorescence was reduced in the SVZ of Sdy mice (section 4.3.2).

On the other hand, polyI:C did not cause further increase in the expression of dysbindin-1, Tlr3 and RelA in Sdy neurospheres nucleofected with dysbindin-1 (Dtnbp1) gene, and this might be because dysbindin-1 was not endogenously expressed in these mutant neurospheres. Nucleofecting Sdy neurospheres with dysbindin-1 (Dtnbp1) gene only transiently rescued the expression of dysbindin-1, Tlr3 and RelA, and therefore the mutant neurospheres were naturally incapable of responding to polyI:C by further inducing the expression of these genes during inflammation as discussed earlier in section 4.3.2.

4.4 Conclusions

A recent genome-wide association study identified a significant association of schizophrenia with immune signalling pathways (Network and Pathway Analysis Subgroup of Psychiatric Genomics, 2015). I report here novel evidence for the role of the schizophrenia-related dysbindin-1 in mediating innate immunity. I demonstrated this in the postnatal GxE model in which disrupted Tlr3-RelA-Sp1 signalling pathway was correlated with reduced SVZ proliferation. This suggests that preventing inflammation in schizophrenia by using anti-inflammatory drugs may alleviate these detrimental effects. The results support previous reports regarding the benefits of using non-steroidal anti-inflammatory drugs (NSAIDs) in reducing symptoms severity in schizophrenic patients (Sommer et al., 2012, Sommer et al., 2014).

Chapter 5

Microglia, leukocyte permeability and cytokine secretion in postnatal SVZ of GxE model of schizophrenia

5.1 Introduction

Microglia are the resident macrophages in the brain and are involved in active immune responses against infection or injury. In rodents, macrophages that are generated in the yolk sac from embryonic day 8 (E8) start to colonize the neuroepithelium from E9/E9.5 and give rise to embryonic microglia (reviewed in (Ginhoux and Prinz, 2015)). These embryonic microglia maintain themselves in the brain parenchyma through local proliferation during late gestation and early postnatal development as shown in figure 5.1 (reviewed in (Ginhoux and Prinz, 2015)). Increased microglial density (Radewicz et al., 2000) as well as microglial activation (van Berckel et al., 2008) has been reported in human schizophrenic patients. Given the neurodevelopmental etiology of schizophrenia, this suggests microglia may be dysfunctional during early brain development. In this chapter, I have addressed this hypothesis using postnatal Sdy mice that were given peripheral polyI:C injections, which together represent gene x environment (GxE) model of schizophrenia. On the other hand, increased lymphocyte infiltration has been found in the hippocampus of schizophrenic patients (Busse et al., 2012). Therefore, I sought to address whether our postnatal GxE model might show enhanced leukocyte infiltration into the developing brain. Given the possible association of schizophrenia with abnormal cytokine expression (reviewed in (Watanabe et al., 2010)), I investigated whether our GxE model also show abnormal cytokine secretion. Together, I have addressed these aims in the subventricular zone (SVZ) since it is in contact with the cerebrospinal fluid (CSF), the major source of substance exchange between the systemic circulation and the brain.

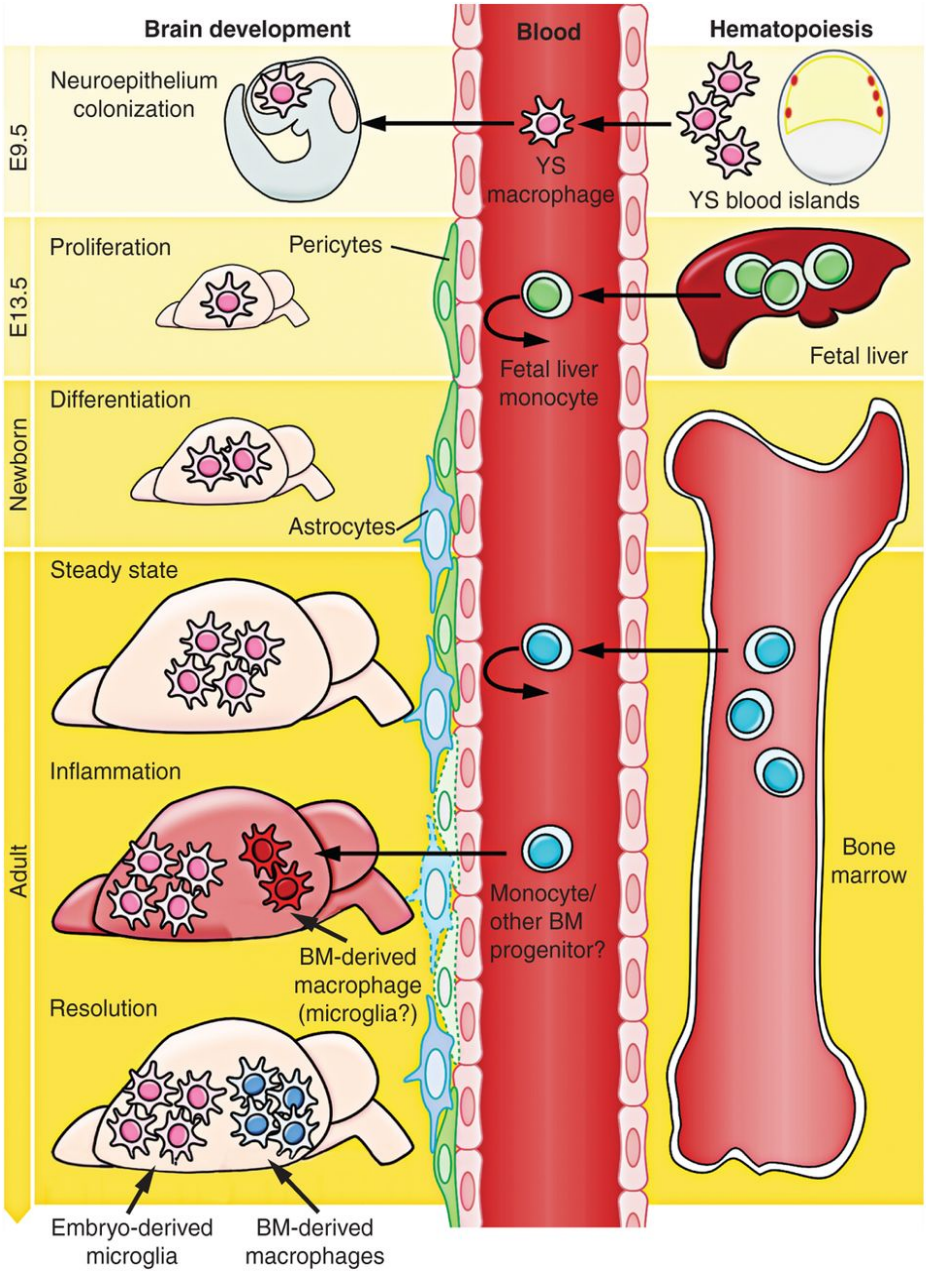

Figure 5.1 Origin of microglia during brain development

Microglia are first established at around E9.0/E9.5 when macrophages derived from the yolk sac (YS) start to colonize the neuroepithelium. The blood-brain barrier (BBB) starts to build from E13.5 isolating the CNS from peripheral macrophages. Resident microglia in the brain expand through local proliferation during late embryonic to early postnatal development. In adulthood, bone marrow (BM) derived macrophages may cross the BBB during inflammation in order supplement local microglial population in the brain.

Image adapted from (Ginhoux and Prinz, 2015).

5.1.1 Microglia are inherently activated in the postnatal SVZ

Surprisingly, very little is known about SVZ microglia in the normal developing brain. To the best of my knowledge, only two recent *in vivo* studies looked at SVZ microglia during normal and early postnatal development (Shigemoto-Mogami et al., 2014, Xavier et al., 2015). In the absence of any inflammation or injury, microglial activation might be age dependent. In control embryos, more than 95% of microglia revealed activated morphology (Cunningham et al., 2013). Postnatally, SVZ microglia showed high activation at P1 (amoeboid shaped and positive for CD68) and this activation gradually decreased at P4 and P10 with less activation at P30 (more ramified and less positive for CD68) (Shigemoto-Mogami et al., 2014). This is in agreement with a study by another group that confirmed that SVZ microglia at P1 and P7 were more activated (CD68+) (Xavier et al., 2015) than in adulthood at P60 which showed reduced CD68 labeling of microglia (Ribeiro Xavier et al., 2015). Although SVZ microglial activation gradually decreased with age, microglia were generally more activated in the SVZ than in the surrounding regions during early postnatal age (Shigemoto-Mogami et al., 2014) and adulthood (Goings et al., 2006).

In order to study microglial activation in postnatal SVZ, I have used two markers (Iba1 and CD68). Iba1 is an ionized calcium-binding adapter molecule 1 that has a role in calcium homeostasis. In immunohistochemistry, Iba1 strongly labels both resting and activated microglia in the brain (Ito et al., 1998), but not macrophages and monocytes (myeloid-cell lineage) (Imai et al., 1996). In order to differentiate activated from resting microglia, I have co-labeled Iba1 with another marker, CD68 or Macrosialin. CD68 is primarily localized in lysosomes and

endosomes and it is involved in promoting phagocytosis and clearing of cellular debris (Holness et al., 1993). Since CD68 also labels monocytes, co-labeling CD68 with Iba1 specifically represents activated microglia, whereas Iba1+ but CD68 negative are resting microglia.

5.1.2 Inflammation may induce leukocyte recruitment into the brain

Systemic inflammation may trigger leukocyte (immune cells) migration from the bloodstream into the CNS where they differentiate into resident macrophages or dendritic cells (reviewed in (Yang et al., 2014)). The likelihood of leukocyte infiltration into the brain may rely on the blood-brain barrier, which is developmentally regulated with a gradual increase in permeability with age. The blood-brain barrier collectively describes four main interfaces between the CNS and periphery: Blood-brain barrier, blood-CSF barrier, outer CSF-brain barrier and inner CSF-brain barrier. Interestingly, the blood-CSF barrier at the choroid plexus has higher permeability than the other barriers (reviewed in (Stolp et al., 2013)), and the SVZ is located adjacent to the choroid plexus. Therefore, infiltration of systemic molecules or cells can be best investigated in the SVZ region.

Here, CD45 antibody was used to label infiltrating leukocytes into the SVZ. CD45 is a leukocyte common antigen which is highly expressed in all leukocytes but only weakly in resident microglia (reviewed in (Guillemin and Brew, 2004)). As discussed earlier, Iba1 antibody strongly labels microglia but not leukocytes, therefore bright amoeboid CD45+ cells but Iba1 negative represent infiltrating leukocytes. Because CD45 marker is broadly expressed in all leukocytes, it cannot be used alone

to detect specific cell type (e.g. monocytes or macrophages) without the use of multiple specific markers. However, the aim of this study was just to determine whether there is immune cell infiltration from the periphery into the SVZ following systemic polyI:C injections.

5.1.3 Neural progenitor cells in the SVZ as a potential source of secreted cytokines

Cytokines are small secretory proteins that are constitutively produced and become upregulated in response to inflammatory stimuli in order to regulate immune function. Cytokines signal through cytokine receptors and are subdivided into different groups, which include lymphokines, interleukins and chemokines (short for chemotactic cytokines) and the latter are mainly involved in chemoattraction and recruitment of leukocytes into inflamed tissue (reviewed in (Zhang and An, 2007)). Determining the function of an individual cytokine can be difficult because several cytokines are produced and interact with each other following immune insult, which together determine the type of immune response (i.e. pro-inflammatory versus anti-inflammatory). Moreover, each cytokine may have a completely different function depending on the cell type from which it is secreted, the target cell and the specific stage of immune response in which it is released (reviewed in (Borish and Steinke, 2003)).

Although cytokines are extensively studied in the peripheral immune system, it has now become clear that cytokines are also produced in the CNS. Microglia, astrocytes and neurons all express cytokine receptors and also secrete cytokines under

normal and inflammatory conditions (reviewed in (Woodroofe, 1995)). In comparison to non-neurogenic brain regions, SVZ is unique in containing neural progenitor cells (NPCs) that maintain themselves into adulthood. Given that microglia are differentially regulated in neurogenic SVZ versus non-neurogenic regions (Goings et al., 2006), this brings the question of whether NPCs might contribute in differentially regulating immune function in the SVZ. One way to address this question is by determining whether NPCs in the SVZ are capable of releasing cytokines and therefore may participate in differential regulation of SVZ immune function through extracellular cytokine signalling.

Interestingly, NPCs in SVZ-derived neurospheres were shown to express chemokine receptors (Ji et al., 2004, Gordon et al., 2009) and were also directly responsive to exogenous chemokines (Gordon et al., 2009, Gordon et al., 2012). Although gene expression of various chemokines were detected in NPCs in SVZ neurosphere assay (Turbic et al., 2011), it is still to be determined if NPCs are also capable of releasing chemokines and/or cytokines. Therefore, one aim of this chapter was to find whether NPCs in the SVZ may release cytokines and hence might be involved in regulating SVZ immune function. Another aim was to determine if cytokine secretion from NPCs might be altered in the GxE model. This can be ideally addressed in SVZ-derived neurospheres that predominately consist of NPCs (reviewed in (Conti and Cattaneo, 2010, Jensen and Parmar, 2006)) and any secreted cytokines in culture medium can be easily harvested and analyzed.

5.1.4 Research questions

Current animal models of schizophrenia have not examined the effect of both GxE factors on microglia and brain permeability during early postnatal development. Furthermore, it is still unclear if NPCs might regulate SVZ immune function through cytokine secretion, and whether this might be modulated in GxE model. In order to address these questions, postnatal Sdy mice in combination with systemic inflammation was used as model of GxE in schizophrenia. The aim of this chapter was to specifically study in the SVZ: 1) microglial cell number, 2) microglial activation, 3) leukocyte infiltration and cytokine secretion in a postnatal GxE model of schizophrenia.

5.2 Results

5.2.1 Dysbindin-1 loss was associated with increased microglial number in the SVZ

Microglia in the SVZ were analyzed at P12 following repeated (P5-9) saline or polyI:C injections to WT (N=4) and Sdy (N=6) pups. Using Iba1 marker, total number of microglial cells were quantified in the whole dorsal SVZ in all the four groups. However, morphological differences of individual cells were not taken into consideration at this stage. Two-way ANOVA revealed a main effect of the genotype ($F(1,16)=18.93$; $P<0.001$; N=4-6 per group) regardless of the treatment (fig. 5.2A). Specifically, Sdy mice showed significantly higher density of Iba1+ microglia in the dorsal SVZ in comparison to WT mice. Representative images for Iba1+ cells in dorsal SVZ are shown in figure 5.2 for WT saline group (B-B') and Sdy polyI:C group (C-C'). Surprisingly, polyI:C treatment within WT or Sdy groups resulted in slight, but not significant, reduction in total number of microglia in the postnatal SVZ (fig. 5.2A).

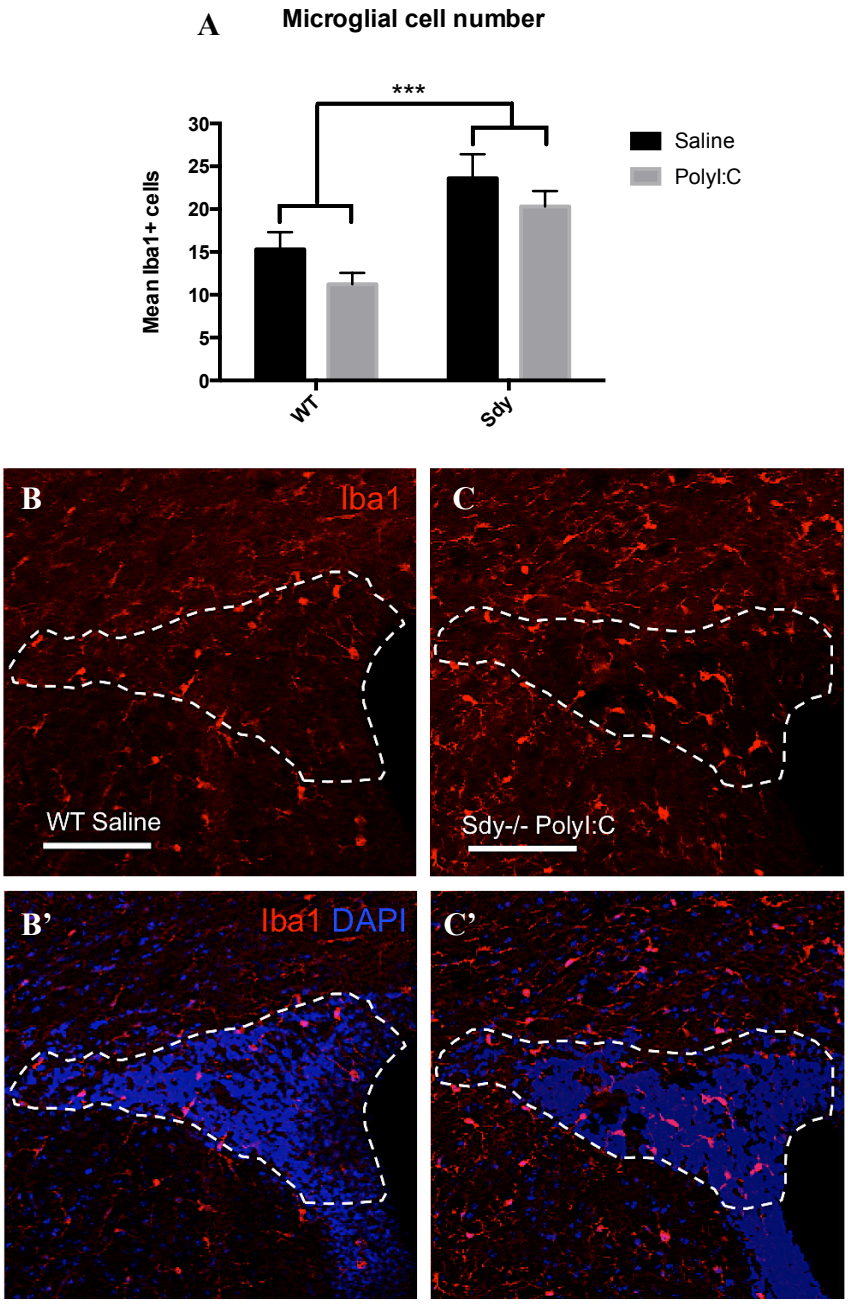

Figure 5.2 Abnormal microglia population numbers in the postnatal SVZ of Sdy mice

(A) Mean number of Iba1+ microglia cells in the dorsal SVZ at P12. Mean ± SEM. Data were analyzed using two-way ANOVA. N=4-6 per group. ***P<0.001.

(B-C') Representative images of Iba1+ microglia in the dorsal SVZ (dotted lines) in WT saline (B-B') and Sdy polyI:C (C-C') groups. Scale bar 100µm.

5.2.2 Microglia were activated in the normal developing SVZ

In the postnatal SVZ, the number of Iba1+ cells that co-expressed the activation marker CD68 were quantified in order to determine the effect of polyI:C injections and/or dysbindin-1 mutation on microglial activation. As shown in figure 5.3A, the number of Iba1+/CD68+ cells seemed slightly reduced in WT polyI:C group. Overall, there was a significant main effect of polyI:C injections in the number of Iba1+/CD68+ cells (two-way ANOVA; $F(1,8)=6.84$; $P<0.05$; N=3 per group; fig.5.3A), however Tukey's multiple comparisons test did not reveal a specific difference among the four groups. Hence, a priori power analysis was performed in GPower Software using the effect size of ($f=0.908$) from my data, an alpha of 0.05 and a power of 0.80. Based on these parameters, a total of 13 mice are needed in order to reach >80% chance for detecting differences between groups in the number of Iba1+/CD68+ SVZ cells.

Interestingly, a distinct phenotype was observed when analyzing the proportion of microglia per group that were either activated and non-activated. In the healthy brain at P12, more than 70% of resident microglia Iba1+ expressed the activation marker CD68 in the dorsal SVZ (fig. 5.3B). This was analyzed using Student's two-tailed t-test that showed 71.5% of the total Iba1+ microglia in WT saline group co-expressed CD68 relative to 28.5% that were CD68 negative ($t(4)=16.40$; $P<0.0001$; N=3; fig. 5.3B). However, only 46% of microglia were activated Iba1+/CD68+ in Sdy saline group compared to 54% that were Iba1+/CD68- cells. A similar trend was also found in both WT and Sdy pups following polyI:C treatment (fig.5.3B). By comparing the percentage of activated microglia among all groups, I found a significantly higher percent of activated microglia (Iba1+/CD68+)

in WT saline group than the other three groups as determined using two-way ANOVA followed by Tukey's multiple comparisons test ($P<0.05$; N=3 per group; fig.5.3B). Representative images for the co-localisation of Iba1+/CD68+ are shown in figure 5.3 for WT saline group (C-C") versus Sdy polyI:C group (D-D"). Conversely, the proportion of inactive microglia Iba1+/CD68- is significantly less in the WT saline in comparison to the remaining groups (two-way ANOVA followed by Tukey's multiple comparisons test; $P<0.05$; N=3 per group; fig.5.3A).

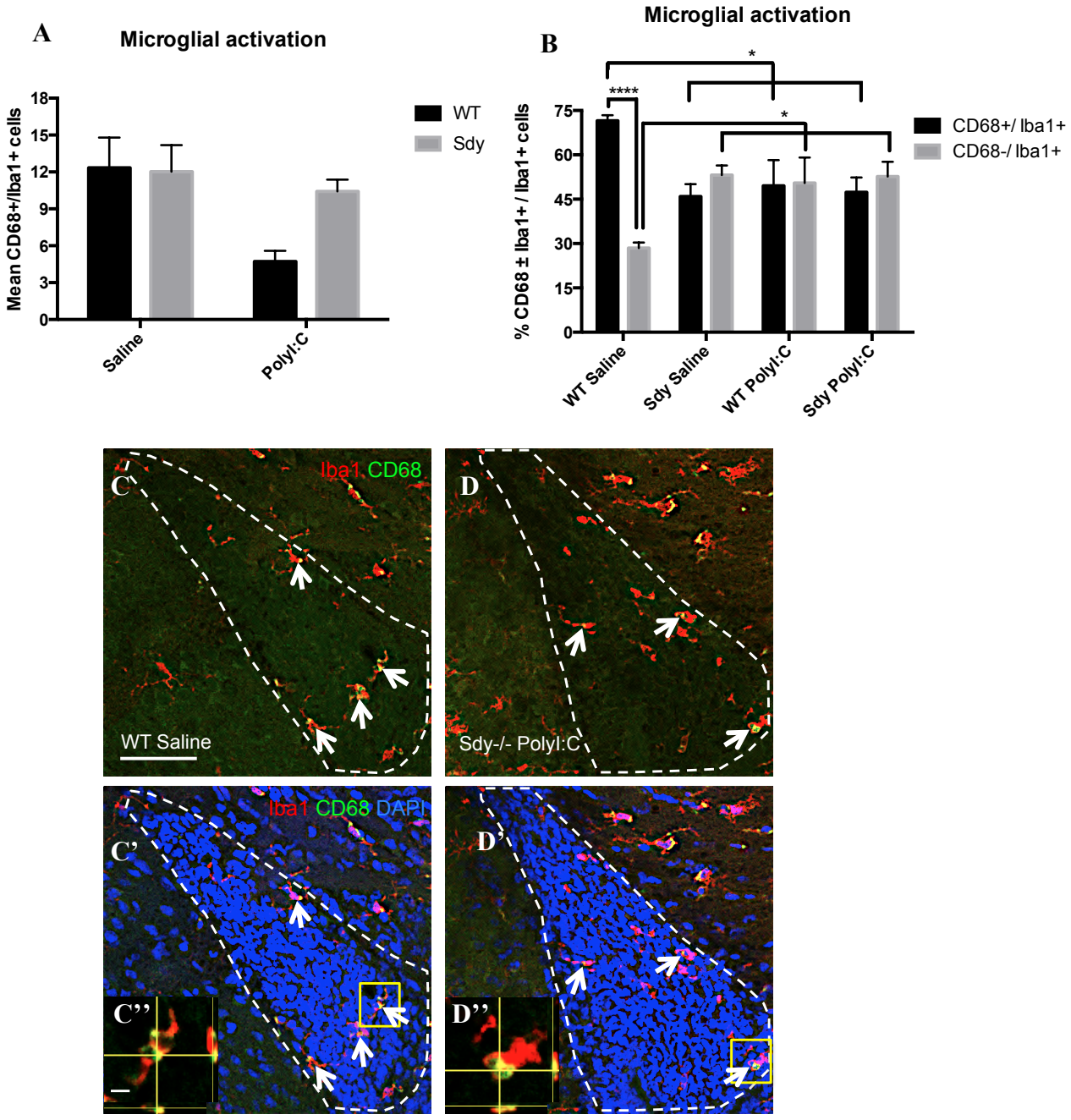

Figure 5.3 Intrinsic microglia activation in the normal developing SVZ

(A) Mean number of Iba1+/CD68+ cells in the dorsal SVZ at P12. N=3 per group.

(B) Percent of microglia Iba1+ cells that are either in active CD68+ or resting CD68- state in the dorsal SVZ at P12. Mean ± SEM. Data were analyzed using Student's two-tailed t-test or two-way ANOVA with Tukey's post-hoc test as appropriate. N=3 per group. *P<0.05; ****P<0.0001.

(C-D') Representative images of co-localized Iba1+/CD68+ cells (arrows) in the dorsal SVZ (dotted lines) in WT saline (C-C') and Sdy polyI:C (D-D') groups. Scale bar 50µm.

(C"-D") Orthogonal views of Iba1+/CD68+ cells in WT saline (C") and Sdy polyI:C (D") groups magnified from the yellow-boxed areas in C' and D', respectively. Scale bar 5µm.

5.2.3 High leukocyte infiltration into the SVZ of GxE model

The infiltrating leukocytes that were quantified in this study showed amoeboid morphology and expressed very high CD45 expression with total absence of Iba1 staining. Intraperitoneal injections of polyI:C resulted in significant immigration of CD45+/Iba1- circulating leukocytes into the dorsal SVZ of Sdy pups. By using two-way ANOVA there was a significant increase in CD45+/Iba1- cells in the Sdy polyI:C group (mean=5; N=4) in comparison to WT saline group (mean=1; N=6) as identified using Tukey's multiple comparison test ($P<0.001$; fig. 5.4A). Representative images of CD45+/Iba1- cells are shown in the Sdy polyI:C group (fig.5.4C-C') but not in WT saline group (fig.5.4B-B'). However, polyI:C injections to WT pups (mean=2.33; N=6) resulted in slight but non-significant infiltration of leukocytes into SVZ compared to WT saline group (mean=1; N=6).

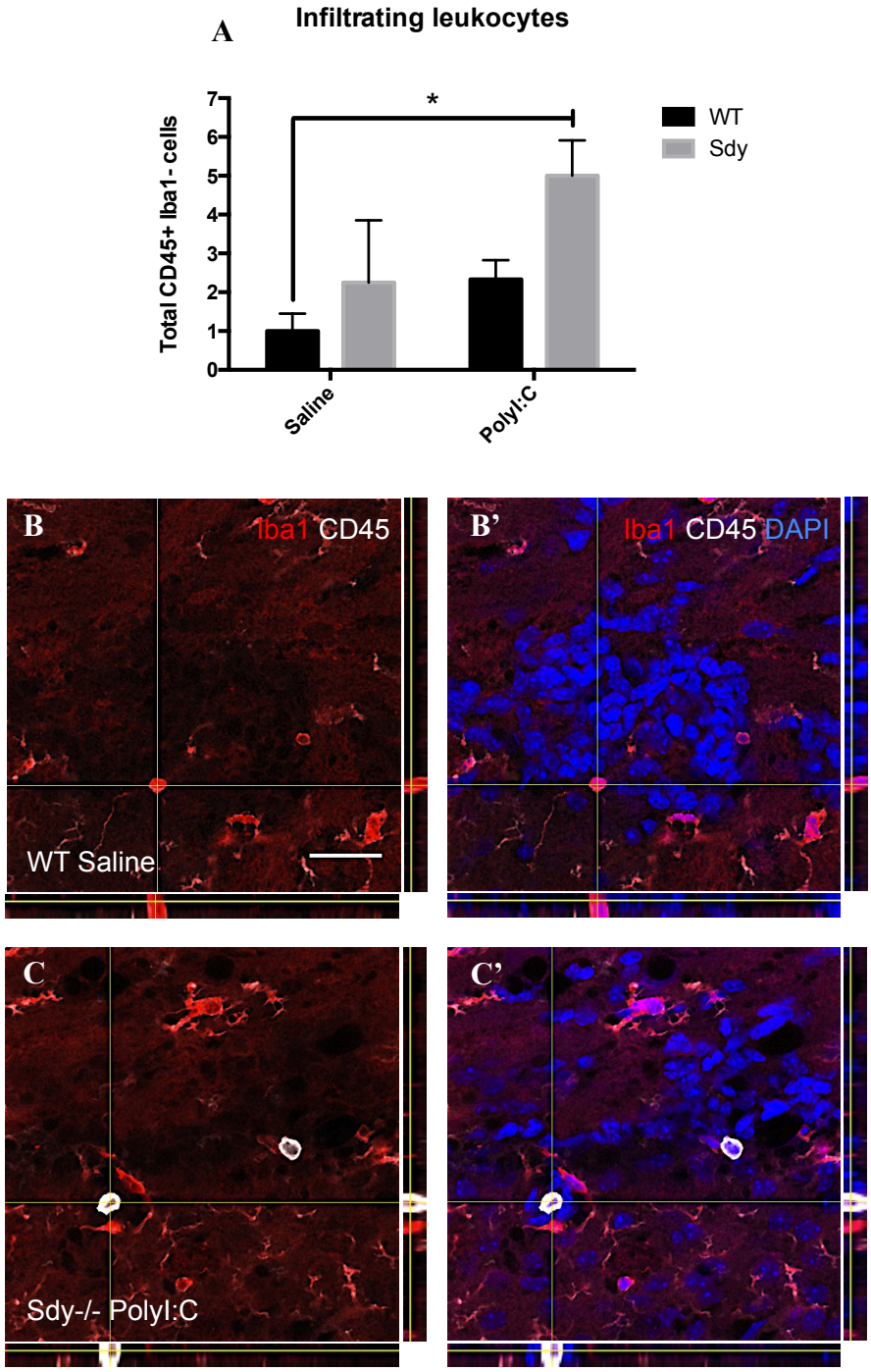

Figure 5.4 Increased leukocyte infiltration into the postnatal SVZ of Sdy mice post inflammation

(A) Total number of infiltrating leukocytes that are CD45+ but Iba1- cells in the dorsal SVZ at P12. Mean ± SEM. Data were analyzed using two-way ANOVA N=4-6 per group. *P<0.05.

(B-C') Orthogonal view images showing CD45+ but Iba1- cells in the dorsal SVZ of Sdy polyI:C group (C-C') but not in WT saline group (B-B'). Scale bar 25µm.

5.2.4 SVZ-derived neurospheres were capable of releasing cytokines and were modulated by dysbindin-1 mutation under baseline and inflammatory conditions

In order to determine the effect of GxE factors on cytokine release, SVZ neurospheres from P5 WT and Sdy pups were incubated with saline or polyI:C for 24 hours and supernatants were collected and analyzed. As illustrated in figure 5.5(A-D), I show novel preliminary data that SVZ neurospheres released cytokines under normal conditions in WT saline group. The baseline level of CXCL10, TIMP-1 and CCL2 secretion was roughly ten times more strongly expressed than the level of CXCL1, M-CSF, CCL5 and CXCL12 secretion from WT saline neurospheres (fig.5.5C-D). Furthermore, WT neurospheres responded to polyI:C induced inflammation by enhancing the release of CXCL10, CCL2, CXCL1 and CCL5 chemokines (fig.5.5C-D). Although CXCL10 and CCL5 secretions were induced in WT and Sdy neurospheres during inflammation, CCL2 release was only induced in WT polyI:C neurospheres whereas CXCL1 secretion was more strongly induced in Sdy polyI:C than WT polyI:C neurospheres (fig.5.5C-D). This could indicate that dysbindin-1 mutation in Sdy neurospheres may cause differential response to inflammation in comparison to WT polyI:C neurospheres. Compared to WT saline neurospheres, the release of CXCL10 and CCL2 were reduced in Sdy saline neurospheres and also TIMP-1, M-CSF and CXCL12 were all reduced in Sdy neurospheres (with or without polyI:C) indicating a role of dysbindin-1 in regulating cytokine release in both baseline and inflammatory conditions (fig. 5.5C-D).

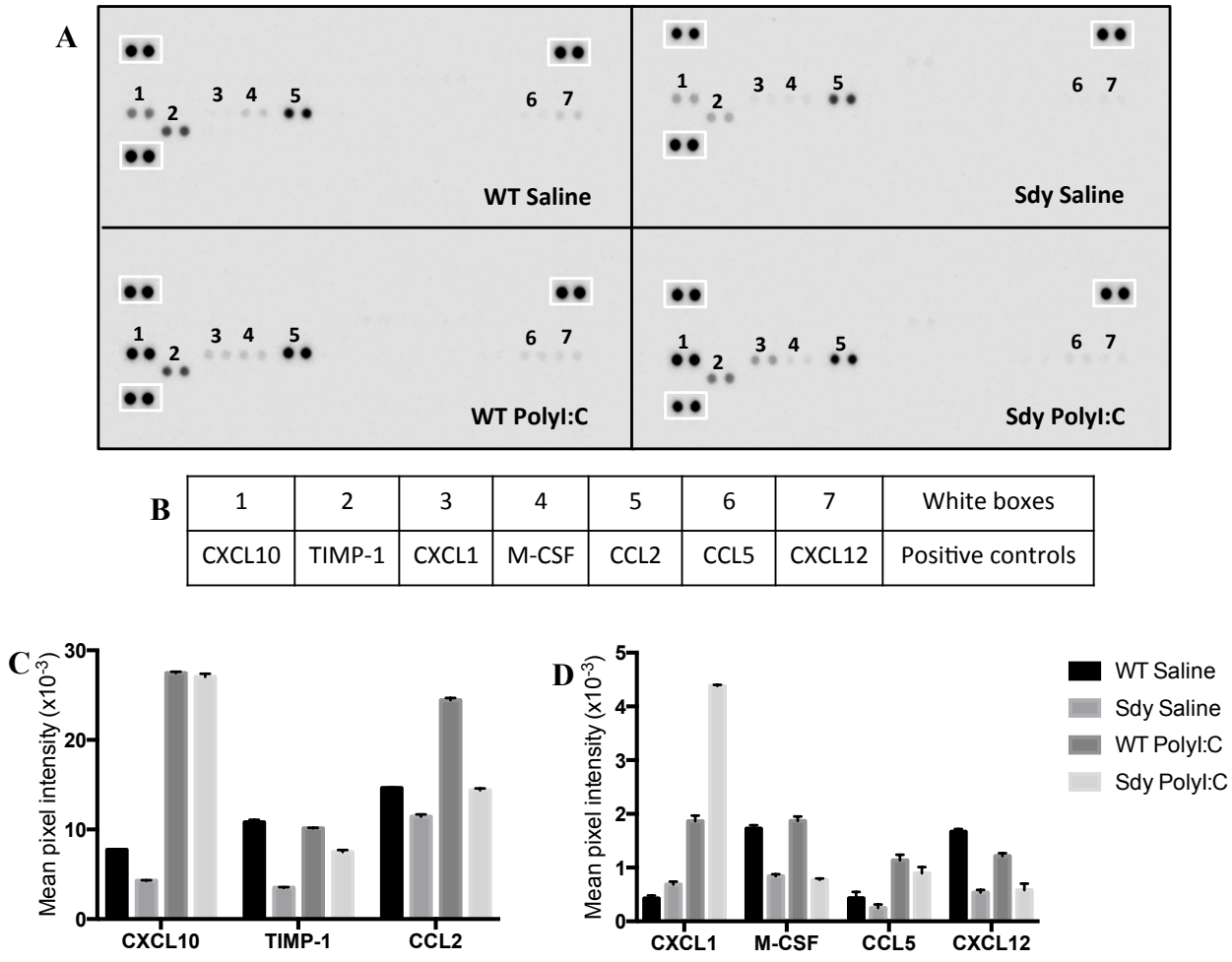

Figure 5.5 Differential cytokine release from WT and Sdy neurospheres following incubation in saline or polyI:C

(A-B) Representative images of detected cytokines in proteome arrays that were incubated separately with supernatants from cultured WT or Sdy neurospheres that were incubated with saline or polyI:C for 24 hours. Each detected cytokine in duplicate is numbered, and the numbers (1-7) corresponds to cytokines in (B). White boxes are positive control spots.

(C-D) Pixel intensity of each detected cytokine was quantified and represented as mean ± SEM from duplicate. Signal intensity is proportional to the amount of cytokines present in the sample. Data are representative of one experiment.

5.3 Discussion

I have shown here increased microglial density in the postnatal SVZ of the schizophrenia-related Sdy model. Also, I found that the majority of Iba1+ microglia co-expressed CD68 activation marker in the normal developing SVZ. Combining Sdy model with polyI:C-induced inflammation resulted in significant infiltration of leukocytes into the postnatal SVZ. Furthermore, abnormal cytokine secretion was detected in Sdy neurospheres with or without inflammation.

5.3.1 Increased microglial density in Sandy mice

Loss of dysbindin-1 in Sdy model of schizophrenia resulted in increased number of microglia in the dorsal SVZ. These results are interestingly similar to another study that showed increase in microglial density in postmortem schizophrenic brains (Radewicz et al., 2000).

Given the germinal mutation of dysbindin-1 in Sdy model, it suggests two possible hypotheses for the postnatal increase in microglial number: embryonic origin and/or postnatal origin. Dysbindin-1 was shown to be strongly expressed during late embryonic development (E14/E18) (Ghiani et al., 2010), which coincided with massive proliferative potential of microglia at E16 (Alliot et al., 1999). This may suggest a role of dysbindin-1 in regulating embryonic microglial pool, in which dysbindin-1 loss resulted in over-expansion of prenatal microglial population that continued at least to P12.

On the other hand, dysbindin-1 showed a higher expression during the first postnatal week than in young adulthood at P21 or P45 (Ghiani et al., 2010). Interestingly, the first postnatal week also corresponded to a high microglial proliferation (PCNA+) at P1 and P9 especially in the SVZ (Alliot et al., 1999). Similarly, microglia showed a significantly higher (~40%) proliferative capacity in microglial cell culture derived from mice during their first postnatal week than at P11 to P14 (Alliot et al., 1999). Interestingly, these might explain the massive increase (~50%) in microglial population (Iba1+) in the SVZ at P10 compared to P1 and P4 (Shigemoto-Mogami et al., 2014), which might be due to continual accumulation of microglial cells in the SVZ due to intense microglial proliferation during the first postnatal week. However, it should be noted that another study reported no microglial proliferation in the postnatal murine SVZ (P1 and P7) following a single pulse of BrdU (only very few cells were co-labeled) (Xavier et al., 2015). Also I found no proliferative microglia at P12 in the dorsal SVZ of all four groups (i.e. PHi3/Iba1 double-labeling; data not shown). This discrepancy might be due to the use of different markers. PCNA labels proliferative cells during all phases of the cell cycle, except G0 (Kurki et al., 1986). However, BrdU and PHi3 only label cells during S-phase and M-phase, respectively. Therefore PCNA marker might "catch" more proliferative microglia than using BrdU and PHi3 antibodies. Taken together, dysbindin-1 might be involved in regulating microglial proliferation during the first postnatal week and that dysbindin-1 dysregulation (as in our Sdy model) resulted in abnormally increased microglial density at P12.

5.3.2 Microglia were more activated in normal than immune challenged postnatal SVZ

In postnatal SVZ, I found that the majority of microglia (>70%) were activated under normal conditions. This may suggest the importance of activated microglia in immune surveillance and clearance of cellular debris in order to maintain normal brain development during early postnatal age (Paolicelli et al., 2011).

Contrary to my expectation, systemic inflammation did not cause further activation of WT microglia but rather caused a reduction by 22% in comparison to WT control. Previous studies showed that systemic challenge with LPS induced microglial activation (CD68+) in the adult hippocampus (Sierra et al., 2010, Monje et al., 2003). Also, intracerebroventricular administration of polyI:C was shown to activate microglia in the cerebral cortex of adult mice (Town et al., 2006). However, no studies have looked at postnatal SVZ microglia in response to peripheral inflammation, which is especially interesting since SVZ microglia were differentially activated in comparison to other brain regions (Goings et al., 2006, Shigemoto-Mogami et al., 2014). Taken together, the postnatal SVZ may respond differently to inflammatory challenges, and caution should be taken when comparing data with variable age, route of administration or even brain region of study.

In the postnatal Sdy mice (regardless of treatment), about 50% of total microglia in the dorsal SVZ were co-labelled with CD68 activation marker. Here, the interpretation of data is complex since CD68 is a lysosome-associated marker, and Sdy mice are phenotypically associated with lysosomal dysfunction (Li et al., 2003, Swank et al., 1991). Therefore, other activation markers that are not expressed in

lysosomes should be considered in the future when studying microglial activation in Sdy model.

5.3.3 Systemic inflammation induced leukocyte recruitment into the postnatal SVZ of Sdy but not WT mice

Following polyI:C-induced inflammation, there was no increase in leukocyte infiltration into the SVZ of postnatal WT mice. This might be due to the intact brain barrier during early development. A previous study reported that prolonged systemic inflammation during postnatal age resulted in increased brain permeability in adult but not in postnatal age (Stolp et al., 2005). This was also true in a stroke model in which there was increased brain permeability in adult but not in early postnatal rats (Fernandez-Lopez et al., 2012). Interestingly, the same study reported low neutrophil infiltration into the postnatal brains (Fernandez-Lopez et al., 2012) consistent with my data of limited leukocyte infiltration into the SVZ of WT polyIC group.

On the other hand, inflammation in Sdy mice increased leukocyte permeability into the postnatal SVZ. Since Tlr3 is expressed in the choroid plexus (Stridh et al., 2013), it may suggest that Tlr3 might be involved in the choroid plexus barrier function. In the SVZ, I found inhibited Tlr3 response to polyI:C in Sdy mice (Chapter 4), however is still to be determined if Tlr3 inflammatory response might also be disrupted in the choroid plexus. This might explain the increased infiltration of peripheral immune cells into the SVZ of Sdy but not WT after inflammation. Also, chemokines are involved in promoting leukocyte entry into the brain (reviewed in (Williams et al., 2014)). Here, I found strong upregulation of CXCL1 release from

NPCs in Sdy polyI:C group, suggesting a role of CXCL1 chemokine in attracting leukocytes into the brain although this needs to be tested *in vivo*.

Interestingly, increased leukocyte recruitment into the SVZ of Sdy polyIC group was also associated with reduced locomotion in adulthood (Chapter 3). This is in agreement with previous studies showing that liver inflammation in adulthood resulted in increased monocyte recruitment into the brain (D'Mello et al., 2009, Kerfoot et al., 2006), which was also associated with sickness behavior (i.e. decreased locomotor activity). Remarkably, this sickness behavior was improved (i.e. increased social interaction and reduced immobility) by inhibiting monocyte recruitment into the brain during inflammation (D'Mello et al., 2009). Taken together, combining dysbindin-1 loss with systemic polyI:C-induced inflammation resulted in abnormal leukocyte permeability into the postnatal brain, and this may explain the reduced locomotion reported in adulthood.

5.3.4 Dysbindin-1 mediated cytokine secretion from SVZ NPCs during normal and inflammatory conditions

I have demonstrated that NPCs in SVZ-derived neurospheres from P5 mouse pups were capable of secreting cytokines. Interestingly, this is consistent with a previous report that showed cytokine secretion from cortical NPCs, which were isolated from P0 mouse pups (Mosher et al., 2012). Furthermore, I showed that SVZ NPCs were also responsive to inflammatory stimuli through regulation of cytokine release. The proteome array used in this study showed that the majority of secreted cytokines from NPCs were specifically chemokines (i.e. CXCL10, CCL2, CXCL1, CCL5 and

CXCL12) and only one cytokine (M-CSF) and another protein (TIMP-1) were detected. Loss of dysbindin-1 in Sdy neurospheres disrupted cytokine secretion under both normal and inflammatory conditions.

Chemokines can be classified according to function into two groups: homeostatic and inflammatory chemokines. Homeostatic chemokines are constitutively produced whereas inflammatory chemokines are only upregulated in response to inflammatory stimuli (reviewed in (Borish and Steinke, 2003, Cartier et al., 2005)). Here, I found that the level of chemokine secretion was generally reduced in Sdy saline neurospheres in comparison to baseline level in WT saline neurospheres. This may suggest a novel role of dysbindin-1 in regulating chemokine secretion from NPCs under normal conditions especially since dysbindin-1 is involved in intracellular vesicle trafficking (Li et al., 2003) and exocytosis (Chen et al., 2008).

Following polyI:C-induced inflammation in WT neurospheres, I found that the release of CXCL10, CCL2, CXCL1 and CCL5 chemokines were all upregulated whereas CXCL12 remained unchanged. Interestingly, CXCL10, CCL2, CXCL1 and CCL5 are already described as inflammatory chemokines whereas CXCL12 mainly acts as a homeostatic chemokine (reviewed in (Borish and Steinke, 2003, Cartier et al., 2005)). In Sdy neurospheres, CCL2 was not upregulated in response to polyI:C whereas CXCL1 was far more upregulated than in WT polyI:C neurospheres. Taken together, the response of homeostatic and inflammatory chemokines in NPCs of WT polyI:C group was consistent with their physiological features, however loss of dysbindin-1 caused abnormal chemokine secretion during inflammation.

On the other hand, M-CSF and TIMP-1 were also secreted from SVZ neurospheres. M-CSF regulates NPCs survival and proliferation (reviewed (Chitu et al., 2016)) whereas TIMP-1 is involved in repair mechanisms, cell survival and inflammatory responses through inhibition of matrix metalloproteinases (MMP) (Gardner and Ghorpade, 2003). Here, I found that the level of M-CSF and TIMP-1 secretion in WT neurospheres was unaltered in response to polyI:C, however the level of M-CSF and TIMP-1 release was reduced in Sdy neurospheres under normal and inflammatory conditions. Taken together, polyI:C did not induce M-CSF and TIMP-1 secretion from WT NPCs whereas dysbindin-1 loss in NPCs resulted in inhibited M-CSF secretion together with imbalance of TIMP-1/MMP regulation.

5.4 Conclusions

Microglial dysfunction has been reported in schizophrenic patients although little is known about its possible causes. I have shown here abnormal microglial density in the SVZ of postnatal Sdy mice suggesting a developmental origin of microglial dysregulation in schizophrenia. In addition, my postnatal GxE model of schizophrenia showed enhanced leukocyte infiltration into the SVZ. Since SVZ NPCs from WTs differentially released cytokines in response to inflammation, this may suggest a role of NPCs in regulating SVZ immune function. Interestingly, I found abnormal cytokine release from dysbindin-1 mutant NPCs under both baseline and inflammatory conditions. Therefore, it would be interesting in the future to determine how altered cytokine secretion from NPCs of GxE model might directly regulate microglial function and leukocyte permeability into the SVZ. On the other hand, I have reported massive microglial activation in the normal developing SVZ although the phenotypic identity of these microglia is not clear. This can be addressed using M1 (i.e. cytotoxic) and M2 (i.e. neuroprotective) activation markers, which may also determine whether dysbindin-1 loss and inflammation might push microglia towards a specific polarity during postnatal development

Chapter 6

General discussion

6.1 Overall view

In schizophrenia, several genetic and environmental (GxE) risk factors are well characterized. In addition, decreased adult hippocampal neurogenesis was reported in schizophrenic patients (Reif et al., 2006). Abnormal subventricular zone (SVZ) neurogenesis may also contribute to schizophrenia since newborn neurons in the adult humans are thought to migrate to the striatum (Ernst et al., 2014), a region that is possibly involved in cognitive deficits in schizophrenia (Simpson et al., 2010). However, it is still unclear whether genetic and environmental factors of schizophrenia may directly interact and regulate adult neurogenesis. In my thesis, I have shown that polyI:C-induced inflammation in postnatal dysbindin-1 mutant mice (GxE model) resulted in reduced adult SVZ proliferation and neuroblast populations in the rostral migratory stream (RMS). In the GxE model, behavioural abnormalities relevant to schizophrenia were also found adulthood. Since genetic and environmental factors alone did not alter adult SVZ proliferation or RMS neuroblast populations, this suggested that a functional interaction between the two factors may amplify the observed phenotypes. Mutations in other risk genes (Nrg1 type I and Snap25) did not cause a significant effect on adult SVZ proliferation or RMS neuroblast populations. However, it is still to be determined whether combining these mutations with neonatal inflammation may impact adult SVZ proliferation and RMS neuroblast populations.

Given the abnormal adult SVZ proliferation in the GxE model, SVZ proliferation was analyzed at postnatal day 12 (P12) in order to determine if this abnormality may originate during early development. Similar to adulthood, I found reduced SVZ proliferation in the postnatal GxE model, suggesting a neurodevelopmental origin of the reduced SVZ proliferation in adulthood. In postnatal brains, radial glial cells are neural stem cells (NSCs) which gradually decrease and transform into adult NSCs during the first two postnatal weeks (Tramontin et al., 2003). Therefore, it remains to be determined whether repeated postnatal polyI:C injections in combination with dysbindin-1 mutation might deplete the adult NSC pool, resulting in the observed reduction in adult SVZ proliferation.

Since SVZ proliferation was reduced in dysbindin-1 mutant, but not WT, mice given polyI:C this suggested that dysbindin-1 was required for maintaining SVZ proliferation. This hypothesis was addressed by analysing expression of Tlr3, RelA and Sp1 genes that are involved in both the innate immune response to polyI:C and also play important functions in regulating cell proliferation. Although the expression of these genes was induced in WT mice and neurospheres in response to polyI:C, this effect was inhibited in dysbindin-1 mutant mice and neurospheres. Therefore, these *in vivo* and *in vitro* data indicated that loss of dysbindin-1 may cause defects in normal immune response to inflammatory challenge, resulting in reduced postnatal SVZ proliferation that continued to adulthood. However, future studies are still to confirm if dysbindin-1 (Dtnbp1) gene may rescue SVZ proliferation in the GxE model.

Importantly, dysbindin-1 expression was also induced in WT mice and neurospheres in response to polyI:C, providing further evidence for the role of dysbindin-1 in innate immune response. Although dysbindin-1 (Dtnbp1) gene was not identified within 108 genetic loci that were significantly associated with schizophrenia (Schizophrenia Working Group of the Psychiatric Genomics, 2014), the work presented here may still provide insights into the immune signalling pathways that might be common outcomes of various risk genes of schizophrenia. This is especially true since genome-wide association studies supported a strong link between immune function and schizophrenia (Network and Pathway Analysis Subgroup of Psychiatric Genomics, 2015, Schizophrenia Working Group of the Psychiatric Genomics, 2014).

In order to gain a bigger picture of what caused the proliferative deficits in the GxE model, microglia were characterized during postnatal development. Microglia are local brain immune cells and therefore were expected to rapidly respond to repeated inflammatory challenges with polyI:C. In addition, leukocytes infiltrating into the SVZ were considered since polyI:C was peripherally administered. Dysbindin-1 mutation caused an abnormally high number of SVZ microglia whereas an increased number of leukocytes was found in the SVZ following postnatal polyI:C injections in Sdy mice. Together, these further emphasise the importance of dysbindin-1 in regulating immune function. A previous study reported that stimulated microglia may release cytokines that affected neurogenesis (Monje et al., 2003). This brings the question of whether inflammation and/or dysbindin-1 mutation may differentially affect cytokines release from microglia and/or infiltrating leukocytes and the impact of this on SVZ proliferation.

Although microglial activation was evaluated in this study using the lysosomal-related CD68 marker, this marker may not be appropriate for use in our GxE model since loss of dysbindin-1 in Sdy mice is associated with lysosomal dysfunction as discussed in Chapter 5. Therefore, M1 (neurotoxic) and M2 (neuroprotective) markers may clarify whether dysbindin-1 mutation and/or postnatal inflammation differentially affect the phenotype of the activated microglia, and the correlation of this with SVZ proliferation. Since increased number of leukocytes were found in the postnatal SVZ of the GxE model, it would be interesting to determine whether leukocytes permeability into the SVZ also persisted or worsened in adulthood.

In addition to the potential regulation of SVZ proliferation through immune-related genes and microglia/leukocytes, cytokines are also involved in regulating proliferation and neuroblast migration (reviewed in (Williams et al., 2014)). Therefore, I have investigated cytokine release from SVZ-derived neural progenitor cells (NPCs) in order to determine the impact of GxE factors on cytokine secretion and the correlation of this with reduced SVZ proliferation and RMS neuroblast populations in the GxE model. Furthermore, investigating cytokine secretion from NPCs may also clarify whether NPCs themselves communicate with each other and with other SVZ cells, such as microglia, through cytokine signalling. Interestingly, SVZ-derived NPCs differentially released cytokines in dysbindin-1 mutant cells and also in the GxE model. Hence, NPCs may participate through cytokine secretion in regulating SVZ proliferation, migratory neuroblasts and microglia in addition to leukocytes permeability into the SVZ.

Taken together, the GxE model used in my thesis revealed abnormalities in the SVZ proliferation, microglial density and infiltrating leukocyte numbers in addition to the disrupted neuroblast populations in the RMS. These abnormal phenotypes in the GxE model might be due to the disrupted intracellular Tlr3-RelA-Sp1 signalling and abnormal extracellular cytokine secretion. Therefore, my work showed novel functions of the schizophrenia-related dysbindin-1 in regulating intracellular immune signalling and extracellular cytokine secretion, which together might modulate SVZ homeostasis under baseline and inflammatory conditions.

6.2 Limitations

I have listed in table 6.1 the limitations of my work described in Chapters 3, 4 and 5.

Table 6.1 Limitations of the current study

Chapter 3
1) Used one marker (PHi3) to assess SVZ proliferation 2) Not determined which cell types specifically showed reduced proliferation 3) Did not give multiple BrdU injections to assess SVZ proliferation and neuroblast migration to the RMS 4) Did not quantitatively determine if postnatal inflammation continued to adulthood
Chapter 4
1) Used one marker (PHi3) to assess SVZ proliferation 2) For *in vivo* RT-qPCR experiments, RNA integrity number (RIN) of the extracted RNA was assessed during initial experiments. RIN was in the range (7.2 to 8.3) of all the measured six separate samples indicating good quality to be used for qRT-PCR. However, it was not possible to assess RIN in subsequent experiments due to limited samples. Given that exact experimental protocol was followed in all subsequent experiments, it can be assumed that they may have similar quality. 3) Two commonly used reference genes (β-actin and Rn18s) were used as reference genes in my current study. However, stability of these genes in my particular tissue and experimental setup was not tested. Since Tlr3 immunohistochemistry confirmed my qRT-PCR, it is likely that these two genes might be suitable for my particular experiments. 4) Nucleofection efficiency was not determined since Dtnbp1 cDNA clone was not tagged with a fluorescent protein. However, Dtnbp1 gene was only expressed in Dtnbp1 nucleofected samples (positive control) and was absent in all mock nucleofected mutant cells (negative control), indicating that nucleofection was working.
Chapter 5
1) Used one marker (Iba1) for microglia 2) Morphology of microglia was not assessed 3) Used one marker CD68 with Iba1 as indicative of microglial activation 4) Not included M1 and M2 phenotypic markers for microglia 5) Did not confirm the cell-types in the neurosphere culture

In addition to the limitations listed in table 6.1, I find that the use of Sdy mice might also have some limitations. In Sdy brain, both dysbindin-1A and -1C were reported to be absent (reviewed in (Talbot, 2009)). However, I propose that dysbindin-1A, but not dysbindin-1C, is absent in Sdy brain. I propose this for the following reasons. First, dysbindin-1C was shown not to be a subunit of BLOC-1 complex in mouse brain (Wang et al., 2014), therefore absence of intact CCD may not affect the stability of dysbindin-1C in the brain. Given that dysbindin-1A is a stable component of BLOC-1 complex (Wang et al., 2014), phenotypic abnormalities in Sdy mice might be attributed to loss of dysbindin-1A but not dysbindin-1C. Second, dysbindin-1A and -1C are only detected in the CNS (i.e. brain and spinal cord) (Wang et al., 2014), and the earlier report for complete absence of dysbindin-1 in Sdy mice was based on non-CNS tissues (i.e. kidney) in which dysbindin-1A, but not dysbindin-1C, is expressed (Li et al., 2003). Third, dysbindin-1A is absent in the brain of mice deficient in muted or pallidin (both BLOC-1 subunits) but dysbindin-1C is unaltered, providing some indication that dysbindin-1C might also remain stable in Sdy brain. Future studies are still needed to determine if dysbindin-1A, but not dysbindin-1C, is absent in Sdy brain. This will clarify whether the abnormal phenotypes in Sdy brain were specifically due to the loss of dysbindin-1A isoform.

6.3 Future directions

To follow up from current work, I suggest looking at how dysbindin-1 mutation may affect neuron-microglia interaction in the OB. Emerging evidences suggest a crucial role of neuron-microglia communication in maintaining proper synaptic connections, and that deficit in this key interaction may lead to excessive or reduced synaptic pruning by microglia resulting in disrupted synaptic transmission (Paolicelli et al., 2011, Sekar et al., 2016, Zhan et al., 2014). However, it is not clear whether neurotransmitters may instruct synaptic pruning activity by microglia. Therefore, I propose looking at how deficit in neurotransmitter release as previously reported in Sdy mice may directly impact synaptic pruning by microglia in the OB.

In schizophrenia, abnormal dopaminergic signalling is consistently reported. Dysbindin-1 was shown to play critical functions in controlling synaptic homeostasis in a dose-dependent manner (Dickman and Davis, 2009). Loss of dysbindin-1 in Sdy mice results in neurosecretion defects such as reduced rate of vesicle release (30% reduction) as well as decreased readily releasable vesicle pool (Chen et al., 2008). Specifically, dopamine levels are reduced in Sdy mice under baseline conditions (Murotani et al., 2007). Also, the releasable pool of dopamine is reduced in Sdy mice (Nagai et al., 2010). Therefore, Sdy mice can be used as a model of dopamine release deficit.

On the other hand, increased dopamine 2 receptor (D2R) density is also reported in the brain of schizophrenia patients and all anti-psychotic drugs block D2R (reviewed in (Howes and Kapur, 2009, Miyamoto et al., 2005)). Increased accumulation of D2R in cell surface was reported in the brain of Sdy mice as well as following dysbindin-1 knockdown (Iizuka et al., 2007, Ji et al., 2009), however dysbindin-1 overexpression reduced cell surface expression of D2R (Schmieg et al., 2015). Together, these indicate a role of dysbindin-1 in regulating D2R expression. Interestingly, functional D2R is expressed in rodent and human microglia (Farber et al., 2005, Huck et al., 2015, Mastroeni et al., 2009). For example, chronic stimulation with dopamine was shown to modulate microglial release and induced microglial migration (Farber et al., 2005). Taken together, Sdy mice might also show increased D2R expression in microglia.

Synaptic dysconnection and reduced dendritic spine density are reported in the brains of schizophrenic patients, which might be attributed to abnormal synaptic pruning (reviewed in (Stephan et al., 2006, Glausier and Lewis, 2013)). A study reported that dysbindin-1 was enriched in dendritic spines and formed a stable complex with WAVE2 and Abi-1 that are involved in dendritic spine morphogenesis, and knockdown of dysbindin-1 led to the formation of immature dendritic spines (Ito et al., 2010). Another study demonstrated that the dendritic spine abnormality in Sdy mice might be due to over-activation of D2R, and that pharmacological blocking of D2R rescued dendritic spine formation in Sdy mice (Jia et al., 2013). However, it is still to be determined if abnormal D2R due to dysbindin-1 mutation may directly trigger synaptic pruning by microglia resulting in dendritic spine deficits.

Here, I propose the following questions:

1) Does reduced SVZ proliferation in the GxE model result in reduced number of differentiated dopaminergic neurons in the OB?

2) Does reduced dopamine release as in Sdy mice "induce" D2R generation and recruitment to cell surface of microglia?

3) Does dopamine release from dopaminergic neurons in the OB act as "inhibitory" signal on microglia via D2R, and therefore control synaptic pruning?

I hypothesize that dopamine may directly control synaptic pruning activity of microglia via D2R. As illustrated in figure 6.1, dopamine release is normal in WT mice and might act as inhibitory signal on microglia via D2R. However, reduced dopamine release in Sdy may cause dis-inhibited effect on D2R resulting in stimulated microglia (fig. 6.1). This stimulatory effect might be further amplified due to increased microglial density in Sdy mice (fig.6.1). Therefore, over-stimulated D2R in microglia may lead to excessive synaptic pruning of dendritic spines in Sdy mice as shown in figure 6.2.

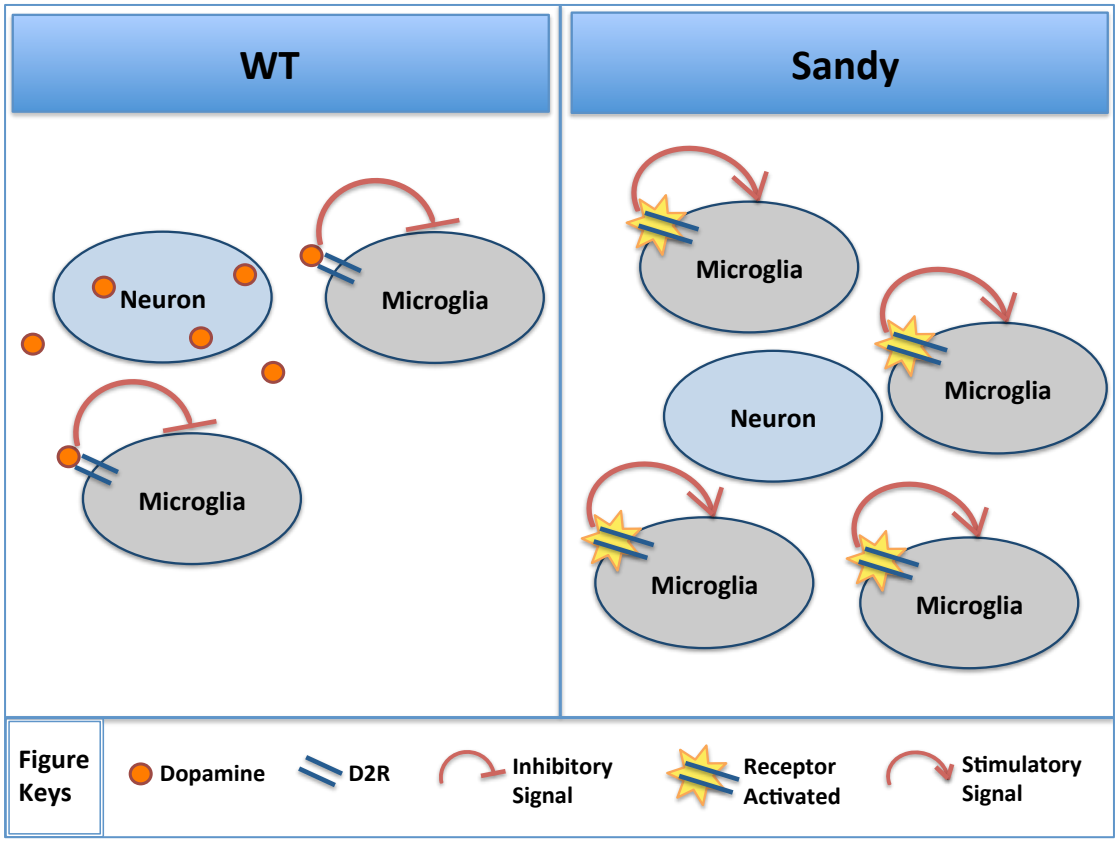

Figure 6.1 Proposed regulation of microglia through dopamine and dopamine 2 receptor (D2R)

Dopamine is normally released from WT dopaminergic neurons and may have inhibitory effect on microglial activity via D2R. However, reduced dopamine release and increased D2R in Sdy mice may stimulate microglia. Microglial cell numbers were increased in Sdy mice as I showed in Chapter 5.

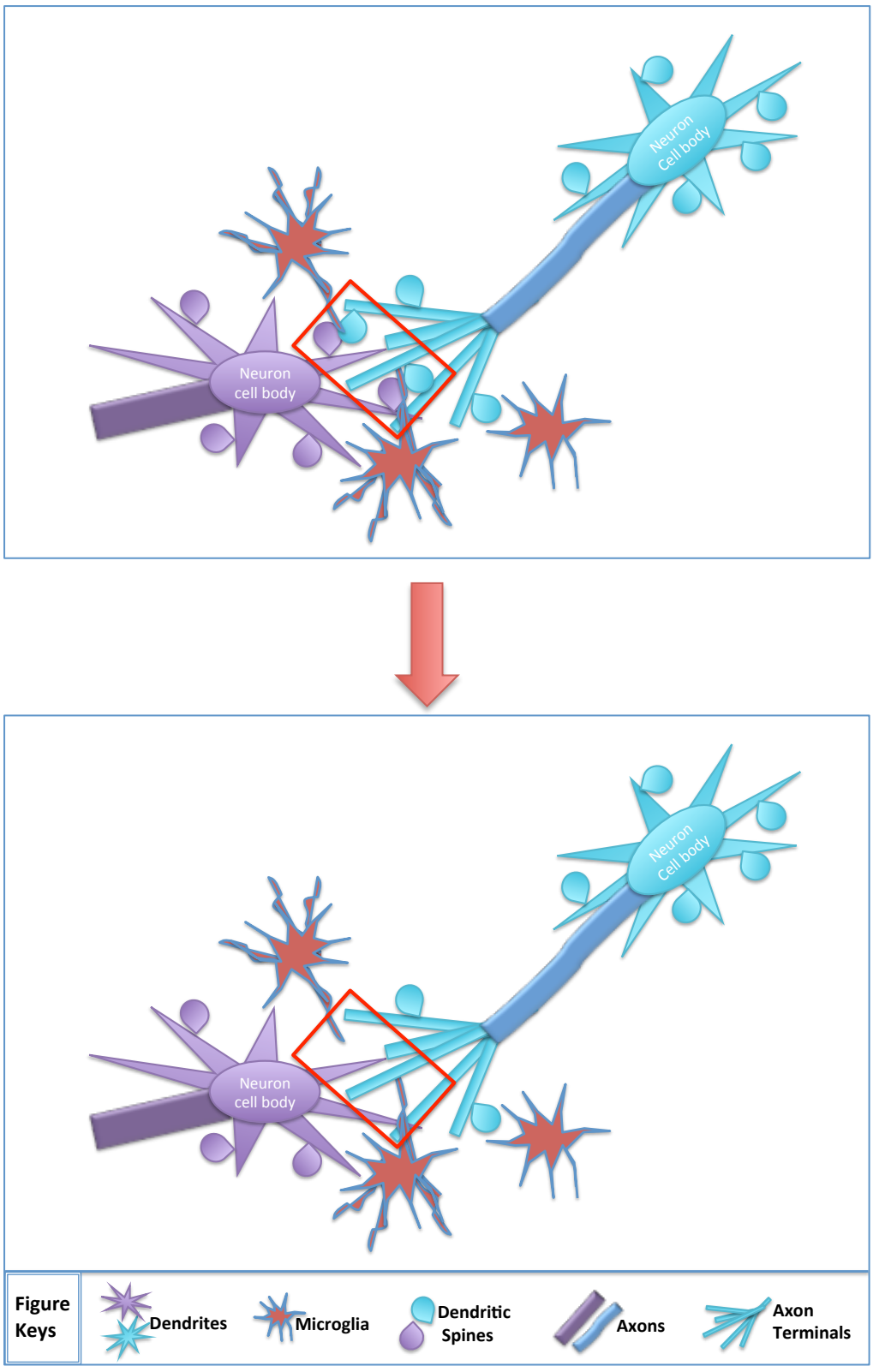

Figure 6.2 Excessive synaptic pruning by microglia due to D2R over-expression in Sdy mice

Following on from my proposed hypothesis in figure 6.1, increased synaptic pruning in Sdy mice may lead to the loss of contact between dendritic spines (Red boxed area).

Taken together, many schizophrenia-related genes, including dysbindin-1, encode synaptic proteins that are essential for normal neurotransmission; however how neurons and microglia directly interact through synaptic signalling is still unclear. Here, I proposed some questions to understand how neurotransmission abnormality due to dysbindin-1 mutation may directly influence microglial function via D2R and the impact of this in neuronal connectivity and spine formation. These can be addressed in the olfactory bulb in which continuous adult neurogenesis takes place. In addition, the impact of gene x environment risk factors of schizophrenia in the neuron-microglia communication can also be investigated. The long-term benefits of these questions might be to understand how antipsychotic drugs work. In general, anti-psychotic drugs block D2R in all cell-types, however targeting D2R specifically in microglia might prove more efficient while maintaining normal neuron-neuron transmission.

References

ALEXOPOULOU, L., HOLT, A. C., MEDZHITOV, R. & FLAVELL, R. A. 2001. Recognition of double-stranded RNA and activation of NF-kappaB by Toll-like receptor 3. *Nature,* 413**,** 732-8.

ALLIOT, F., GODIN, I. & PESSAC, B. 1999. Microglia derive from progenitors, originating from the yolk sac, and which proliferate in the brain. *Brain Res Dev Brain Res,* 117**,** 145-52.

ALVAREZ-BUYLLA, A. & LIM, D. A. 2004. For the long run: maintaining germinal niches in the adult brain. *Neuron,* 41**,** 683-6.

ANTON, E. S., GHASHGHAEI, H. T., WEBER, J. L., MCCANN, C., FISCHER, T. M., CHEUNG, I. D., GASSMANN, M., MESSING, A., KLEIN, R., SCHWAB, M. H., LLOYD, K. C. & LAI, C. 2004. Receptor tyrosine kinase ErbB4 modulates neuroblast migration and placement in the adult forebrain. *Nat Neurosci,* 7**,** 1319-28.

ARNOLD, S. E., HAN, L. Y., MOBERG, P. J., TURETSKY, B. I., GUR, R. E., TROJANOWSKI, J. Q. & HAHN, C. G. 2001. Dysregulation of olfactory receptor neuron lineage in schizophrenia. *Arch Gen Psychiatry,* 58**,** 829-35.

ARNOLD, S. E., SMUTZER, G. S., TROJANOWSKI, J. Q. & MOBERG, P. J. 1998. Cellular and molecular neuropathology of the olfactory epithelium and central olfactory pathways in Alzheimer's disease and schizophrenia. *Ann N Y Acad Sci,* 855**,** 762-75.

BARAK, B., FELDMAN, N. & OKUN, E. 2014. Toll-like receptors as developmental tools that regulate neurogenesis during development: an update. *Front Neurosci,* 8**,** 272.

BARK, C., BELLINGER, F. P., KAUSHAL, A., MATHEWS, J. R., PARTRIDGE, L. D. & WILSON, M. C. 2004. Developmentally regulated switch in alternatively spliced SNAP-25 isoforms alters facilitation of synaptic transmission. *J Neurosci,* 24**,** 8796-805.

BARK, I. C., HAHN, K. M., RYABININ, A. E. & WILSON, M. C. 1995. Differential expression of SNAP-25 protein isoforms during divergent vesicle fusion events of neural development. *Proc Natl Acad Sci U S A,* 92**,** 1510-4.

BEISHLINE, K. & AZIZKHAN-CLIFFORD, J. 2015. Sp1 and the 'hallmarks of cancer'. *FEBS J,* 282**,** 224-58.

BELL, J. K., BOTOS, I., HALL, P. R., ASKINS, J., SHILOACH, J., SEGAL, D. M. & DAVIES, D. R. 2005. The molecular structure of the Toll-like receptor 3 ligand-binding domain. *Proc Natl Acad Sci U S A,* 102**,** 10976-80.

BEN-SHACHAR, D. & KARRY, R. 2007. Sp1 expression is disrupted in schizophrenia; a possible mechanism for the abnormal expression of mitochondrial complex I genes, NDUFV1 and NDUFV2. *PLoS One,* 2**,** e817.

BENES, F. M., PASKEVICH, P. A., DAVIDSON, J. & DOMESICK, V. B. 1985. The effects of haloperidol on synaptic patterns in the rat striatum. *Brain Res,* 329**,** 265-73.

BENSON, M. A., NEWEY, S. E., MARTIN-RENDON, E., HAWKES, R. & BLAKE, D. J. 2001. Dysbindin, a novel coiled-coil-containing protein that interacts with the dystrobrevins in muscle and brain. *J Biol Chem,* 276**,** 24232-41.

BHARDWAJ, S. K., BAHARNOORI, M., SHARIF-ASKARI, B., KAMATH, A., WILLIAMS, S. & SRIVASTAVA, L. K. 2009. Behavioral characterization of dysbindin-1 deficient sandy mice. *Behav Brain Res,* 197**,** 435-41.

BORISH, L. C. & STEINKE, J. W. 2003. 2. Cytokines and chemokines. *J Allergy Clin Immunol,* 111**,** S460-75.

BORTOLOTTO, V., CUCCURAZZU, B., CANONICO, P. L. & GRILLI, M. 2014. NF-kappaB mediated regulation of adult hippocampal neurogenesis: relevance to mood disorders and antidepressant activity. *Biomed Res Int,* 2014**,** 612798.

BRAFF, D. L. & GEYER, M. A. 1990. Sensorimotor gating and schizophrenia. Human and animal model studies. *Arch Gen Psychiatry,* 47**,** 181-8.

BRAIDA, D., PONZONI, L., MATTEOLI, M. & SALA, M. M. 2016. Different attentional abilities among inbred mice strains using virtual object recognition task (VORT): SNAP25(+)/(-) mice as a model of attentional deficit. *Behav Brain Res,* 296**,** 393-400.

BRINKMANN, B. G., AGARWAL, A., SEREDA, M. W., GARRATT, A. N., MULLER, T., WENDE, H., STASSART, R. M., NAWAZ, S., HUMML, C., VELANAC, V., RADYUSHKIN, K., GOEBBELS, S., FISCHER, T. M., FRANKLIN, R. J., LAI, C., EHRENREICH, H., BIRCHMEIER, C., SCHWAB, M. H. & NAVE, K. A. 2008. Neuregulin-1/ErbB signaling serves distinct functions in myelination of the peripheral and central nervous system. *Neuron,* 59**,** 581-95.

BROWN, A. S. 2011. The environment and susceptibility to schizophrenia. *Prog Neurobiol,* 93**,** 23-58.

BROZ, P. & MONACK, D. M. 2013. Newly described pattern recognition receptors team up against intracellular pathogens. *Nat Rev Immunol,* 13**,** 551-65.

BSIBSI, M., RAVID, R., GVERIC, D. & VAN NOORT, J. M. 2002. Broad expression of Toll-like receptors in the human central nervous system. *J Neuropathol Exp Neurol,* 61**,** 1013-21.

BUSSE, S., BUSSE, M., SCHILTZ, K., BIELAU, H., GOS, T., BRISCH, R., MAWRIN, C., SCHMITT, A., JORDAN, W., MULLER, U. J., BERNSTEIN, H. G., BOGERTS, B. & STEINER, J. 2012. Different distribution patterns of lymphocytes and microglia in the hippocampus of patients with residual versus paranoid schizophrenia: further evidence for disease course-related immune alterations? *Brain Behav Immun,* 26**,** 1273-9.

CAMERON, H. A., WOOLLEY, C. S., MCEWEN, B. S. & GOULD, E. 1993. Differentiation of newly born neurons and glia in the dentate gyrus of the adult rat. *Neuroscience,* 56**,** 337-44.

CARLSON, G. C., TALBOT, K., HALENE, T. B., GANDAL, M. J., KAZI, H. A., SCHLOSSER, L., PHUNG, Q. H., GUR, R. E., ARNOLD, S. E. & SIEGEL, S. J. 2011. Dysbindin-1 mutant mice implicate reduced fast-phasic inhibition as a final common disease mechanism in schizophrenia. *Proc Natl Acad Sci U S A,* 108**,** E962-70.

CARTIER, L., HARTLEY, O., DUBOIS-DAUPHIN, M. & KRAUSE, K. H. 2005. Chemokine receptors in the central nervous system: role in brain inflammation and neurodegenerative diseases. *Brain Res Brain Res Rev,* 48**,** 16-42.

CHAKOS, M. H., SHIRAKAWA, O., LIEBERMAN, J., LEE, H., BILDER, R. & TAMMINGA, C. A. 1998. Striatal enlargement in rats chronically treated with neuroleptic. *Biol Psychiatry,* 44**,** 675-84.

CHEN, X. W., FENG, Y. Q., HAO, C. J., GUO, X. L., HE, X., ZHOU, Z. Y., GUO, N., HUANG, H. P., XIONG, W., ZHENG, H., ZUO, P. L., ZHANG, C. X., LI, W. & ZHOU, Z. 2008. DTNBP1, a schizophrenia susceptibility gene, affects kinetics of transmitter release. *J Cell Biol,* 181**,** 791-801.

CHITU, V., GOKHAN, S., NANDI, S., MEHLER, M. F. & STANLEY, E. R. 2016. Emerging Roles for CSF-1 Receptor and its Ligands in the Nervous System. *Trends Neurosci,* 39**,** 378-93.

CHOE, J., KELKER, M. S. & WILSON, I. A. 2005. Crystal structure of human toll-like receptor 3 (TLR3) ectodomain. *Science,* 309**,** 581-5.

CLARKE, M. C., TANSKANEN, A., HUTTUNEN, M., WHITTAKER, J. C. & CANNON, M. 2009. Evidence for an interaction between familial liability and prenatal exposure to infection in the causation of schizophrenia. *Am J Psychiatry,* 166**,** 1025-30.

COMTE, I., KOTAGIRI, P. & SZELE, F. G. 2012. Regional differences in human ependymal and subventricular zone cytoarchitecture are unchanged in neuropsychiatric disease. *Dev Neurosci,* 34**,** 299-309.

CONTI, L. & CATTANEO, E. 2010. Neural stem cell systems: physiological players or in vitro entities? *Nat Rev Neurosci,* 11**,** 176-87.

CORRADINI, I., DONZELLI, A., ANTONUCCI, F., WELZL, H., LOOS, M., MARTUCCI, R., DE ASTIS, S., PATTINI, L., INVERARDI, F., WOLFER, D., CALEO, M., BOZZI, Y., VERDERIO, C., FRASSONI, C., BRAIDA, D., CLERICI, M., LIPP, H. P., SALA, M. & MATTEOLI, M. 2014. Epileptiform activity and cognitive deficits in SNAP-25(+/-) mice are normalized by antiepileptic drugs. *Cereb Cortex,* 24**,** 364-76.

CORSON, P. W., NOPOULOS, P., ANDREASEN, N. C., HECKEL, D. & ARNDT, S. 1999. Caudate size in first-episode neuroleptic-naive schizophrenic patients measured using an artificial neural network. *Biol Psychiatry,* 46**,** 712-20.

COX, M. M., TUCKER, A. M., TANG, J., TALBOT, K., RICHER, D. C., YEH, L. & ARNOLD, S. E. 2009. Neurobehavioral abnormalities in the dysbindin-1 mutant, sandy, on a C57BL/6J genetic background. *Genes Brain Behav,* 8**,** 390-7.

CUNNINGHAM, C., CAMPION, S., TEELING, J., FELTON, L. & PERRY, V. H. 2007. The sickness behaviour and CNS inflammatory mediator profile induced by systemic challenge of mice with synthetic double-stranded RNA (poly I:C). *Brain Behav Immun,* 21**,** 490-502.

CUNNINGHAM, C. L., MARTINEZ-CERDENO, V. & NOCTOR, S. C. 2013. Microglia regulate the number of neural precursor cells in the developing cerebral cortex. *J Neurosci,* 33**,** 4216-33.

CURTIS, M. A., PENNEY, E. B., PEARSON, A. G., VAN ROON-MOM, W. M., BUTTERWORTH, N. J., DRAGUNOW, M., CONNOR, B. & FAULL, R. L. 2003. Increased cell proliferation and neurogenesis in the adult human Huntington's disease brain. *Proc Natl Acad Sci U S A,* 100**,** 9023-7.

D'MELLO, C., LE, T. & SWAIN, M. G. 2009. Cerebral microglia recruit monocytes into the brain in response to tumor necrosis factoralpha signaling during peripheral organ inflammation. *J Neurosci,* 29**,** 2089-102.

DE MIRANDA, J., YADDANAPUDI, K., HORNIG, M., VILLAR, G., SERGE, R. & LIPKIN, W. I. 2010. Induction of Toll-like receptor 3-mediated immunity during gestation inhibits cortical neurogenesis and causes behavioral disturbances. *MBio,* 1.

DEAKIN, I. H., LAW, A. J., OLIVER, P. L., SCHWAB, M. H., NAVE, K. A., HARRISON, P. J. & BANNERMAN, D. M. 2009. Behavioural characterization of neuregulin 1 type I overexpressing transgenic mice. *Neuroreport,* 20**,** 1523-8.

DEAKIN, I. H., NISSEN, W., LAW, A. J., LANE, T., KANSO, R., SCHWAB, M. H., NAVE, K. A., LAMSA, K. P., PAULSEN, O., BANNERMAN, D. M. & HARRISON, P. J. 2012. Transgenic overexpression of the type I isoform of neuregulin 1 affects working memory and hippocampal oscillations but not long-term potentiation. *Cereb Cortex,* 22**,** 1520-9.

DELISI, L. E., HOLCOMB, H. H., COHEN, R. M., PICKAR, D., CARPENTER, W., MORIHISA, J. M., KING, A. C., KESSLER, R. & BUCHSBAUM, M. S. 1985. Positron emission tomography in schizophrenic patients with and without neuroleptic medication. *J Cereb Blood Flow Metab,* 5**,** 201-6.

DELISI, L. E., SAKUMA, M., TEW, W., KUSHNER, M., HOFF, A. L. & GRIMSON, R. 1997. Schizophrenia as a chronic active brain process: a study of progressive brain structural change subsequent to the onset of schizophrenia. *Psychiatry Res,* 74**,** 129-40.

DICKMAN, D. K. & DAVIS, G. W. 2009. The schizophrenia susceptibility gene dysbindin controls synaptic homeostasis. *Science,* 326**,** 1127-30.

DOETSCH, F. & ALVAREZ-BUYLLA, A. 1996. Network of tangential pathways for neuronal migration in adult mammalian brain. *Proc Natl Acad Sci U S A,* 93**,** 14895-900.

DOYLE, S. L., SHIREY, K. A., MCGETTRICK, A. F., KENNY, E. F., CARPENTER, S., CAFFREY, B. E., GARGAN, S., QUINN, S. R., CAAMANO, J. H., MOYNAGH, P., VOGEL, S. N. & O'NEILL, L. A. 2013. Nuclear factor kappaB2 p52 protein has a role in antiviral immunity through IkappaB kinase epsilon-dependent induction of Sp1 protein and interleukin 15. *J Biol Chem,* 288**,** 25066-75.

DYNAN, W. S. & TJIAN, R. 1983. The promoter-specific transcription factor Sp1 binds to upstream sequences in the SV40 early promoter. *Cell,* 35**,** 79-87.

ELVEVAG, B. & GOLDBERG, T. E. 2000. Cognitive impairment in schizophrenia is the core of the disorder. *Crit Rev Neurobiol,* 14**,** 1-21.

ERNST, A., ALKASS, K., BERNARD, S., SALEHPOUR, M., PERL, S., TISDALE, J., POSSNERT, G., DRUID, H. & FRISEN, J. 2014. Neurogenesis in the Striatum of the Adult Human Brain. *Cell*.

FALCAO, A. M., MARQUES, F., NOVAIS, A., SOUSA, N., PALHA, J. A. & SOUSA, J. C. 2012. The path from the choroid plexus to the subventricular zone: go with the flow! *Front Cell Neurosci,* 6**,** 34.

FARBER, K., PANNASCH, U. & KETTENMANN, H. 2005. Dopamine and noradrenaline control distinct functions in rodent microglial cells. *Mol Cell Neurosci,* 29**,** 128-38.

FENG, Y. Q., ZHOU, Z. Y., HE, X., WANG, H., GUO, X. L., HAO, C. J., GUO, Y., ZHEN, X. C. & LI, W. 2008. Dysbindin deficiency in sandy mice causes reduction of snapin and displays behaviors related to schizophrenia. *Schizophr Res,* 106**,** 218-28.

FERNANDEZ-LOPEZ, D., FAUSTINO, J., DANEMAN, R., ZHOU, L., LEE, S. Y., DERUGIN, N., WENDLAND, M. F. & VEXLER, Z. S. 2012. Blood-brain barrier permeability is increased after acute adult stroke but not neonatal stroke in the rat. *J Neurosci,* 32**,** 9588-600.

FLAMES, N., LONG, J. E., GARRATT, A. N., FISCHER, T. M., GASSMANN, M., BIRCHMEIER, C., LAI, C., RUBENSTEIN, J. L. & MARIN, O. 2004. Short- and long-range attraction of cortical GABAergic interneurons by neuregulin-1. *Neuron,* 44**,** 251-61.

FRANKLIN, K. B. J. & PAXINOS, G. 2001. *The Mouse Brain in Stereotaxic Coordinates,* San Diego, CA, Academic Press.

FU, C., CHEN, D., CHEN, R., HU, Q. & WANG, G. 2015. The Schizophrenia-Related Protein Dysbindin-1A Is Degraded and Facilitates NF-Kappa B Activity in the Nucleus. *PLoS One,* 10**,** e0132639.

GARDNER, J. & GHORPADE, A. 2003. Tissue inhibitor of metalloproteinase (TIMP)-1: the TIMPed balance of matrix metalloproteinases in the central nervous system. *J Neurosci Res,* 74**,** 801-6.

GHASHGHAEI, H. T., WEBER, J., PEVNY, L., SCHMID, R., SCHWAB, M. H., LLOYD, K. C., EISENSTAT, D. D., LAI, C. & ANTON, E. S. 2006. The role of neuregulin-ErbB4 interactions on the proliferation and organization of cells in the subventricular zone. *Proc Natl Acad Sci U S A,* 103**,** 1930-5.

GHIANI, C. A., STARCEVIC, M., RODRIGUEZ-FERNANDEZ, I. A., NAZARIAN, R., CHELI, V. T., CHAN, L. N., MALVAR, J. S., DE VELLIS, J., SABATTI, C. & DELL'ANGELICA, E. C. 2010. The dysbindin-containing complex (BLOC-1) in brain: developmental regulation, interaction with SNARE proteins and role in neurite outgrowth. *Mol Psychiatry,* 15**,** 115, 204-15.

GINHOUX, F. & PRINZ, M. 2015. Origin of microglia: current concepts and past controversies. *Cold Spring Harb Perspect Biol,* 7**,** a020537.

GLAUSIER, J. R. & LEWIS, D. A. 2013. Dendritic spine pathology in schizophrenia. *Neuroscience,* 251**,** 90-107.

GOINGS, G. E., KOZLOWSKI, D. A. & SZELE, F. G. 2006. Differential activation of microglia in neurogenic versus non-neurogenic regions of the forebrain. *Glia,* 54**,** 329-42.

GORDON, R. J., MCGREGOR, A. L. & CONNOR, B. 2009. Chemokines direct neural progenitor cell migration following striatal cell loss. *Mol Cell Neurosci,* 41**,** 219-32.

GORDON, R. J., MEHRABI, N. F., MAUCKSCH, C. & CONNOR, B. 2012. Chemokines influence the migration and fate of neural precursor cells from the young adult and middle-aged rat subventricular zone. *Exp Neurol,* 233**,** 587-94.

GU, L., FINDLEY, H. W. & ZHOU, M. 2002. MDM2 induces NF-kappaB/p65 expression transcriptionally through Sp1-binding sites: a novel, p53-independent role of MDM2 in doxorubicin resistance in acute lymphoblastic leukemia. *Blood,* 99**,** 3367-75.

GUAN, H., CAI, J., ZHANG, N., WU, J., YUAN, J., LI, J. & LI, M. 2012. Sp1 is upregulated in human glioma, promotes MMP-2-mediated cell invasion and predicts poor clinical outcome. *Int J Cancer,* 130**,** 593-601.

GUILLEMIN, G. J. & BREW, B. J. 2004. Microglia, macrophages, perivascular macrophages, and pericytes: a review of function and identification. *J Leukoc Biol,* 75**,** 388-97.

GUR, R. E., MAANY, V., MOZLEY, P. D., SWANSON, C., BILKER, W. & GUR, R. C. 1998. Subcortical MRI volumes in neuroleptic-naive and treated patients with schizophrenia. *Am J Psychiatry,* 155**,** 1711-7.

GUTTRIDGE, D. C., ALBANESE, C., REUTHER, J. Y., PESTELL, R. G. & BALDWIN, A. S., JR. 1999. NF-kappaB controls cell growth and differentiation through transcriptional regulation of cyclin D1. *Mol Cell Biol,* 19**,** 5785-99.

HAFNER, H., LOFFLER, W., MAURER, K., HAMBRECHT, M. & AN DER HEIDEN, W. 1999. Depression, negative symptoms, social stagnation and social decline in the early course of schizophrenia. *Acta Psychiatr Scand,* 100**,** 105-18.

HARRISON, P. J. 1999. The neuropathology of schizophrenia. A critical review of the data and their interpretation. *Brain,* 122 (Pt 4)**,** 593-624.

HARRISON, P. J. & LAW, A. J. 2006. Neuregulin 1 and schizophrenia: genetics, gene expression, and neurobiology. *Biol Psychiatry,* 60**,** 132-40.

HARVEY, L. & BOKSA, P. 2012. Prenatal and postnatal animal models of immune activation: relevance to a range of neurodevelopmental disorders. *Dev Neurobiol,* 72**,** 1335-48.

HASHIMOTO, R., STRAUB, R. E., WEICKERT, C. S., HYDE, T. M., KLEINMAN, J. E. & WEINBERGER, D. R. 2004. Expression analysis of neuregulin-1 in the dorsolateral prefrontal cortex in schizophrenia. *Mol Psychiatry,* 9**,** 299-307.

HATTORI, S., MUROTANI, T., MATSUZAKI, S., ISHIZUKA, T., KUMAMOTO, N., TAKEDA, M., TOHYAMA, M., YAMATODANI, A., KUNUGI, H. & HASHIMOTO, R. 2008. Behavioral abnormalities and dopamine reductions in sdy mutant mice with a deletion in Dtnbp1, a susceptibility gene for schizophrenia. *Biochem Biophys Res Commun,* 373**,** 298-302.

HOLLADAY, S. D. & SMIALOWICZ, R. J. 2000. Development of the murine and human immune system: differential effects of immunotoxicants depend on time of exposure. *Environ Health Perspect,* 108 Suppl 3**,** 463-73.

HOLNESS, C. L., DA SILVA, R. P., FAWCETT, J., GORDON, S. & SIMMONS, D. L. 1993. Macrosialin, a mouse macrophage-restricted glycoprotein, is a member of the lamp/lgp family. *J Biol Chem,* 268**,** 9661-6.

HOSHINO, K., TAKEUCHI, O., KAWAI, T., SANJO, H., OGAWA, T., TAKEDA, Y., TAKEDA, K. & AKIRA, S. 1999. Cutting edge: Toll-like receptor 4 (TLR4)-deficient mice are hyporesponsive to lipopolysaccharide: evidence for TLR4 as the Lps gene product. *J Immunol,* 162**,** 3749-52.

HOWES, O. D. & KAPUR, S. 2009. The dopamine hypothesis of schizophrenia: version III--the final common pathway. *Schizophr Bull,* 35**,** 549-62.

HUCK, J. H., FREYER, D., BOTTCHER, C., MLADINOV, M., MUSELMANN-GENSCHOW, C., THIELKE, M., GLADOW, N., BLOOMQUIST, D., MERGENTHALER, P. & PRILLER, J. 2015. De novo expression of dopamine D2 receptors on microglia after stroke. *J Cereb Blood Flow Metab,* 35**,** 1804-11.

HUNG, W. C., TSENG, W. L., SHIEA, J. & CHANG, H. C. 2010. Skp2 overexpression increases the expression of MMP-2 and MMP-9 and invasion of lung cancer cells. *Cancer Lett,* 288**,** 156-61.

IBI, D., NAGAI, T., KITAHARA, Y., MIZOGUCHI, H., KOIKE, H., SHIRAKI, A., TAKUMA, K., KAMEI, H., NODA, Y., NITTA, A., NABESHIMA, T., YONEDA, Y. & YAMADA, K. 2009. Neonatal polyI:C treatment in mice results in schizophrenia-like behavioral and neurochemical abnormalities in adulthood. *Neurosci Res,* 64**,** 297-305.

IBI, D., NAGAI, T., KOIKE, H., KITAHARA, Y., MIZOGUCHI, H., NIWA, M., JAARO-PELED, H., NITTA, A., YONEDA, Y., NABESHIMA, T., SAWA, A. & YAMADA,

K. 2010. Combined effect of neonatal immune activation and mutant DISC1 on phenotypic changes in adulthood. *Behav Brain Res,* 206**,** 32-7.

IHRIE, R. A. & ALVAREZ-BUYLLA, A. 2008. Cells in the astroglial lineage are neural stem cells. *Cell Tissue Res,* 331**,** 179-91.

IHRIE, R. A. & ALVAREZ-BUYLLA, A. 2011. Lake-front property: a unique germinal niche by the lateral ventricles of the adult brain. *Neuron,* 70**,** 674-86.

IIJIMA, S., MASAKI, H., WAKAYAMA, Y., INOUE, M., JIMI, T., HARA, H., UNAKI, A., ONIKI, H., NAKANO, K., HIRAYAMA, Y. & KISHIMOTO, K. 2009. Immunohistochemical detection of dysbindin at the astroglial endfeet around the capillaries of mouse brain. *J Mol Histol,* 40**,** 117-21.

IIZUKA, Y., SEI, Y., WEINBERGER, D. R. & STRAUB, R. E. 2007. Evidence that the BLOC-1 protein dysbindin modulates dopamine D2 receptor internalization and signaling but not D1 internalization. *J Neurosci,* 27**,** 12390-5.

IMAI, Y., IBATA, I., ITO, D., OHSAWA, K. & KOHSAKA, S. 1996. A novel gene iba1 in the major histocompatibility complex class III region encoding an EF hand protein expressed in a monocytic lineage. *Biochem Biophys Res Commun,* 224**,** 855-62.

ITO, D., IMAI, Y., OHSAWA, K., NAKAJIMA, K., FUKUUCHI, Y. & KOHSAKA, S. 1998. Microglia-specific localisation of a novel calcium binding protein, Iba1. *Brain Res Mol Brain Res,* 57**,** 1-9.

ITO, H., MORISHITA, R., SHINODA, T., IWAMOTO, I., SUDO, K., OKAMOTO, K. & NAGATA, K. 2010. Dysbindin-1, WAVE2 and Abi-1 form a complex that regulates dendritic spine formation. *Mol Psychiatry,* 15**,** 976-86.

JACOBS, B. L. & LANGLAND, J. O. 1996. When two strands are better than one: the mediators and modulators of the cellular responses to double-stranded RNA. *Virology,* 219**,** 339-49.

JEANS, A. F., OLIVER, P. L., JOHNSON, R., CAPOGNA, M., VIKMAN, J., MOLNAR, Z., BABBS, A., PARTRIDGE, C. J., SALEHI, A., BENGTSSON, M., ELIASSON, L., RORSMAN, P. & DAVIES, K. E. 2007. A dominant mutation in Snap25 causes impaired vesicle trafficking, sensorimotor gating, and ataxia in the blind-drunk mouse. *Proc Natl Acad Sci U S A,* 104**,** 2431-6.

JENSEN, J. B. & PARMAR, M. 2006. Strengths and limitations of the neurosphere culture system. *Mol Neurobiol,* 34**,** 153-61.

JENTSCH, J. D., TRANTHAM-DAVIDSON, H., JAIRL, C., TINSLEY, M., CANNON, T. D. & LAVIN, A. 2009. Dysbindin modulates prefrontal cortical glutamatergic circuits and working memory function in mice. *Neuropsychopharmacology,* 34**,** 2601-8.

JI, J. F., HE, B. P., DHEEN, S. T. & TAY, S. S. 2004. Expression of chemokine receptors CXCR4, CCR2, CCR5 and CX3CR1 in neural progenitor cells isolated from the subventricular zone of the adult rat brain. *Neurosci Lett,* 355**,** 236-40.

JI, Y., YANG, F., PAPALEO, F., WANG, H. X., GAO, W. J., WEINBERGER, D. R. & LU, B. 2009. Role of dysbindin in dopamine receptor trafficking and cortical GABA function. *Proc Natl Acad Sci U S A,* 106**,** 19593-8.

JIA, J. M., ZHAO, J., HU, Z., LINDBERG, D. & LI, Z. 2013. Age-dependent regulation of synaptic connections by dopamine D2 receptors. *Nat Neurosci,* 16**,** 1627-36.

JIN, K., GALVAN, V., XIE, L., MAO, X. O., GOROSTIZA, O. F., BREDESEN, D. E. & GREENBERG, D. A. 2004. Enhanced neurogenesis in Alzheimer's disease transgenic (PDGF-APPSw,Ind) mice. *Proc Natl Acad Sci U S A,* 101**,** 13363-7.

JOYAL, C. C., LAAKSO, M. P., TIIHONEN, J., SYVALAHTI, E., VILKMAN, H., LAAKSO, A., ALAKARE, B., RAKKOLAINEN, V., SALOKANGAS, R. K. & HIETALA, J. 2002. A volumetric MRI study of the entorhinal cortex in first episode neuroleptic-naive schizophrenia. *Biol Psychiatry,* 51**,** 1005-7.

KADONAGA, J. T., CARNER, K. R., MASIARZ, F. R. & TJIAN, R. 1987. Isolation of cDNA encoding transcription factor Sp1 and functional analysis of the DNA binding domain. *Cell,* 51**,** 1079-90.

KATAOKA, M., YAMAMORI, S., SUZUKI, E., WATANABE, S., SATO, T., MIYAOKA, H., AZUMA, S., IKEGAMI, S., KUWAHARA, R., SUZUKI-MIGISHIMA, R., NAKAHARA, Y., NIHONMATSU, I., INOKUCHI, K., KATOH-FUKUI, Y., YOKOYAMA, M. & TAKAHASHI, M. 2011. A single amino acid mutation in SNAP-25 induces anxiety-related behavior in mouse. *PLoS One,* 6**,** e25158.

KAWAI, T. & AKIRA, S. 2010. The role of pattern-recognition receptors in innate immunity: update on Toll-like receptors. *Nat Immunol,* 11**,** 373-84.

KERFOOT, S. M., D'MELLO, C., NGUYEN, H., AJUEBOR, M. N., KUBES, P., LE, T. & SWAIN, M. G. 2006. TNF-alpha-secreting monocytes are recruited into the brain of cholestatic mice. *Hepatology,* 43**,** 154-62.

KERNS, J. M., SIERENS, D. K., KAO, L. C., KLAWANS, H. L. & CARVEY, P. M. 1992. Synaptic plasticity in the rat striatum following chronic haloperidol treatment. *Clin Neuropharmacol,* 15**,** 488-500.

KESHAVAN, M. S., ROSENBERG, D., SWEENEY, J. A. & PETTEGREW, J. W. 1998. Decreased caudate volume in neuroleptic-naive psychotic patients. *Am J Psychiatry,* 155**,** 774-8.

KIM, Y., WANG, W. Z., COMTE, I., PASTRANA, E., TRAN, P. B., BROWN, J., MILLER, R. J., DOETSCH, F., MOLNAR, Z. & SZELE, F. G. 2010. Dopamine stimulation of postnatal murine subventricular zone neurogenesis via the D3 receptor. *J Neurochem,* 114**,** 750-60.

KIPPIN, T. E., KAPUR, S. & VAN DER KOOY, D. 2005. Dopamine specifically inhibits forebrain neural stem cell proliferation, suggesting a novel effect of antipsychotic drugs. *J Neurosci,* 25**,** 5815-23.

KRAMER, R., BUCAY, N., KANE, D. J., MARTIN, L. E., TARPLEY, J. E. & THEILL, L. E. 1996. Neuregulins with an Ig-like domain are essential for mouse myocardial and neuronal development. *Proc Natl Acad Sci U S A,* 93**,** 4833-8.

KUMAR, H., KAWAI, T. & AKIRA, S. 2009. Pathogen recognition in the innate immune response. *Biochem J,* 420**,** 1-16.

KURKI, P., VANDERLAAN, M., DOLBEARE, F., GRAY, J. & TAN, E. M. 1986. Expression of proliferating cell nuclear antigen (PCNA)/cyclin during the cell cycle. *Exp Cell Res,* 166**,** 209-19.

LAFON, M., MEGRET, F., LAFAGE, M. & PREHAUD, C. 2006. The innate immune facet of brain: human neurons express TLR-3 and sense viral dsRNA. *J Mol Neurosci,* 29**,** 185-94.

LARIMORE, J., ZLATIC, S. A., GOKHALE, A., TORNIERI, K., SINGLETON, K. S., MULLIN, A. P., TANG, J., TALBOT, K. & FAUNDEZ, V. 2014. Mutations in the

BLOC-1 subunits dysbindin and muted generate divergent and dosage-dependent phenotypes. *J Biol Chem,* 289**,** 14291-300.

LATHIA, J. D., OKUN, E., TANG, S. C., GRIFFIOEN, K., CHENG, A., MUGHAL, M. R., LARYEA, G., SELVARAJ, P. K., FFRENCH-CONSTANT, C., MAGNUS, T., ARUMUGAM, T. V. & MATTSON, M. P. 2008. Toll-like receptor 3 is a negative regulator of embryonic neural progenitor cell proliferation. *J Neurosci,* 28**,** 13978-84.

LAW, A. J., LIPSKA, B. K., WEICKERT, C. S., HYDE, T. M., STRAUB, R. E., HASHIMOTO, R., HARRISON, P. J., KLEINMAN, J. E. & WEINBERGER, D. R. 2006. Neuregulin 1 transcripts are differentially expressed in schizophrenia and regulated by 5' SNPs associated with the disease. *Proc Natl Acad Sci U S A,* 103**,** 6747-52.

LEE, J. C., YAU, S. Y., LEE, T. M., LAU, B. W. & SO, K. F. 2016. Voluntary wheel running reverses the decrease in subventricular zone neurogenesis caused by corticosterone. *Cell Transplant*.

LEE, S. R., KIM, H. Y., ROGOWSKA, J., ZHAO, B. Q., BHIDE, P., PARENT, J. M. & LO, E. H. 2006. Involvement of matrix metalloproteinase in neuroblast cell migration from the subventricular zone after stroke. *J Neurosci,* 26**,** 3491-5.

LEMAITRE, B., NICOLAS, E., MICHAUT, L., REICHHART, J. M. & HOFFMANN, J. A. 1996. The dorsoventral regulatory gene cassette spatzle/Toll/cactus controls the potent antifungal response in Drosophila adults. *Cell,* 86**,** 973-83.

LEONARD, J. N., GHIRLANDO, R., ASKINS, J., BELL, J. K., MARGULIES, D. H., DAVIES, D. R. & SEGAL, D. M. 2008. The TLR3 signaling complex forms by cooperative receptor dimerization. *Proc Natl Acad Sci U S A,* 105**,** 258-63.

LEWIS, C. M., LEVINSON, D. F., WISE, L. H., DELISI, L. E., STRAUB, R. E., HOVATTA, I., WILLIAMS, N. M., SCHWAB, S. G., PULVER, A. E., FARAONE, S. V., BRZUSTOWICZ, L. M., KAUFMANN, C. A., GARVER, D. L., GURLING, H. M., LINDHOLM, E., COON, H., MOISES, H. W., BYERLEY, W., SHAW, S. H., MESEN, A., SHERRINGTON, R., O'NEILL, F. A., WALSH, D., KENDLER, K. S., EKELUND, J., PAUNIO, T., LONNQVIST, J., PELTONEN, L., O'DONOVAN, M. C., OWEN, M. J., WILDENAUER, D. B., MAIER, W., NESTADT, G., BLOUIN, J. L., ANTONARAKIS, S. E., MOWRY, B. J., SILVERMAN, J. M., CROWE, R. R., CLONINGER, C. R., TSUANG, M. T., MALASPINA, D., HARKAVY-FRIEDMAN, J. M., SVRAKIC, D. M., BASSETT, A. S., HOLCOMB, J., KALSI, G., MCQUILLIN, A., BRYNJOLFSON, J., SIGMUNDSSON, T., PETURSSON, H., JAZIN, E., ZOEGA, T. & HELGASON, T. 2003. Genome scan meta-analysis of schizophrenia and bipolar disorder, part II: Schizophrenia. *Am J Hum Genet,* 73**,** 34-48.

LI, W., ZHANG, Q., OISO, N., NOVAK, E. K., GAUTAM, R., O'BRIEN, E. P., TINSLEY, C. L., BLAKE, D. J., SPRITZ, R. A., COPELAND, N. G., JENKINS, N. A., AMATO, D., ROE, B. A., STARCEVIC, M., DELL'ANGELICA, E. C., ELLIOTT, R. W., MISHRA, V., KINGSMORE, S. F., PAYLOR, R. E. & SWANK, R. T. 2003. Hermansky-Pudlak syndrome type 7 (HPS-7) results from mutant dysbindin, a member of the biogenesis of lysosome-related organelles complex 1 (BLOC-1). *Nat Genet,* 35**,** 84-9.

LIAO, H. M. & CHEN, C. H. 2004. Mutation analysis of the human dystrobrevin-binding protein 1 gene in schizophrenic patients. *Schizophr Res,* 71**,** 185-9.

LIEBERMAN, J., CHAKOS, M., WU, H., ALVIR, J., HOFFMAN, E., ROBINSON, D. & BILDER, R. 2001. Longitudinal study of brain morphology in first episode schizophrenia. *Biol Psychiatry,* 49**,** 487-99.

LIU, L., BOTOS, I., WANG, Y., LEONARD, J. N., SHILOACH, J., SEGAL, D. M. & DAVIES, D. R. 2008. Structural basis of toll-like receptor 3 signaling with double-stranded RNA. *Science,* 320**,** 379-81.

LIU, Y. H., LAI, W. S., TSAY, H. J., WANG, T. W. & YU, J. Y. 2013. Effects of maternal immune activation on adult neurogenesis in the subventricular zone-olfactory bulb pathway and olfactory discrimination. *Schizophr Res*.

LIVAK, K. J. & SCHMITTGEN, T. D. 2001. Analysis of relative gene expression data using real-time quantitative PCR and the 2(-Delta Delta C(T)) Method. *Methods,* 25**,** 402-8.

LUO, J., WANG, X., XIA, Z., YANG, L., DING, Z., CHEN, S., LAI, B. & ZHANG, N. 2015. Transcriptional factor specificity protein 1 (SP1) promotes the proliferation of glioma cells by up-regulating midkine (MDK). *Mol Biol Cell,* 26**,** 430-9.

MAES, M., BERK, M., GOEHLER, L., SONG, C., ANDERSON, G., GALECKI, P. & LEONARD, B. 2012. Depression and sickness behavior are Janus-faced responses to shared inflammatory pathways. *BMC Med,* 10**,** 66.

MAHAR, I., TAN, S., DAVOLI, M. A., DOMINGUEZ-LOPEZ, S., QIANG, C., RACHALSKI, A., TURECKI, G. & MECHAWAR, N. 2011. Subchronic peripheral neuregulin-1 increases ventral hippocampal neurogenesis and induces antidepressant-like effects. *PLoS One,* 6**,** e26610.

MAO, X., YANG, S. H., SIMPKINS, J. W. & BARGER, S. W. 2007. Glutamate receptor activation evokes calpain-mediated degradation of Sp3 and Sp4, the prominent Sp-family transcription factors in neurons. *J Neurochem,* 100**,** 1300-14.

MAO, X. R., MOERMAN-HERZOG, A. M., CHEN, Y. & BARGER, S. W. 2009. Unique aspects of transcriptional regulation in neurons--nuances in NFkappaB and Sp1-related factors. *J Neuroinflammation,* 6**,** 16.

MASTROENI, D., GROVER, A., LEONARD, B., JOYCE, J. N., COLEMAN, P. D., KOZIK, B., BELLINGER, D. L. & ROGERS, J. 2009. Microglial responses to dopamine in a cell culture model of Parkinson's disease. *Neurobiol Aging,* 30**,** 1805-17.

MEDZHITOV, R., PRESTON-HURLBURT, P. & JANEWAY, C. A., JR. 1997. A human homologue of the Drosophila Toll protein signals activation of adaptive immunity. *Nature,* 388**,** 394-7.

MEI, L. & XIONG, W. C. 2008. Neuregulin 1 in neural development, synaptic plasticity and schizophrenia. *Nat Rev Neurosci,* 9**,** 437-52.

MESHUL, C. K. & CASEY, D. E. 1989. Regional, reversible ultrastructural changes in rat brain with chronic neuroleptic treatment. *Brain Res,* 489**,** 338-46.

MICHAILOV, G. V., SEREDA, M. W., BRINKMANN, B. G., FISCHER, T. M., HAUG, B., BIRCHMEIER, C., ROLE, L., LAI, C., SCHWAB, M. H. & NAVE, K. A. 2004. Axonal neuregulin-1 regulates myelin sheath thickness. *Science,* 304**,** 700-3.

MIURA, A., ODAHARA, N., TOMINAGA, A., INOUE, K., KAMBE, Y., KURIHARA, T. & MIYATA, A. 2012. Regulatory mechanism of PAC1 gene expression via Sp1 by nerve growth factor in PC12 cells. *FEBS Lett,* 586**,** 1731-5.

MIYAMOTO, S., DUNCAN, G. E., MARX, C. E. & LIEBERMAN, J. A. 2005. Treatments for schizophrenia: a critical review of pharmacology and mechanisms of action of antipsychotic drugs. *Mol Psychiatry,* 10**,** 79-104.

MOBERG, P. J., AGRIN, R., GUR, R. E., GUR, R. C., TURETSKY, B. I. & DOTY, R. L. 1999. Olfactory dysfunction in schizophrenia: a qualitative and quantitative review. *Neuropsychopharmacology,* 21**,** 325-40.

MONJE, M. L., TODA, H. & PALMER, T. D. 2003. Inflammatory blockade restores adult hippocampal neurogenesis. *Science,* 302**,** 1760-5.

MOSHER, K. I., ANDRES, R. H., FUKUHARA, T., BIERI, G., HASEGAWA-MORIYAMA, M., HE, Y., GUZMAN, R. & WYSS-CORAY, T. 2012. Neural progenitor cells regulate microglia functions and activity. *Nat Neurosci,* 15**,** 1485-7.

MULLER, N., WAGNER, J. K., KRAUSE, D., WEIDINGER, E., WILDENAUER, A., OBERMEIER, M., DEHNING, S., GRUBER, R. & SCHWARZ, M. J. 2012. Impaired monocyte activation in schizophrenia. *Psychiatry Res,* 198**,** 341-6.

MUROTANI, T., ISHIZUKA, T., HATTORI, S., HASHIMOTO, R., MATSUZAKI, S. & YAMATODANI, A. 2007. High dopamine turnover in the brains of Sandy mice. *Neurosci Lett,* 421**,** 47-51.

NAGAI, T., KITAHARA, Y., SHIRAKI, A., HIKITA, T., TAYA, S., KAIBUCHI, K. & YAMADA, K. 2010. Dysfunction of dopamine release in the prefrontal cortex of dysbindin deficient sandy mice: an in vivo microdialysis study. *Neurosci Lett,* 470**,** 134-8.

NAIT-OUMESMAR, B., PICARD-RIERA, N., KERNINON, C., DECKER, L., SEILHEAN, D., HOGLINGER, G. U., HIRSCH, E. C., REYNOLDS, R. & BARON-VAN EVERCOOREN, A. 2007. Activation of the subventricular zone in multiple sclerosis: evidence for early glial progenitors. *Proc Natl Acad Sci U S A,* 104**,** 4694-9.

NETWORK & PATHWAY ANALYSIS SUBGROUP OF PSYCHIATRIC GENOMICS, C. 2015. Psychiatric genome-wide association study analyses implicate neuronal, immune and histone pathways. *Nat Neurosci,* 18**,** 199-209.

NEWELL-LITWA, K., SEONG, E., BURMEISTER, M. & FAUNDEZ, V. 2007. Neuronal and non-neuronal functions of the AP-3 sorting machinery. *J Cell Sci,* 120**,** 531-41.

NIHONMATSU-KIKUCHI, N., HASHIMOTO, R., HATTORI, S., MATSUZAKI, S., SHINOZAKI, T., MIURA, H., OHOTA, S., TOHYAMA, M., TAKEDA, M. & TATEBAYASHI, Y. 2011. Reduced rate of neural differentiation in the dentate gyrus of adult dysbindin null (sandy) mouse. *PLoS One,* 6**,** e15886.

NISHIYA, T. & DEFRANCO, A. L. 2004. Ligand-regulated chimeric receptor approach reveals distinctive subcellular localization and signaling properties of the Toll-like receptors. *J Biol Chem,* 279**,** 19008-17.

NIWA, M., JAARO-PELED, H., TANKOU, S., SESHADRI, S., HIKIDA, T., MATSUMOTO, Y., CASCELLA, N. G., KANO, S., OZAKI, N., NABESHIMA, T. & SAWA, A. 2013. Adolescent stress-induced epigenetic control of dopaminergic neurons via glucocorticoids. *Science,* 339**,** 335-9.

NUMAKAWA, T., YAGASAKI, Y., ISHIMOTO, T., OKADA, T., SUZUKI, T., IWATA, N., OZAKI, N., TAGUCHI, T., TATSUMI, M., KAMIJIMA, K., STRAUB, R. E., WEINBERGER, D. R., KUNUGI, H. & HASHIMOTO, R. 2004. Evidence of novel neuronal functions of dysbindin, a susceptibility gene for schizophrenia. *Hum Mol Genet,* 13**,** 2699-708.

O'NEILL, L. 2000. The Toll/interleukin-1 receptor domain: a molecular switch for inflammation and host defence. *Biochem Soc Trans,* 28**,** 557-63.

OHIRA, K., KOBAYASHI, K., TOYAMA, K., NAKAMURA, H. K., SHOJI, H., TAKAO, K., TAKEUCHI, R., YAMAGUCHI, S., KATAOKA, M., OTSUKA, S., TAKAHASHI, M. & MIYAKAWA, T. 2013. Synaptosomal-associated protein 25 mutation induces immaturity of the dentate granule cells of adult mice. *Mol Brain,* 6**,** 12.

OLIVER, P. L. & DAVIES, K. E. 2009. Interaction between environmental and genetic factors modulates schizophrenic endophenotypes in the Snap-25 mouse mutant blind-drunk. *Hum Mol Genet,* 18**,** 4576-89.

OLIVER, P. L., SOBCZYK, M. V., MAYWOOD, E. S., EDWARDS, B., LEE, S., LIVIERATOS, A., OSTER, H., BUTLER, R., GODINHO, S. I., WULFF, K., PEIRSON, S. N., FISHER, S. P., CHESHAM, J. E., SMITH, J. W., HASTINGS, M. H., DAVIES, K. E. & FOSTER, R. G. 2012. Disrupted circadian rhythms in a mouse model of schizophrenia. *Curr Biol,* 22**,** 314-9.

OOSTING, M., CHENG, S. C., BOLSCHER, J. M., VESTERING-STENGER, R., PLANTINGA, T. S., VERSCHUEREN, I. C., ARTS, P., GARRITSEN, A., VAN EENENNAAM, H., STURM, P., KULLBERG, B. J., HOISCHEN, A., ADEMA, G. J., VAN DER MEER, J. W., NETEA, M. G. & JOOSTEN, L. A. 2014. Human TLR10 is an anti-inflammatory pattern-recognition receptor. *Proc Natl Acad Sci U S A,* 111**,** E4478-84.

OSHIUMI, H., MATSUMOTO, M., FUNAMI, K., AKAZAWA, T. & SEYA, T. 2003. TICAM-1, an adaptor molecule that participates in Toll-like receptor 3-mediated interferon-beta induction. *Nat Immunol,* 4**,** 161-7.

PAOLICELLI, R. C., BOLASCO, G., PAGANI, F., MAGGI, L., SCIANNI, M., PANZANELLI, P., GIUSTETTO, M., FERREIRA, T. A., GUIDUCCI, E., DUMAS, L., RAGOZZINO, D. & GROSS, C. T. 2011. Synaptic pruning by microglia is necessary for normal brain development. *Science,* 333**,** 1456-8.

PERKINS, N. D., AGRANOFF, A. B., PASCAL, E. & NABEL, G. J. 1994. An interaction between the DNA-binding domains of RelA(p65) and Sp1 mediates human immunodeficiency virus gene activation. *Mol Cell Biol,* 14**,** 6570-83.

PINACHO, R., VALDIZAN, E. M., PILAR-CUELLAR, F., PRADES, R., TARRAGO, T., HARO, J. M., FERRER, I. & RAMOS, B. 2014. Increased SP4 and SP1 transcription factor expression in the postmortem hippocampus of chronic schizophrenia. *J Psychiatr Res,* 58**,** 189-96.

RADEWICZ, K., GAREY, L. J., GENTLEMAN, S. M. & REYNOLDS, R. 2000. Increase in HLA-DR immunoreactive microglia in frontal and temporal cortex of chronic schizophrenics. *J Neuropathol Exp Neurol,* 59**,** 137-50.

RAIS, M., CAHN, W., SCHNACK, H. G., HULSHOFF POL, H. E., KAHN, R. S. & VAN HAREN, N. E. 2012. Brain volume reductions in medication-naive patients with schizophrenia in relation to intelligence quotient. *Psychol Med,* 42**,** 1847-56.

RANGREZ, A. Y., BERNT, A., POYANMEHR, R., HARAZIN, V., BOOMGAARDEN, I., KUHN, C., ROHRBECK, A., FRANK, D. & FREY, N. 2013. Dysbindin is a potent inducer of RhoA-SRF-mediated cardiomyocyte hypertrophy. *J Cell Biol,* 203**,** 643-56.

REIF, A., FRITZEN, S., FINGER, M., STROBEL, A., LAUER, M., SCHMITT, A. & LESCH, K. P. 2006. Neural stem cell proliferation is decreased in schizophrenia, but not in depression. *Mol Psychiatry,* 11**,** 514-22.

RIBEIRO XAVIER, A. L., KRESS, B. T., GOLDMAN, S. A., LACERDA DE MENEZES, J. R. & NEDERGAARD, M. 2015. A Distinct Population of Microglia Supports Adult Neurogenesis in the Subventricular Zone. *J Neurosci,* 35**,** 11848-61.

ROLLS, A., SHECHTER, R., LONDON, A., ZIV, Y., RONEN, A., LEVY, R. & SCHWARTZ, M. 2007. Toll-like receptors modulate adult hippocampal neurogenesis. *Nat Cell Biol,* 9**,** 1081-8.

SAGGU, S., CANNON, T. D., JENTSCH, J. D. & LAVIN, A. 2013. Potential molecular mechanisms for decreased synaptic glutamate release in dysbindin-1 mutant mice. *Schizophr Res,* 146**,** 254-63.

SCARDIGLI, R., CAPELLI, P., VIGNONE, D., BRANDI, R., CECI, M., LA REGINA, F., PIRAS, E., CINTOLI, S., BERARDI, N., CAPSONI, S. & CATTANEO, A. 2014. Neutralization of nerve growth factor impairs proliferation and differentiation of adult neural progenitors in the subventricular zone. *Stem Cells,* 32**,** 2516-28.

SCHIZOPHRENIA WORKING GROUP OF THE PSYCHIATRIC GENOMICS, C. 2014. Biological insights from 108 schizophrenia-associated genetic loci. *Nature,* 511**,** 421-7.

SCHMIEG, N., ROCCHI, C., ROMEO, S., MAGGIO, R., MILLAN, M. J. & MANNOURY LA COUR, C. 2015. Dysbindin-1 modifies signaling and cellular localization of recombinant, human D and D receptors. *J Neurochem*.

SCHULTZ, S. H., NORTH, S. W. & SHIELDS, C. G. 2007. Schizophrenia: a review. *Am Fam Physician,* 75**,** 1821-9.

SCHULZ, O., DIEBOLD, S. S., CHEN, M., NASLUND, T. I., NOLTE, M. A., ALEXOPOULOU, L., AZUMA, Y. T., FLAVELL, R. A., LILJESTROM, P. & REIS E SOUSA, C. 2005. Toll-like receptor 3 promotes cross-priming to virus-infected cells. *Nature,* 433**,** 887-92.

SEKAR, A., BIALAS, A. R., DE RIVERA, H., DAVIS, A., HAMMOND, T. R., KAMITAKI, N., TOOLEY, K., PRESUMEY, J., BAUM, M., VAN DOREN, V., GENOVESE, G., ROSE, S. A., HANDSAKER, R. E., SCHIZOPHRENIA WORKING GROUP OF THE PSYCHIATRIC GENOMICS, C., DALY, M. J., CARROLL, M. C., STEVENS, B. & MCCARROLL, S. A. 2016. Schizophrenia risk from complex variation of complement component 4. *Nature*.

SEN, R. & BALTIMORE, D. 1986. Multiple nuclear factors interact with the immunoglobulin enhancer sequences. *Cell,* 46**,** 705-16.

SHAO, L., SHUAI, Y., WANG, J., FENG, S., LU, B., LI, Z., ZHAO, Y., WANG, L. & ZHONG, Y. 2011. Schizophrenia susceptibility gene dysbindin regulates glutamatergic and dopaminergic functions via distinctive mechanisms in Drosophila. *Proc Natl Acad Sci U S A,* 108**,** 18831-6.

SHEN, H., MORRISON, C. D., ZHANG, J., UNDERWOOD, W., 3RD, YANG, N., FRANGOU, C., ENG, K., HEAD, K., BOLLAG, R. J., KAVURI, S. K., ROJIANI, A. M., LI, Y., YAN, L., HILL, A., WOLOSZYNSKA-READ, A., WANG, J., LIU, S., TRUMP, D. L. & CANDACE, J. S. 2013. 6p22.3 amplification as a biomarker and potential therapeutic target of advanced stage bladder cancer. *Oncotarget,* 4**,** 2124-34.

SHI, H., GABARIN, N., HICKEY, E. & ASKALAN, R. 2013. TLR-3 receptor activation protects the very immature brain from ischemic injury. *J Neuroinflammation,* 10**,** 104.

SHIGEMOTO-MOGAMI, Y., HOSHIKAWA, K., GOLDMAN, J. E., SEKINO, Y. & SATO, K. 2014. Microglia enhance neurogenesis and oligodendrogenesis in the early postnatal subventricular zone. *J Neurosci,* 34**,** 2231-43.

SHIHABUDDIN, L., BUCHSBAUM, M. S., HAZLETT, E. A., HAZNEDAR, M. M., HARVEY, P. D., NEWMAN, A., SCHNUR, D. B., SPIEGEL-COHEN, J., WEI, T., MACHAC, J., KNESAUREK, K., VALLABHAJOSULA, S., BIREN, M. A., CIARAVOLO, T. M. & LUU-HSIA, C. 1998. Dorsal striatal size, shape, and metabolic rate in never-medicated and previously medicated schizophrenics performing a verbal learning task. *Arch Gen Psychiatry,* 55**,** 235-43.

SIERRA, A., ENCINAS, J. M., DEUDERO, J. J., CHANCEY, J. H., ENIKOLOPOV, G., OVERSTREET-WADICHE, L. S., TSIRKA, S. E. & MALETIC-SAVATIC, M. 2010. Microglia shape adult hippocampal neurogenesis through apoptosis-coupled phagocytosis. *Cell Stem Cell,* 7**,** 483-95.

SIMPSON, E. H., KELLENDONK, C. & KANDEL, E. 2010. A possible role for the striatum in the pathogenesis of the cognitive symptoms of schizophrenia. *Neuron,* 65**,** 585-96.

SNYDER, J. S., SOUMIER, A., BREWER, M., PICKEL, J. & CAMERON, H. A. 2011. Adult hippocampal neurogenesis buffers stress responses and depressive behaviour. *Nature,* 476**,** 458-61.

SOBUE, S., HAGIWARA, K., BANNO, Y., TAMIYA-KOIZUMI, K., SUZUKI, M., TAKAGI, A., KOJIMA, T., ASANO, H., NOZAWA, Y. & MURATE, T. 2005. Transcription factor specificity protein 1 (Sp1) is the main regulator of nerve growth factor-induced sphingosine kinase 1 gene expression of the rat pheochromocytoma cell line, PC12. *J Neurochem,* 95**,** 940-9.

SOMMER, I. E., DE WITTE, L., BEGEMANN, M. & KAHN, R. S. 2012. Nonsteroidal anti-inflammatory drugs in schizophrenia: ready for practice or a good start? A meta-analysis. *J Clin Psychiatry,* 73**,** 414-9.

SOMMER, I. E., VAN WESTRHENEN, R., BEGEMANN, M. J., DE WITTE, L. D., LEUCHT, S. & KAHN, R. S. 2014. Efficacy of anti-inflammatory agents to improve symptoms in patients with schizophrenia: an update. *Schizophr Bull,* 40**,** 181-91.

SONG, X. Q., LV, L. X., LI, W. Q., HAO, Y. H. & ZHAO, J. P. 2009. The interaction of nuclear factor-kappa B and cytokines is associated with schizophrenia. *Biol Psychiatry,* 65**,** 481-8.

SOUMIYA, H., FUKUMITSU, H. & FURUKAWA, S. 2011. Prenatal immune challenge compromises the normal course of neurogenesis during development of the mouse cerebral cortex. *J Neurosci Res,* 89**,** 1575-85.

STEFANSSON, H., SIGURDSSON, E., STEINTHORSDOTTIR, V., BJORNSDOTTIR, S., SIGMUNDSSON, T., GHOSH, S., BRYNJOLFSSON, J., GUNNARSDOTTIR, S., IVARSSON, O., CHOU, T. T., HJALTASON, O., BIRGISDOTTIR, B., JONSSON, H., GUDNADOTTIR, V. G., GUDMUNDSDOTTIR, E., BJORNSSON, A., INGVARSSON, B., INGASON, A., SIGFUSSON, S., HARDARDOTTIR, H., HARVEY, R. P., LAI, D., ZHOU, M., BRUNNER, D., MUTEL, V., GONZALO, A., LEMKE, G., SAINZ, J., JOHANNESSON, G., ANDRESSON, T., GUDBJARTSSON, D., MANOLESCU, A., FRIGGE, M. L., GURNEY, M. E., KONG, A., GULCHER, J.

R., PETURSSON, H. & STEFANSSON, K. 2002. Neuregulin 1 and susceptibility to schizophrenia. *Am J Hum Genet,* 71**,** 877-92.

STEPHAN, K. E., BALDEWEG, T. & FRISTON, K. J. 2006. Synaptic plasticity and dysconnection in schizophrenia. *Biol Psychiatry,* 59**,** 929-39.

STOLP, H. B., DZIEGIELEWSKA, K. M., EK, C. J., POTTER, A. M. & SAUNDERS, N. R. 2005. Long-term changes in blood-brain barrier permeability and white matter following prolonged systemic inflammation in early development in the rat. *Eur J Neurosci,* 22**,** 2805-16.

STOLP, H. B., LIDDELOW, S. A., SA-PEREIRA, I., DZIEGIELEWSKA, K. M. & SAUNDERS, N. R. 2013. Immune responses at brain barriers and implications for brain development and neurological function in later life. *Front Integr Neurosci,* 7**,** 61.

STRAUB, R. E., JIANG, Y., MACLEAN, C. J., MA, Y., WEBB, B. T., MYAKISHEV, M. V., HARRIS-KERR, C., WORMLEY, B., SADEK, H., KADAMBI, B., CESARE, A. J., GIBBERMAN, A., WANG, X., O'NEILL, F. A., WALSH, D. & KENDLER, K. S. 2002. Genetic variation in the 6p22.3 gene DTNBP1, the human ortholog of the mouse dysbindin gene, is associated with schizophrenia. *Am J Hum Genet,* 71**,** 337-48.

STRIDH, L., EK, C. J., WANG, X., NILSSON, H. & MALLARD, C. 2013. Regulation of Toll-like receptors in the choroid plexus in the immature brain after systemic inflammatory stimuli. *Transl Stroke Res,* 4**,** 220-7.

STRIDH, L., SMITH, P. L., NAYLOR, A. S., WANG, X. & MALLARD, C. 2011. Regulation of toll-like receptor 1 and -2 in neonatal mice brains after hypoxia-ischemia. *J Neuroinflammation,* 8**,** 45.

SWANK, R. T., SWEET, H. O., DAVISSON, M. T., REDDINGTON, M. & NOVAK, E. K. 1991. Sandy: a new mouse model for platelet storage pool deficiency. *Genet Res,* 58**,** 51-62.

TABETA, K., GEORGEL, P., JANSSEN, E., DU, X., HOEBE, K., CROZAT, K., MUDD, S., SHAMEL, L., SOVATH, S., GOODE, J., ALEXOPOULOU, L., FLAVELL, R. A. & BEUTLER, B. 2004. Toll-like receptors 9 and 3 as essential components of innate immune defense against mouse cytomegalovirus infection. *Proc Natl Acad Sci U S A,* 101**,** 3516-21.

TAKAO, K., TOYAMA, K., NAKANISHI, K., HATTORI, S., TAKAMURA, H., TAKEDA, M., MIYAKAWA, T. & HASHIMOTO, R. 2008. Impaired long-term memory retention and working memory in sdy mutant mice with a deletion in Dtnbp1, a susceptibility gene for schizophrenia. *Mol Brain,* 1**,** 11.

TALBOT, K. 2009. The sandy (sdy) mouse: a dysbindin-1 mutant relevant to schizophrenia research. *Prog Brain Res,* 179**,** 87-94.

TALBOT, K., EIDEM, W. L., TINSLEY, C. L., BENSON, M. A., THOMPSON, E. W., SMITH, R. J., HAHN, C. G., SIEGEL, S. J., TROJANOWSKI, J. Q., GUR, R. E., BLAKE, D. J. & ARNOLD, S. E. 2004. Dysbindin-1 is reduced in intrinsic, glutamatergic terminals of the hippocampal formation in schizophrenia. *J Clin Invest,* 113**,** 1353-63.

TALBOT, K., LOUNEVA, N., COHEN, J. W., KAZI, H., BLAKE, D. J. & ARNOLD, S. E. 2011. Synaptic dysbindin-1 reductions in schizophrenia occur in an isoform-specific manner indicating their subsynaptic location. *PLoS One,* 6**,** e16886.

TALBOT, K., ONG, W. Y., BLAKE, D. J., TANG, J., LOUNEVA, N., CARLSON, G. C. & ARNOLD, S. E. 2009. Dysbindin-1 and Its Protein Family. *Handbook of*

Neurochemistry and Molecular Neurobiology: Schizophrenia, Third Edition, 107-241.

TAN, N. Y. & KHACHIGIAN, L. M. 2009. Sp1 phosphorylation and its regulation of gene transcription. *Mol Cell Biol,* 29, 2483-8.

TANG, J., LEGROS, R. P., LOUNEVA, N., YEH, L., COHEN, J. W., HAHN, C. G., BLAKE, D. J., ARNOLD, S. E. & TALBOT, K. 2009. Dysbindin-1 in dorsolateral prefrontal cortex of schizophrenia cases is reduced in an isoform-specific manner unrelated to dysbindin-1 mRNA expression. *Hum Mol Genet,* 18, 3851-63.

THOMPSON, P. M., EGBUFOAMA, S. & VAWTER, M. P. 2003. SNAP-25 reduction in the hippocampus of patients with schizophrenia. *Prog Neuropsychopharmacol Biol Psychiatry,* 27, 411-7.

THOMPSON, P. M., SOWER, A. C. & PERRONE-BIZZOZERO, N. I. 1998. Altered levels of the synaptosomal associated protein SNAP-25 in schizophrenia. *Biol Psychiatry,* 43, 239-43.

TORREY, E. F. 2002. Studies of individuals with schizophrenia never treated with antipsychotic medications: a review. *Schizophr Res,* 58, 101-15.

TOWN, T., JENG, D., ALEXOPOULOU, L., TAN, J. & FLAVELL, R. A. 2006. Microglia recognize double-stranded RNA via TLR3. *J Immunol,* 176, 3804-12.

TRAMONTIN, A. D., GARCIA-VERDUGO, J. M., LIM, D. A. & ALVAREZ-BUYLLA, A. 2003. Postnatal development of radial glia and the ventricular zone (VZ): a continuum of the neural stem cell compartment. *Cereb Cortex,* 13, 580-7.

TURBIC, A., LEONG, S. Y. & TURNLEY, A. M. 2011. Chemokines and inflammatory mediators interact to regulate adult murine neural precursor cell proliferation, survival and differentiation. *PLoS One,* 6, e25406.

TURETSKY, B. I., MOBERG, P. J., YOUSEM, D. M., DOTY, R. L., ARNOLD, S. E. & GUR, R. E. 2000. Reduced olfactory bulb volume in patients with schizophrenia. *Am J Psychiatry,* 157, 828-30.

URANOVA, N. A., ORLOVSKAYA, D. D., APEL, K., KLINTSOVA, A. J., HASELHORST, U. & SCHENK, H. 1991. Morphometric study of synaptic patterns in the rat caudate nucleus and hippocampus under haloperidol treatment. *Synapse,* 7, 253-9.

VAN BERCKEL, B. N., BOSSONG, M. G., BOELLAARD, R., KLOET, R., SCHUITEMAKER, A., CASPERS, E., LUURTSEMA, G., WINDHORST, A. D., CAHN, W., LAMMERTSMA, A. A. & KAHN, R. S. 2008. Microglia activation in recent-onset schizophrenia: a quantitative (R)-[11C]PK11195 positron emission tomography study. *Biol Psychiatry,* 64, 820-2.

VANDESOMPELE, J., DE PRETER, K., PATTYN, F., POPPE, B., VAN ROY, N., DE PAEPE, A. & SPELEMAN, F. 2002. Accurate normalization of real-time quantitative RT-PCR data by geometric averaging of multiple internal control genes. *Genome Biol,* 3, RESEARCH0034.

VONTELL, R., SUPRAMANIAM, V., THORNTON, C., WYATT-ASHMEAD, J., MALLARD, C., GRESSENS, P., RUTHERFORD, M. & HAGBERG, H. 2013. Toll-like receptor 3 expression in glia and neurons alters in response to white matter injury in preterm infants. *Dev Neurosci,* 35, 130-9.

WAKADE, C. G., MAHADIK, S. P., WALLER, J. L. & CHIU, F. C. 2002. Atypical neuroleptics stimulate neurogenesis in adult rat brain. *J Neurosci Res,* 69, 72-9.

WANG, H., YUAN, Y., ZHANG, Z., YAN, H., FENG, Y. & LI, W. 2014. Dysbindin-1C is required for the survival of hilar mossy cells and the maturation of adult newborn neurons in dentate gyrus. *J Biol Chem,* 289**,** 29060-72.

WANG, H. D., DUNNAVANT, F. D., JARMAN, T. & DEUTCH, A. Y. 2004. Effects of antipsychotic drugs on neurogenesis in the forebrain of the adult rat. *Neuropsychopharmacology,* 29**,** 1230-8.

WASHBOURNE, P., THOMPSON, P. M., CARTA, M., COSTA, E. T., MATHEWS, J. R., LOPEZ-BENDITO, G., MOLNAR, Z., BECHER, M. W., VALENZUELA, C. F., PARTRIDGE, L. D. & WILSON, M. C. 2002. Genetic ablation of the t-SNARE SNAP-25 distinguishes mechanisms of neuroexocytosis. *Nat Neurosci,* 5**,** 19-26.

WATANABE, Y., SOMEYA, T. & NAWA, H. 2010. Cytokine hypothesis of schizophrenia pathogenesis: evidence from human studies and animal models. *Psychiatry Clin Neurosci,* 64**,** 217-30.

WEICKERT, C. S., ROTHMOND, D. A., HYDE, T. M., KLEINMAN, J. E. & STRAUB, R. E. 2008. Reduced DTNBP1 (dysbindin-1) mRNA in the hippocampal formation of schizophrenia patients. *Schizophr Res,* 98**,** 105-10.

WEICKERT, C. S., STRAUB, R. E., MCCLINTOCK, B. W., MATSUMOTO, M., HASHIMOTO, R., HYDE, T. M., HERMAN, M. M., WEINBERGER, D. R. & KLEINMAN, J. E. 2004. Human dysbindin (DTNBP1) gene expression in normal brain and in schizophrenic prefrontal cortex and midbrain. *Arch Gen Psychiatry,* 61**,** 544-55.

WIDERA, D., MIKENBERG, I., ELVERS, M., KALTSCHMIDT, C. & KALTSCHMIDT, B. 2006. Tumor necrosis factor alpha triggers proliferation of adult neural stem cells via IKK/NF-kappaB signaling. *BMC Neurosci,* 7**,** 64.

WILLIAMS, J. L., HOLMAN, D. W. & KLEIN, R. S. 2014. Chemokines in the balance: maintenance of homeostasis and protection at CNS barriers. *Front Cell Neurosci,* 8**,** 154.

WOODROOFE, M. N. 1995. Cytokine production in the central nervous system. *Neurology,* 45**,** S6-10.

XAVIER, A. L., LIMA, F. R., NEDERGAARD, M. & MENEZES, J. R. 2015. Ontogeny of CX3CR1-EGFP expressing cells unveil microglia as an integral component of the postnatal subventricular zone. *Front Cell Neurosci,* 9**,** 37.

XU, K. & SHU, H. K. 2007. EGFR activation results in enhanced cyclooxygenase-2 expression through p38 mitogen-activated protein kinase-dependent activation of the Sp1/Sp3 transcription factors in human gliomas. *Cancer Res,* 67**,** 6121-9.

YADDANAPUDI, K., DE MIRANDA, J., HORNIG, M. & LIPKIN, W. I. 2011. Toll-like receptor 3 regulates neural stem cell proliferation by modulating the Sonic Hedgehog pathway. *PLoS One,* 6**,** e26766.

YAMAMOTO, M., SATO, S., HEMMI, H., HOSHINO, K., KAISHO, T., SANJO, H., TAKEUCHI, O., SUGIYAMA, M., OKABE, M., TAKEDA, K. & AKIRA, S. 2003. Role of adaptor TRIF in the MyD88-independent toll-like receptor signaling pathway. *Science,* 301**,** 640-3.

YAMAMOTO, M., SATO, S., MORI, K., HOSHINO, K., TAKEUCHI, O., TAKEDA, K. & AKIRA, S. 2002. Cutting edge: a novel Toll/IL-1 receptor domain-containing adapter that preferentially activates the IFN-beta promoter in the Toll-like receptor signaling. *J Immunol,* 169**,** 6668-72.

YAN, S., BERQUIN, I. M., TROEN, B. R. & SLOANE, B. F. 2000. Transcription of human cathepsin B is mediated by Sp1 and Ets family factors in glioma. *DNA Cell Biol,* 19**,** 79-91.

YANG, J., ZHANG, L., YU, C., YANG, X. F. & WANG, H. 2014. Monocyte and macrophage differentiation: circulation inflammatory monocyte as biomarker for inflammatory diseases. *Biomark Res,* 2**,** 1.

YOUNG, C. E., ARIMA, K., XIE, J., HU, L., BEACH, T. G., FALKAI, P. & HONER, W. G. 1998. SNAP-25 deficit and hippocampal connectivity in schizophrenia. *Cereb Cortex,* 8**,** 261-8.

YOUNG, K. M., BARTLETT, P. F. & COULSON, E. J. 2006. Neural progenitor number is regulated by nuclear factor-kappaB p65 and p50 subunit-dependent proliferation rather than cell survival. *J Neurosci Res,* 83**,** 39-49.

YOUNG, S. Z., TAYLOR, M. M. & BORDEY, A. 2011. Neurotransmitters couple brain activity to subventricular zone neurogenesis. *Eur J Neurosci,* 33**,** 1123-32.

YUROCHKO, A. D., MAYO, M. W., POMA, E. E., BALDWIN, A. S., JR. & HUANG, E. S. 1997. Induction of the transcription factor Sp1 during human cytomegalovirus infection mediates upregulation of the p65 and p105/p50 NF-kappaB promoters. *J Virol,* 71**,** 4638-48.

ZHAN, Y., PAOLICELLI, R. C., SFORAZZINI, F., WEINHARD, L., BOLASCO, G., PAGANI, F., VYSSOTSKI, A. L., BIFONE, A., GOZZI, A., RAGOZZINO, D. & GROSS, C. T. 2014. Deficient neuron-microglia signaling results in impaired functional brain connectivity and social behavior. *Nat Neurosci,* 17**,** 400-6.

ZHANG, J. M. & AN, J. 2007. Cytokines, inflammation, and pain. *Int Anesthesiol Clin,* 45**,** 27-37.

ZHANG, S. Y., JOUANGUY, E., UGOLINI, S., SMAHI, A., ELAIN, G., ROMERO, P., SEGAL, D., SANCHO-SHIMIZU, V., LORENZO, L., PUEL, A., PICARD, C., CHAPGIER, A., PLANCOULAINE, S., TITEUX, M., COGNET, C., VON BERNUTH, H., KU, C. L., CASROUGE, A., ZHANG, X. X., BARREIRO, L., LEONARD, J., HAMILTON, C., LEBON, P., HERON, B., VALLEE, L., QUINTANA-MURCI, L., HOVNANIAN, A., ROZENBERG, F., VIVIER, E., GEISSMANN, F., TARDIEU, M., ABEL, L. & CASANOVA, J. L. 2007. TLR3 deficiency in patients with herpes simplex encephalitis. *Science,* 317**,** 1522-7.

Appendix

Recipes for solutions

1. TAE buffer 1X

2. 0.1M PBS 1X

3. 0.1M PB 1X

4. 4% PFA

5. Cryoprotectant

6. 30% sucrose

TAE buffer 50X (stock solution)

Tris-base	242 g
Glacial acetic acid	57.1 mL
EDTA 0.5M	100 mL
For 250mL 0.5M EDTA pH 8 46.5g EDTA and 5.5g NaOH pellet in fill to 250mL	
distilled water	Up to 1000 ml

Working solution TAE buffer 1X

1M PBS 10X (stock solution)

Sodium chloride	NaCl	80 g
Potassium chloride	KCl	2 g
Potassium dihydrogen phosphate	KH_2PO_4	2.4 g
Sodium phosphate dibasic anhydrous	Na_2HPO_4	14.4 g
Distilled water	dH_2O	Up to 1000 mL

Working solution 0.1M PBS 1X at pH 7.4

0.1M PB 1X

Sodium phosphate monobasic	NaH_2PO_4	3.864 g
Sodium phosphate dibasic anhydrous	Na_2HPO_4	10.22 g
Distilled water	dH_2O	Up to 1000 mL

Adjust pH to 7.2

4% PFA

Paraformaldehyde (PFA)	20 g
0.1M PBS (pH 7.4)	Up to 1000 ml

Heat to 70°C in fume hood on a magnetic stirrer and filter when PFA dissolved and store at 4°C

Cryoprotectant

Sucrose	300 g
Ethylene glycol	300 mL
0.1M PB (pH 7.2)	Up to 1000 ml

Store at 4°C

30% sucrose

Sucrose	30 g
0.1M PB (pH 7.2)	Up to 100 ml

Store at 4°C